ACKNOWLEDGEMENT

"Of making many books there is no end, and
much study is a weariness of the flesh."

Ecclesiastes 12.12

The author wishes to thank Dr. V. Ramachandran for taking time and energy to read and comment during preparation of this report, and Dr. Kámilo Feher for having suggested such an interesting research subject.

He is especially indebted to Mr. Michael Ibbitt for the careful revision of the English version. Many thanks to Mrs. Adrienne Sutherland for compiling and typing and to Mr. Gordon Smith for the drawings.

Finally he wishes to thank his wife for all her encouragement and patience during seemingly endless hours spent in the preparation of this report.

TABLE OF CONTENTS

LIST OF FIGURES

LIST OF TABLES

LIST OF SYMBOLS AND ABBREVIATIONS

A	Availability
B=br	Bit rate of binary source
BER	Bit error rate
BPF	Band Pass Filter
β	Pseudoerror decision angle
DM	Delta Modulation
DC	Diphase Coding
DPSK	Differential Phase Shift Keying
DAV	Data Above Voice
DAVID	Data Above Vidio
Δ	$\frac{d-\ell}{d}$
Δt	Sampling Offset
$E_b=E_s$	Energy per Bit
E{ }	Expected Value
erfc	Complementary error function
$\frac{\eta}{2}$=No	Noise power spectral density (noise power in one hertz bandwidth)
E_b	Energy per Bit
f_c	Cut off frequency
FDM	Frequency Division Multiplex
F( )	F-distribution
ISI	Intersymbol Interference
LPF	Low pass Filter
LDM	Bevel Distribution Monitor
LED	Light Emitting Diode
m=L	Number of transmitted level (m-aray transmission signal)

MZP	Multi-zone Pseudoerror Monitor
NRZ	Non-Return to Zero
Ne	Number of bits incorrectly received
Nt	Total Number of Bits
PAM	Pulse Amplitude Modulation
P	A priory probability
P(e)	Probability of error
P(p)	Probability of pseudoerror
PRBS	Pseudo Random Binary Sequence
PCM	Pulse Code Modulation
PEZ	Pseudoerror Zone Monitor
2-PEZ	2-Level Pseudoerror Zone Monitor
2P	MZP's number of slicing levels
$\Phi(n)$	$\frac{1}{\sqrt{2\pi}} \int_o^x \exp -t^2/2 \ .dt$
p.d.f.	Probability of density function
Q	Charge of electron
Q(n)	$\frac{1}{\sqrt{2\pi}} \int_x^\infty \exp -t^2/2.dt$
QPSK	Quarternary Phase Shift Keying
RZ	Return to Zero
S/N	Signal to Noise Ratio
S(t)	Transmitted Signal
T	Band Interval
T_o	Monitoring time
TDM	Time Division Multiplex
TC	Transition Coding
τ	LPF time constant (1/RC)

WGN	White Gaussian Noise
$\sigma n = \sigma_o$	Standard deviation of Gaussian distributed Noise Source
$\oplus$	Modulo-2 addition
$1/f$	Low frequency noise
χ^2	χ^2 distribution

CHAPTER 1

INTRODUCTION

1.1 Principle of Digital Communication

Pseudo-error monitoring (PEM) techniques are a comparatively recent advance in performance monitoring of digital transmission systems and because they can be applied more efficiently and economically than alternative techniques, there is much interest in their development. This report will examine the design and application of various PEM techniques, and the practicality of their use in digital transmission.

Before examining these PEM techniques it is worthwhile to review some basic concepts of digital transmission. A communication system consists of three components: a transmitter, a channel, and a receiver as shown in Fig. 1.1. In digital communication, the data input to the transmitter consists of "bits" or binary digits, and this implies transmission of signals at two levels only. The signalling speed, or the data transmitted per second, is measured in "bauds" and for data transmitted in binary format bits and bauds are numerically equivalent.

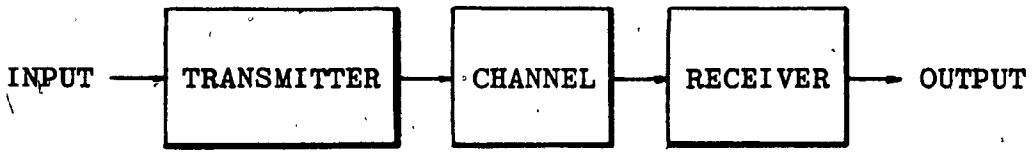

Figure 1.1: Basic Communication System

At present binary information is being generated by many types of equipment. The telegraph system is an example of a binary information source, but this type of information is now being generated mainly by modern digital computers and analog

encoders which encode analog signals in bits by means of Pulse Code Modulation (PCM) or Delta Modulation (DM).

Whatever the source, the transmitter assigns an electrical wave-form to each possible sequence of bits for appropriate transmission through the channel. A channel is an inter-connecting medium between the transmitter and receiver: Telephone cables, radio links, microwave channels and satellite transponders are typical examples. In passing through the channel the transmitted wave-form is distorted, attenuated and corrupted by various forms of "noise": Noise consists of unwanted random signals with certain statistical properties.

The receiver, which performs the inverse function of the transmitter, must recognize on receiving the transmitted data which one of the possible sequences has been transmitted. Due to degradation of the wave-forms by channel impairment, errors are introduced in re-establishing the transmitted information.

As in analog communications, there are many parameters which can be used to characterize the performance of digital communication systems. The most commonly used is the Bit Error Rate (BER) defined as the probability of error, Thus:

$$\begin{aligned} BER &= P(e) \\ &= N_e/N_t \\ &= N_e/Bt_o \end{aligned} \qquad (1.0.1)$$

where P (e) is the probability of an error, N_e the number of bits

incorrectly received, N_t the total number of bits transmitted during the monitoring time, B the bit rate of the binary source, and t_o the monitoring time.

1.2 Functional Diagram of a Basic Communication System

The functional diagram of a wide-band digital transmission system is shown in Fig. 1.2 for 300 to 3400 Hz wire-line applications, the up-and-down convertions do not apply. In this section each block in the transmission path will be described in detail.

The source coder is essentially an analog-to-digital (A/D) convertor containing signal processing circuitry such as conventional PCM or DM, a complex logic circuit, or even a microcomputer device which remains the redundant part of the information from an analog message. More advanced source coding techniques sueh as interframe coders and vocoders can reduce the bit rate and channel bandwidth requirements for digitized audio or video signals significantly. If the source information is in digital format as in digital computers or time-division multiplexers then a digital path which does not include the source coder is used.

The error coder is used to detect and/or correct a certain class of errors, and thereby reduces the probability of error in the overall system. Due to the complexity of processes for efficient error correction and/or detection coding/decoding, and the consequent increase in the transmission bit rate, a larger channel bandwidth is required. Binary data sequences are

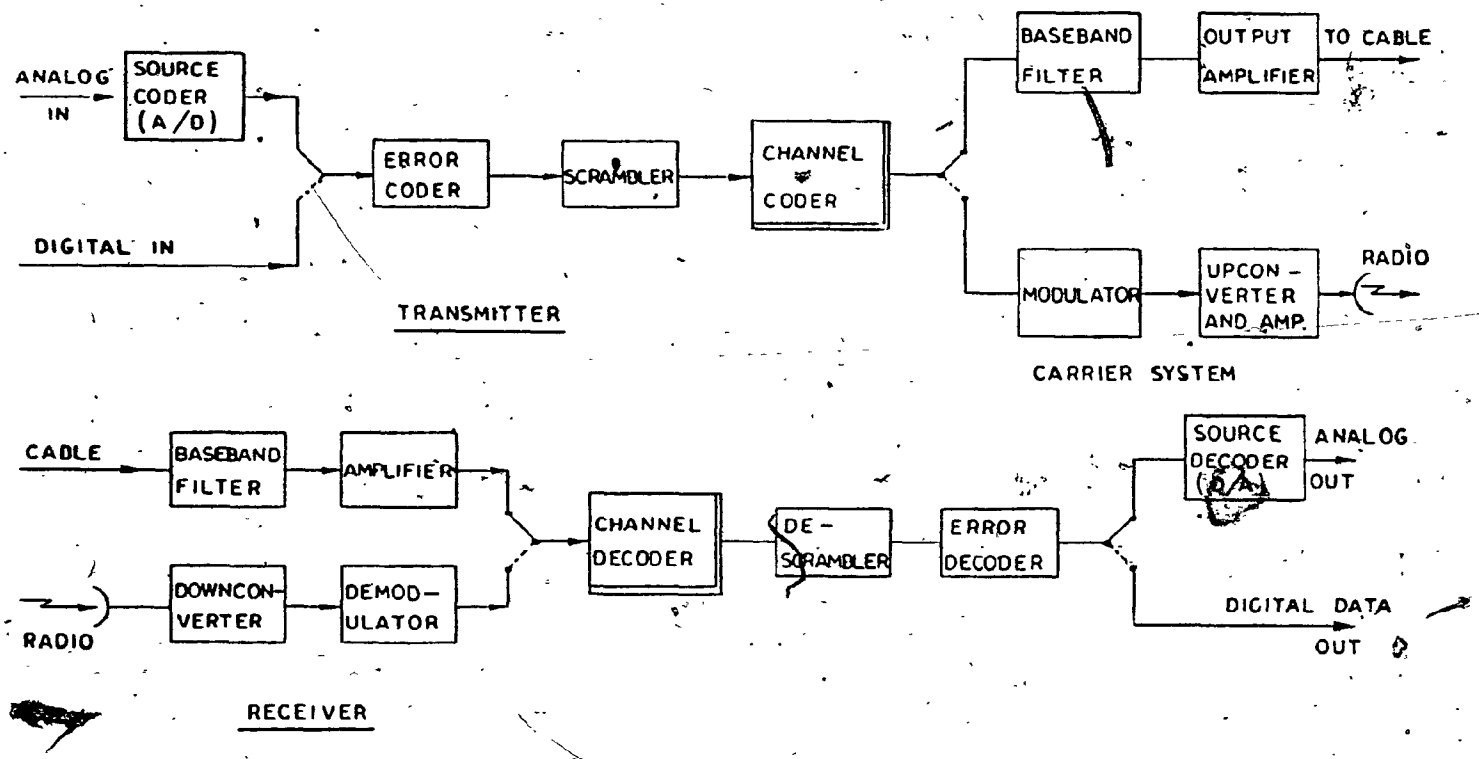

FIG. 1.2 FUNCTIONAL DIAGRAM OF A DIGITAL TRANSMISSON SYSTEM

randomized in scramblers and the resulting sequences generate a continuous spectrum void of discreet spectral lines; thus, there is an improvement in the interference environment. The scrambled data are then processed into multilevel or modified binary spectral-shaped signals in a channel coder which, in turn, feeds the base-band filter and output amplifier of a cable system, or the modulator of a carrier system. Some of the frequently applied channel coders such as those based on non-return to zero and return to zero signalling, are studied briefly in the following section.

1.3 Channel Coding

Various types of channel coding techniques are employed in digital communication. Applications differ from one type to another due to differences in time-domain representation and corresponding spectral densities. The channel bandwidth and signal-to-noise (S/N) ratio required to transmit a predetermined bit rate with a specified probability of error P(e) are the most important channel coding considerations. The following four other criteria are taken into consideration in various applications:

(1) Signal synchronization capability;

(2) Signal error detecting capability;

(3) Signal interference rejection and noise immunity capability;

(4) Cost due to complexity of transmission coder and receiver detector equipment.

In the following description of frequently applied channel codes the same probability of occurrence is assumed for logic state one (mark) and logic state zero (space), i.e. P(1) = P(0) = 0.5. This is a realistic assumption for most systems but if the source data do not meet this condition of equiprobability a scrambler circuit is used.

1.3.1. Baseband Channel Coding Technicques

In digital communication systems the channel coder generates random sequences of bits. Each bit, in synchronous communication, has a time interval of T (seconds) assigned for its transmission. A "one" is usually represented by a square pulse of amplitude V_p volts and durations t_p seconds while the absence of a pulse indicates a "zero".

a) Non-Return to Zero (NRZ) Coding

If the pulse duration, t_p seconds, (Fig. 1-3a and b) is equal to the bit interval T seconds the signal is called a Non-Return to Zero (NRZ) signal Ref. 1, page 27. This signal has an average DC-component value of VP/2 volts (Fig. 1-3a) and a normalized mean power of $V_p^2/2$ watts, if zero volts denotes logic zero. If the signal is transmitted through an AC-coupled channel as is usually the case, then the DC component is removed (Fig. 1-3b); the normalized mean power of this signal is then V_p^2 watts.

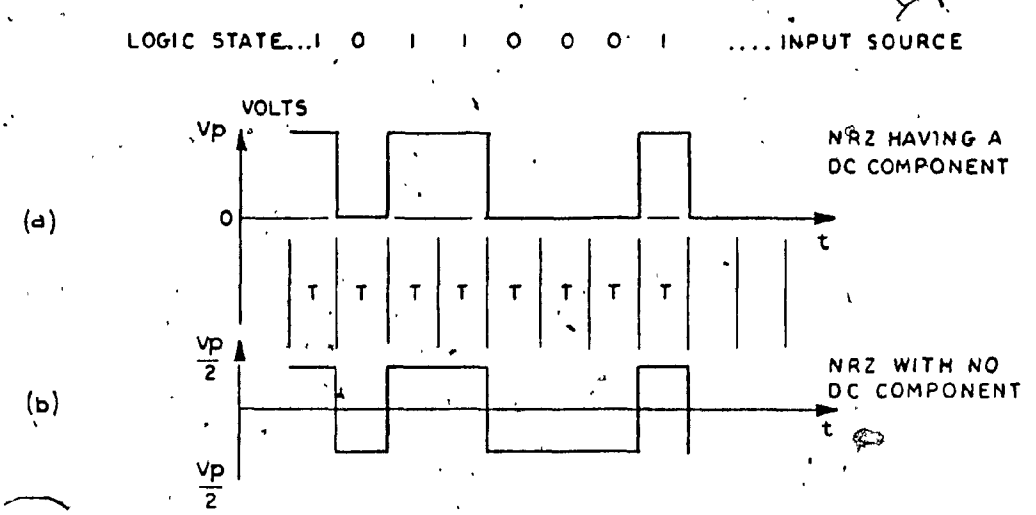

FIG. 1.3 NRZ DATA WITH AND WITHOUT D.C. COMPONENT

NRZ is one of the most frequently applied coding techniques. PCM convertors and outputs from A/D convertors of Time Division Multiplexed (TDM) circuits are therefore very often suitable for processing NRZ data.

b) Return to Zero (RZ) Coding

If the pulse duration t_p (Fig. 1-4) is less than the bit interval T, the signal is referred to as a Return to Zero (RZ) signal Ref. 1, page 27. The duty cycle, or duration cycle, of an RZ signal is defined (Ref. 1) as the ratio of the pulse width (t_p) to the bit interval (T). Usually, RZ pulses have a 50% duty cycle (Fig. 1-4).

RZ pulses have a broader spectrum than NRZ pulses and require, for identical bit rates, a greater bandwidth. For this

reason they are seldom used in digital transmission.

c) Bipolar Return to Zero (BRZ) Coding

If the pulse duration t_p equals T/2 and Vp volts denotes the first logic state (logic state one) encountered (Fig. 1-5) and -Vp the next one, then the signal is called a Bipolar Return to Zero (BRZ) signal Ref. 1. The BRZ code has three levels, is sometimes classified as a "pseudo-ternary" signal and is defined in Table 1.1.

TABLE 1.1

BRZ LOGIC TABLE

INPUT LOGIC STATE	OUTPUT BRZ-CODED SIGNAL
First "1" encountered	(bit time slot O,T)
	+ Vp (O,T/2)
	O (T/2, T)
Next "1" encountered	-Vp (O,T/2)
	O (T/2, T)
Zero	O (O,T)

BRZ is a frequently used coding technique. Specifically, the standard North Americal 24 channel, 1.544 Mb/s PCM TDM outputs in BRZ code (2).

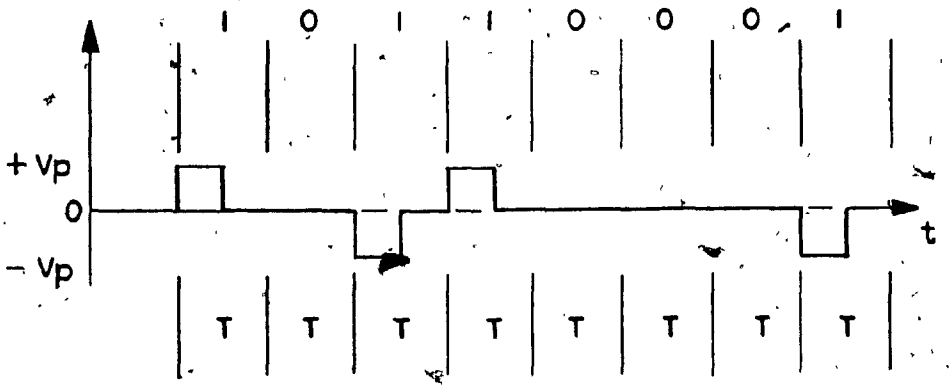

FIG. 1.5 BIPOLAR RETURN TO ZERO (BRZ) PATTERN

The power spectral density of random sequences coded are NRZ, RZ, BRZ, and various other binary formats are described by Bennett (Ref. 1 - Chapter 19); in his study it is shown that the BRZ bandwidth occupancy is the same as that of an NRZ signal.

In BRZ transmission equipment, an invertor operates on every other pulse position so that successive pulse positions of logic state "1" cannot have the same polarity. The receiver is thus capable of estimating the error rate by detecting the number of cases of two or more successive "ones" with the same polarity. This error detection can be carried out by a very simple logic circuit.

The only disadvantage of pulse-polarity error detectors is their inability to detect occurrences of two successive pulses in error. The error rate detector also fails in the event that an even number of successive errors occur in greater than T seconds (two or more) zero states at random in BRZ data.

d) Diphase Coding

If the mirror image (π - phase difference) of an RZ logic state one denotes logic state zero the coding is called Diphase Coding (DC), (Fig. 1-6). Since, at low frequencies, the power spectral density of DC in which the two signals O and 1 are represented by the phase O and π of a square wave of period T is negligible, analog service channel signals are used at these frequencies. This signal has a broader spectrum then NRZ.

e) Transition Coding

In Transition Coding (TC) the transitions of non-transitions between successive states of the signal are the significant features. The states of the signal are the same as for direct coding but since the changes of state contain the information the error rate is doubled (compared to that of direct coding) once the decision is made at the receiver.

In this section some of the more frequently used direct and transition codes were briefly described, and of these NRZ coding is perhaps the most frequently used. Outputs of PCM convertors and A/D convertors of TDM circuits are commonly NRZ pulses. Conventional digital integrated circuits are often suitable for processing NRZ data. Throughout this report, only PEM techniques applied to NRZ signals will be considered. These techniques can also be used to detect errors in a variety of digital base-band signals.

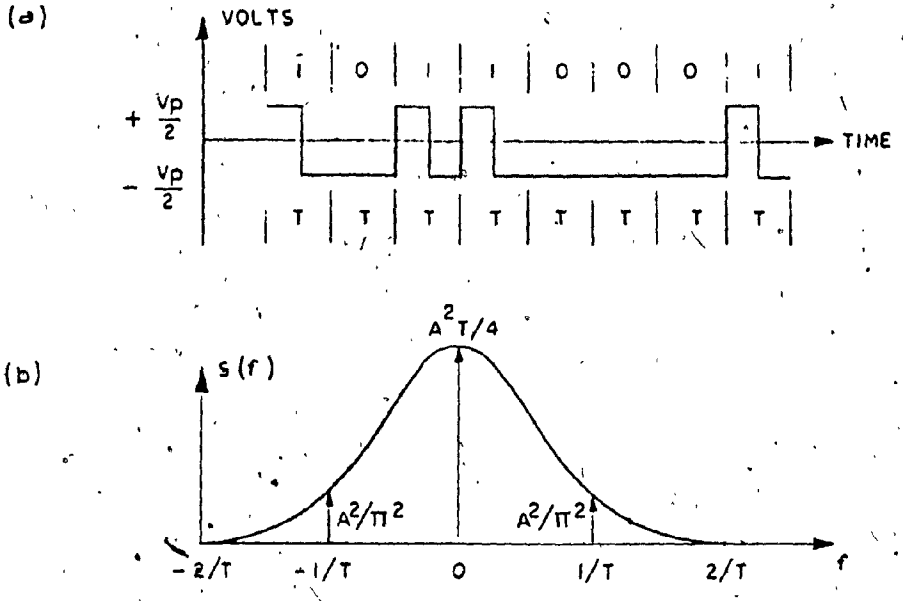

FIG. 1.4 RZ DATA PATTERN AND NORMALIZED RZ POWER SPECTRUM

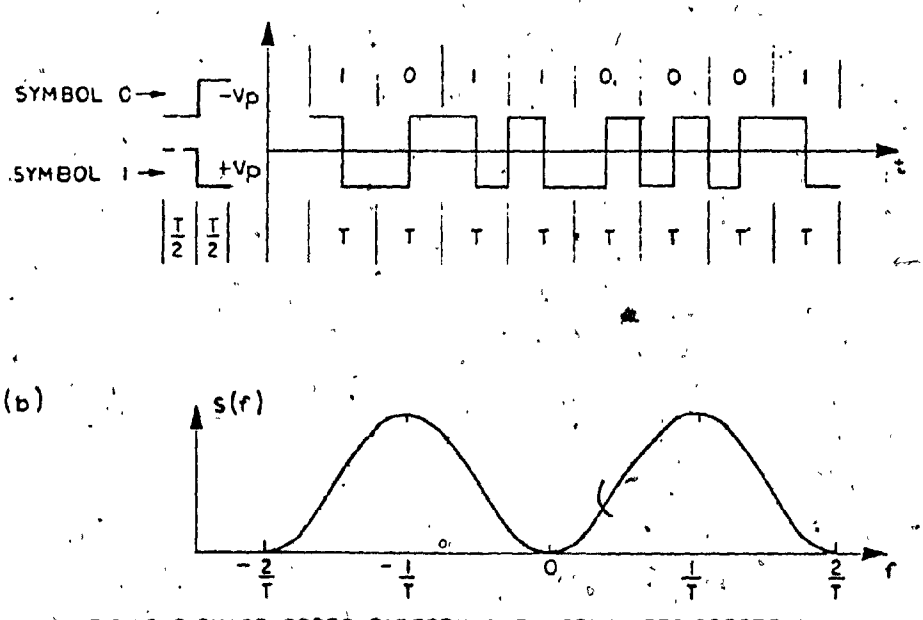

FIG. 1.6 DIPHASE CODED PATTERN AND NORMALIZED SPECTRUM

1.4 Criterion of Performance of Data Transmission Systems.

The final and most important criterion of performance of a data transmission links is the measure of the quantity of errors the system introduces on the average, that is to say, how large is the probability of error, P(e), or the bit error rate (BER). Other important parameters are the total transmitted power, the inband power spectral density and the out of band spectrum which is a cause of interference into other channels, the received carrier to noise (CNR), the carrier to interchannel interference ratio (CIR) and the demodulated baseband signal to noise ratio (SNR). Most well designed transmission systems operate with a very low P(e). Therefore back to back P(e) measurements often give no sufficient indication of the margins required for the system. Channel distortion and intersymbol interference measurements are helpful to obtain this additional information.

In this report frequently used measurements and a recently discovered BER estimation technique, the pseudoerror technique, are discussed.

CHAPTER 2

DATA TRANSMISSION LINES

2.1 Survey of Data Transmission Link

A pulse code modulation (PCM) system using binary encoding transmits a sequence of binary digits that is 1's and 0's. As stated before, these digits may be represented in a number of ways. In general the binary digits are encoded so that a "1" is represented by a signal $S_1(t)$ and an "0" by a signal $S_2(t)$, where $S_1(t)$ and $S_2(t)$ each have a duration T. The resulting signal may be transmitted directly or, as is more usually the case, used to modulate a carrier as in Phase Shift Keying (PSK) Differential Phase Shift Keying (DPSK) or Frequency Shift Keying (FSK). The received signal is corrupted by noise and hence there is a finite probability that the receiver will make an error in determining, within each time slot, whether a "1" or a "0" was transmitted.

The most important feature of digital transmission is the ability to reconstruct the transmitted pulse train after it has travelled through a dispersive and noisy medium. This process of reconstructing the pulses is performed at intervals along the transmission path by regenerative repeaters which equalize, synchronize and regenerate the data. The functional diagram of such a repeater is depicted in Fig. 2.1. For purpose of illustration, it is assumed that an ac-coupled NRZ sequence is transmitted from the previous repeater (Point 1 in the figure). The channel distorts, attenuates, and introduces various types of noise into the transmitted information (Point 2 in the figure). The pulses appearing at Point 3 are then shaped and raised to the level where a pulse, no - pulse decision (decision level) can be made. This is performed

by the preamplifier and equalizer section of a regenerator repeater. Finally, the reconstruction of the pulses is accomplished by the simultaneous operations of the timing and regeneration.

Bit timing recovery is accomplished by Phase Locked Loops or, in many cases, by non-linear processing and filtering of the incoming data stream. The timing path provides narrow pulses (almost impulses), for the following purposes:

(1) to sample the equalized pulse where the signal to interference ratio should be at the maximum;

(2) to maintain the proper pulse spacing.

The primary function of a regenerator is to reconstruct an exact replica of the pulse train at Point 1. The regenerator consists of a sampling device, a threshold comparator and a T-Sec (period of each pulse) level holding device. The regenerator proceeds whereby the incoming composite signal (pulse plus interference), at Point 5 exceeds the decision level (threshold level) and when the timing pulses at the output of the timing device sample the signal at the point where the signal has maximum peak value from the decision level (maximum eye opening).

In the ideal situation, the reconstructed pulse train at Point 6 would be an exact replica of the pulse train at Point 1.

In practice it departs from the ideal in the following ways:

(1) If the interference is sufficiently large at the decision time, the wrong decision will be made and an error will occur.

(2) If the spacing between the pulses departs from its proper value, the resulting pulse position "jitter" introduces distortion and intermodulation noise.

2.2 Error Rates and Eye Diagrams

Performance of a digital transmission system is measured by its error rate. When the bandwidth of such a transmission system is restricted, the wave form of Fig. 2.2a will be distorted (Fig. 2.2b). Errors may then be made at the receiver in determining the voltage level transmitted within the time slot associated with each bit.

Suppose that a pulse, representing a sample of a baseband signal, is applied to the input of a communication channel of limited bandwidth. At the receiving end of the channel the waveform resulting from this input pulse will not be confined to the time interval allocated to this sample. As a result, crosstalk occurs between baseband channels. In unquantized PAM, adjacent time slots are often associated with different message channels,

and the term *crosstalk* is more appropriate. In PCM adjacent bits are more generally symbols in the code representation of a single quantized sample. Hence the term *intersymbol interference*. It has already been noted that intersymbol interference may cause errors in reading the digits of the bit stream transmitted in a digital transmission system. Errors of this type may be avoided by extending the bandwidth. However, errors will still occur, because of the additive noise. More generally, even when the intersymbol interference or the additive noise, acting individually, is too small to cause an error, the two together may combine to cause an error.

A convenient graphical technique for determining the effects of the practical degradations introduced into the pulses as they travel to the regenerator is the "eye diagram". This diagram of two or more signalling intervals is the result of superimposing all possible pulse sequences. Such an eye diagram is given in Fig. 2.2b.

One way to obtain a good qualitative indication of the performance of a digital transmission system is to examine the bit stream on a cathode ray oscilloscope. One way to ensure that such an examination yields a great deal of information at a glance is to set the time base of the scope so that it triggers at the bit rate and yields a sweep lasting one time-slot duration. In the ideal case of no noise and no bandwidth restriction, the bit train waveform would appear as at the left in Fig. 2.2a and the scope pattern as at the right. The scope pattern would consist of two

horizontal lines. In Fig. 2.2b the bit train waveform illustrates the effect of limited bandwidth and the scope pattern resembles an "eye" and is called an "eye diagram". Fig. 2.2b shows an eye diagram for an NRZ random binary sequence in which the individual pulses at the input to the regenerators has a rounded-off shape. The decision area of "eye opening" for the decision level is evident. In an m-level system there will be m-1 separate eyes. Fig. 2.3 illustrates a three-level signal eye pattern and the corresponding decision levels. In Fig. 2.2b, the horizontal lines labelled +Vp/2 and -Vp/2 correspond to ideal received amplitudes. The vertical lines, separated by the signalling interval T, correspond to the ideal-decision times (Maximum eye opening). The decision making process in the regenerator can be represented by crosshairs in each eye as illustrated. The vertical line represents the decision time, while the horizontal hair represents the decision level. In order to regenerate the pulse sequence without error, the eye must be open, thereby meaning a decision area must exist, and the decision crosshairs must be within the open area. The effect of practical degradations of the pulses is to reduce the size of the ideal eye. A measure of the margin against error is the minimum distance between the crosshair and the edges of the eye.

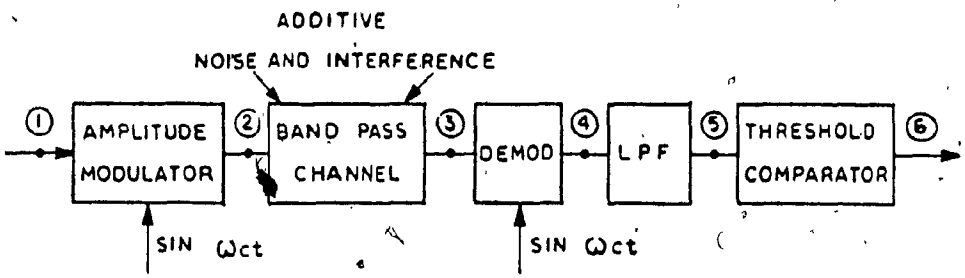

FIG.2.1 A SIMPLE DIGITAL AMPLITUDE MODULATED (AM) SYSTEM

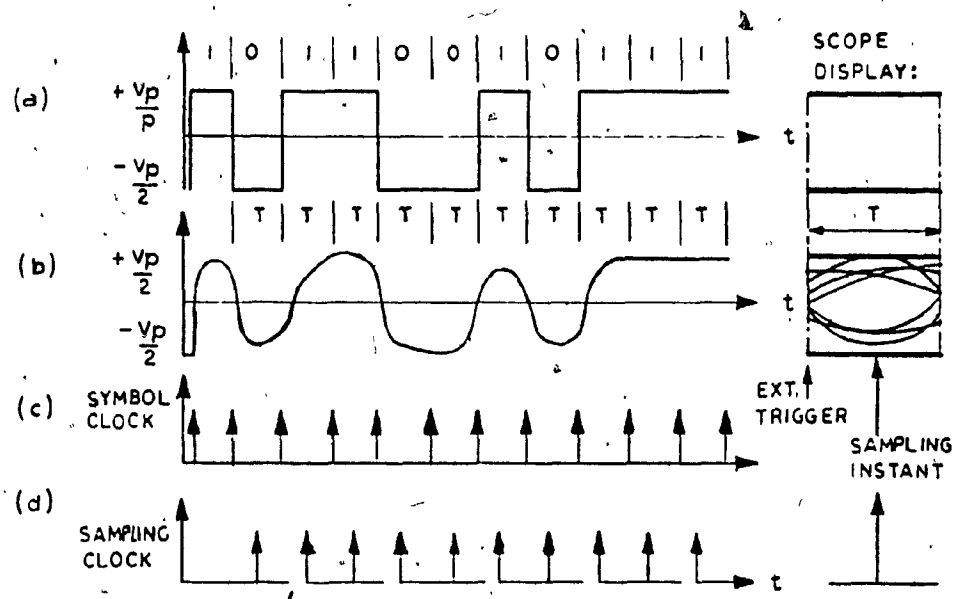

FIG. 2.2 EYE PATTERN OF A DATA STREAM

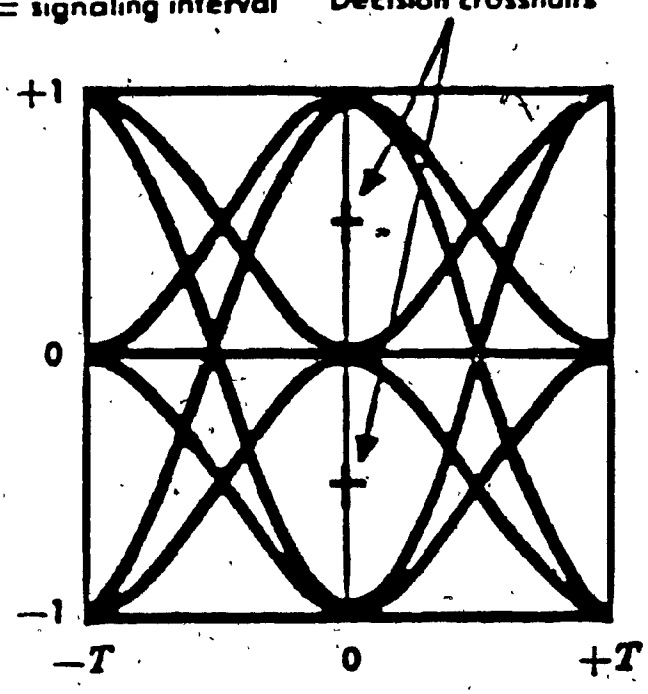

FIG. 2.3 EYE DIAGRAM FOR TERNARY RECEPTION

2.3 Channel Impairments

The modulation channel consists of the transmission medium and whatever transducers are needed to couple the signal to this medium. This transmission medium typically includes cable, microwave, or high-frequency radio links. In any event, for modulation and demodulation, the channel is treated as an analog link and its function is to convey the message presented to it at its input and reproduce it at its output. The real channel output typically differs from its input in two ways. The transmitted signal may be modified in a deterministic, even though not necessarily known, manner such as dispersion, frequency offset, and/or nonlinearities. The message can also be corrupted statistically by the channel. Examples of this type of modification are various types of additive and multiplicative noise such as thermal and impulse noise. Typical impairments encountered in the modulation-demodulation channel are discussed in the following sections.

2.3.1. Noise

Any interference to a communications channel can be considered noise. All unwanted electrical waves corresponding to noise at the system output will be easily characterized. In case of data transmission, the disturbance associated with these generalized electrical noises will effect the accuracy of the received information.

There are many potential sources of noise or interference

in a transmission system. For example, intermodulation noise resulting from nonlinearities in the transmission system, interference produced by one transmission channel being coupled to another (crosstalk), linear distortions representing a kind of deterministic channel impairment, and common types of noise with their characteristically nondeterministic nature.

Common Types of Noise

The most common characteristic of noise is its non-deterministic nature, i.e. its exact waveform cannot be predicted. If prediction were possible, it would be easy to achieve effective noise-free performance. Lack of accurate waveform information does not prevent measuring the amount of noise which can be determined by the rms voltage (or current), average peak, or rectified average voltage (or current), measured on an appropriate meter. For different types of noise the relationships between these qualities are different, and depending on type of noise, passage through a non-linear device will change the frequency spectrum and hence have an effect on the noise.

The use of a probability distribution or probability density function (pdf), is a common way to characterize many types of noise waveforms. If the probability that the voltage is less than V is P(V), then the probability distribution function extends from zero for $V = -\infty$ to one for $V = +\infty$. The probability density function, P(V) is represented by the slope of its distribution function. Since the area under the p.d.f.

curve is equal to unity, the fraction of time or probability of V being in the interval from $V = V_1$ to $V = V_2$ is equal to the area under the P(V) curve within that interval. Level Distribution Monitor (LDM) is used to obtain the probability distribution function of the noise wave. Basically LDM consists of a bank of parallel threshold detectors feeding integrated output meters.

A probability function does not uniquely define random noise. The missing parameter is the frequency (or time) scale. This is usually furnished by the frequency spectrum of the noise wave. Since the wave frequency components are not limited, the Fourier spectrum, which is an energy spectrum for all frequencies, does not exist. Instead, the mean square voltage spectrum, or spectral density which is measurable is commonly used and is identical with the power spectral density, if the load impendance is one ohm.

The autocorrelation function can also be used to characterize the time scale of a noise wave. At any two instants of time, the degree of dependance between amplitudes of the wave is given by this function. Lee {3} has shown that the auto-correlation function and spectral density are Fourier transform pairs.

Sine Wave Interference

Sine Wave Disturbance can theoretically be eliminated by locally producing a sine wave 180 degrees out of phase to cancel the interference. In practice, an interfering sine wave may

originate from an external uncontrolled source and its amplitude, frequency, and/or phase are liable to vary unpredictably. Therefore, it is sometimes convenient to treat sine wave interference as if it were noise with a sinusoidal distribution of magnitude versus time.

The amplitude density function of a sine wave voltage, of peak amplitude A, is given by:

$$\left.\begin{aligned} P(V) &= \frac{1}{\pi\sqrt{A^2 - V^2}} && -A \leq V \leq A \\ &= 0 && |V| > A \end{aligned}\right\} \quad (2.2.1)$$

The corresponding distribution function is:

$$\left.\begin{aligned} P(V) &= \frac{1}{2} + \frac{1}{\pi} \text{ arc Sin } \frac{V}{A} && -A \leq V \leq A \\ &= 0 && V < -A \\ &= 1 && V > A \end{aligned}\right\} \quad (2.2.2)$$

The Average Absolute Value, Root Mean Square voltage and the peak value can be determined by the density function of equation (2.2.1). The peak value of this sine wave is given by A in volts or 20 log A in dBV. The average absolute value is determined by doubling the density function of Eq. (2.2.1), which

corresponds to the density function of a fully rectified sine wave, and by taking the expected value of the peak V, {4}, given by Eq. (2.2.3).

$$E\{|V|\} = \int_0^A \frac{2V}{\pi\sqrt{A^2 - V^2}}\, dV = \frac{2A}{\pi} \qquad (2.2.3)$$

Finally, the rms voltage is given by the square root of the expected value of V^2 derived as follows:

$$Vrms = \sqrt{\int_{-A}^{+A} \frac{V}{\pi\sqrt{A^2 - V^2}}\, dV} = \frac{A}{\sqrt{2}} \qquad (2.2.4)$$

Many voltmeters do not read the peak values but instead rectify the voltage and read the average, or the rms voltage of the input signal. However the average absolute value is 20 log $\pi/2$ = 3.92 dB below the peak value for a sine wave. The rms voltage is then 20 log $\sqrt{2}$ = 3.01 dB below the peak value. Many meters are constructed to respond to the rectified average voltage and yet are calibrated in terms of rms sinewave voltages (i.e. they read 3.92 - 3.01 = .91 dB high). Errors can result when rms voltages of other types of signals are measured on such a meter assumed to be the correct rms value.

Pilots

The reason for classifying single frequency sinusoidal waves as single frequency noise is because they are deliberately placed on a carrier facility as pilots for synchronizing reinserted carriers, and are often employed for line regulation and maintenance, namely, orderwire transmission. Consequently, they can produce undesired interference which is introduced by the nonlinearities in the system. The nonlinearities may produce harmonics of the pilots frequency and if one of these harmonics falls into a FDM voice channel, the demodulated output of that channel will contain a single frequency audio tone. As a consequence in digital radio, a single frequency interference will produce an inter-modulated distorted eye diagram (as illustrated in Fig. 2.4). Thus, the regenerated bit stream contains a higher bit error rate due to the single-frequency interference.

Supervision

In a multichannel system the crosstalk of supervision (and occasionally signalling) tones into adjacent channels are also sources of single frequency interference.

Thermal Noise

In accordance with the kinetic theory of heat, thermal noise is a phenomenon associated with the continual random motion of the electrons in a conductor in thermal equilibrium with the

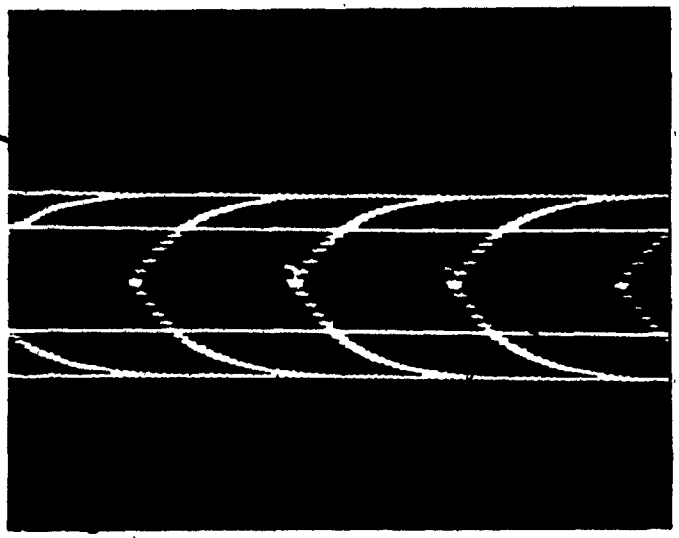

FIG.2.4 PILOT INTER-MODULATED DISTORTED EYE DIAGRAM

molecules. The results given by the equipartition law of Boltzmann and Maxwell states that for a thermal noise source, the power density spectrum is independant of frequency. In all reported measurements, the available power of a thermal noise source has been found to be proportional to the bandwidth over any range from direct current to the highest microwave frequencies commonly used. Because of this property, a thermal noise source is referred to as a white noise source (analogy to white light which contains all visible wavelengths of lights). The term white noise has become well established to imply a uniform distribution with frequency and will be so used here. If the bandwidths are unlimited, the Equipartition Theory states that the available power of the Thermal noise source is also unlimited.

For most practical purposes the available noise power of a thermal noise source is directly proportional to the product of the bandwidth of the system and the absolute temperature of the source.

Gaussian Distribution

According to the "central limit theorem", the outcome of the sum of large numbers of independent events tends to have a Gaussian distribution. Thermal noise, which may be regarded as the superposition of an exceedingly large number of random independent electronic signals, satisfies theoretical conditions for a Gaussian distribution. The Gaussian distribution function for zero mean is shown in Fig. 2-5A, and its equation is:

$$P(V) = \frac{1}{\sigma_n\sqrt{2\pi}} \int_{-\infty}^{V} \exp \frac{-x^2}{2\sigma_n^2}\, dx \qquad (2.2.5)$$

Values for this integral have been tabulated for various values of V/σ_n. The density function is also shown in Fig. 2-5b and is given by the differential of Eq. 2.2.5.

$$P(V) = \frac{1}{\sigma_n\sqrt{2\pi}} d\left[\frac{\int_{-\infty}^{V} \exp\frac{-x^2}{2\sigma n^2}\, dx}{dx}\right] = \frac{1}{\sigma_n\sqrt{2\pi}} \exp \frac{-V^2}{2\sigma_n^2} \qquad (2.2.6)$$

The "mean square voltage" (the expected value of V^2) is equal to the variance, σ_n^2. Thus, the standard deviation of a Gaussian distributed noise source, σ_n, stands for the rms voltage. The expected value of the random variable V which is the full wave rectified average voltage of Gaussian Noise is equal to:

$$E(|V|) = \frac{2}{\sigma_n\sqrt{2\pi}} \int_{o}^{\infty} \exp\left(-V^2/2\sigma_n^2\right) dv = \sigma_n\sqrt{\frac{2}{\pi}} \qquad (2.2.7)$$

The ratio of rms to average absolute voltage is given by $\sqrt{\pi/2} = 1.253$ which is equivalent to 1.96 dB. From the previous analysis of a sine wave, the rms to average absolute voltage of a sine wave is 0.91dB. Thus, the rms value indicated for thermal

noise, from a rectifying-type meter calibrated to read rms values for a sine wave, will be 1.05 dB lower than the actual value.

For a thermal noise signal the definition of peak factor differs from other signals. This is because Gaussian noise has a probability greater than zero of exceeding any finite magnitude no matter how great. Thus, the peak factor given by the ratio of peak to rms voltage does not exist for a thermal noise signal. Therefore, the definition of peak factor for thermal noise is modified to be the ratio of the value exceeded by the noise a certain percentage of the time to the rms noise value. Due to the statistical properties and behavior of thermal noise this percentage of time is chosen to be 0.01 percent. Peak magnitudes greater than 3.89 σ_n (i.e. $|V| > 3.89\ \sigma_n$) occur less than 0.01 percent of the time. Thus, the peak factor for a thermal noise signal is 3.89, or 11.80 dB. Inclusion of 0.001 percent peaks increases the peak factor by only 1.1 dB to 12.9 dB.

When making thermal noise loading tests on amplifiers, repeater telephone systems and active filters, the peak factor must be considered. The active devices can handle only a limited amplitude range before the signal is clipped or otherwise distorted. As an example, if the amplifier is to be used to amplify a sine wave signal or a thermal noise signal without distorting the waveforms, the power handling capacity of thermal noise is 8.8 dB less than that for a sine wave.

The fact that thermal noise is white as well as Gaussian has led many engineers into carelessly treating white and

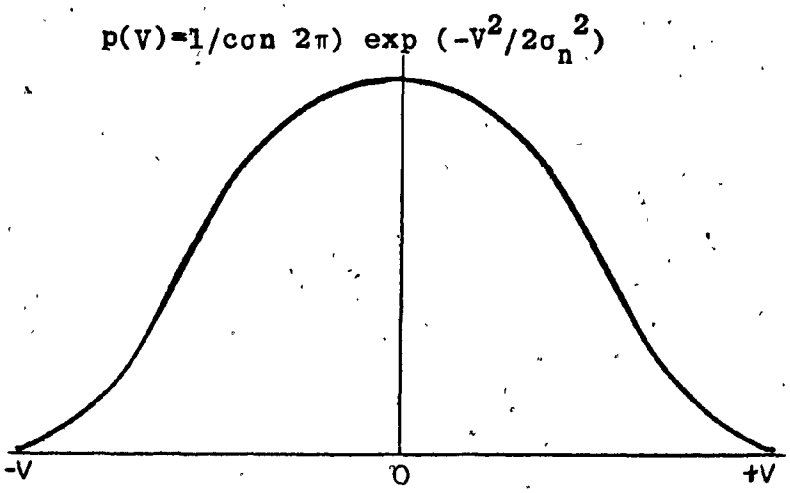

(a) Gaussian Density Function

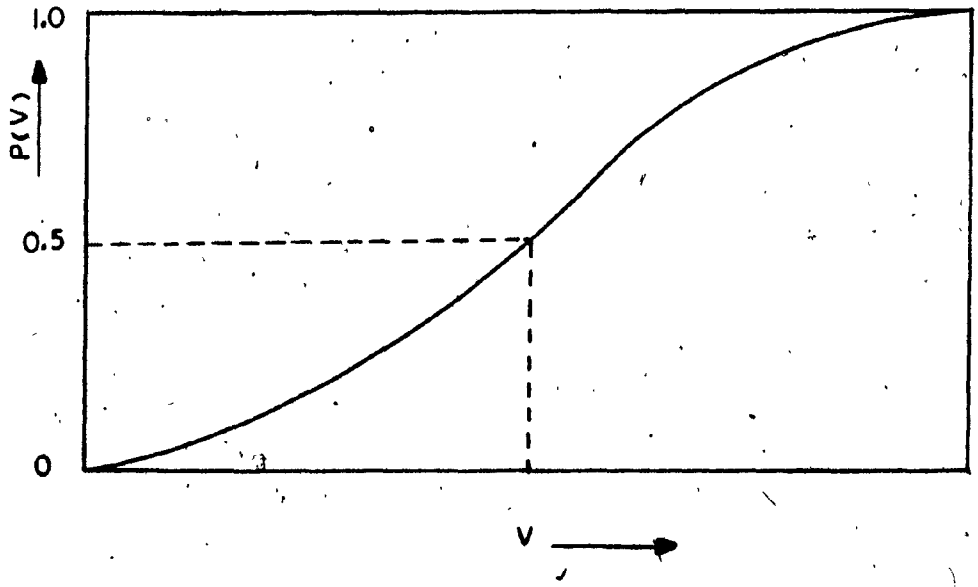

(b) Gaussian Distribution Function

FIG. 2.5 GAUSSIAN PROBABILITY DENSITY AND DISTRIBUTION FUNCTIONS

Gaussian noise as synonymous. Such is not always the case. For example, passing Gaussian Noise through a linear network such as a filter will leave it Gaussian but may considerably change the frequency spectrum. On the other hand, a single impulse will not have a Gaussian amplitude distribution but will have a flat or white frequency spectrum.

Shot Noise

Shot Noise is due to the discreet nature of electron flow and is found in most active devices. It was first observed in the anode current in vacuum-tube amplifiers and was described by W. Schottky in 1918. The mean square shot noise current in a 1-HZ bandwidth is:

$$i^2 \text{ rms} = 2QI \qquad (2.2.8)$$

Where Q = charge of the electron = $1.6(10)^{-19}$ Coulombs, and I = direct current through the device in amperes.

According to the central limit theorem, since shot noise is made up of a very large number of independent contributors the amplitude distribution of shot noise is Gaussian with variance $\sigma = i^2 = 2QI$. Observations confirm this assumption. Similarly, it is often accurate to assume that each impulsive component of the shot noise contains frequency components of equal magnitude (uniformly distributed) across all frequencies of practical interest, with the result that shot noise is considered white as well as

thermal noise.

In summary, both shot noise and thermal noise are white with Gaussian distributed amplitudes. Linear filtering or shaping of them does not affect their Gaussian properties but certainly does not leave them white. Again, the terms white and Gaussian are not synonymous. However, the magnitude of thermal noise is proportional to absolute temperature, whereas the magnitude of shot noise is proportional to the square root of current. Thus, it is related to signal amplitude.

Low Frequency (1/f) Noise

The random signal voltages associated with contact and surface irregularities in cathodes and semiconductors is called "Low-frequency (1/f) noise". This noise is caused by fluctuations in conductivity of the medium and it appears to be a Gaussian distributed noise. The effects of low-frequency noise have been reduced by cleaning and passivating semi-conductor surfaces. A good device may have negligible low-frequency noise above about 1 kHz although the corner frequency for high-frequency low noise transistors can be a few decades higher.

Impulse Noise

Due to corona-type discharges that occur along a repeater line and also switching transients in central offices, short spikes of energy having an approximately flat frequency spectrum over the frequency range of interest will appear. This type of noise is

called impulse noise, and appears to have an insignificant effect on human hearing, i.e. the impulses are below levels which might cause hearing damage. However, digital receivers are relatively intolerant of these impulses since they cannot distinguish between impulse noise and the pulses to be detected. Therefore, current study and control of impulse noise have marked effects on digital transmission. In any fixed interval the number of pulses occurring independently at random times follows a Poisson process. Mathematically this process is given by:

$$P(n) = \frac{(\nu T)^n \, e^{-\nu T}}{n!} \qquad (2.2.9)$$

where $P(n)$ is the probability that exactly n pulses occur in a time interval of duration, T, and ν is the average number of pulses occurring in unit time. It has been found experimentally that the number of events per unit time can be approximated by a log-normal distribution.

2.4 Probability of Error in a Gaussian Noise Environment

To detect reliably the correct symbol at the input to the regenerator, some minimum "signal-to-Noise" ratio is required. First, consider the code in which at the output of the channel coder, (see overall Block Diagram of Fig. 1.2) infinite bandwidth NRZ pulses of amplitude $+V_p$ or $-V_p$ are transmitted with equal probability (Fig. 2.2a). The received bandlimit and distorted

signal has a rounded-off shape after passing through the channel (Fig. 2.2b). For this situation, the decision threshold would be set at zero volt. At the decision time, if the composite signal is greater than zero the regenerator would make the decision that a positive pulse had been transmitted and, if the received signal plus noise is less than zero, a negative pulse would be regenerated. To find the probability of error, assume that the noise added to the signal has a Gaussian Distribution function. If, at the decision time, the noise level is more negative than $-V_p$, for a positive transmitted bit, error is introduced; for a negative pulse an error occurs if the noise is more positive than $+V_p$.

The probability of making such an error is:

$$\left.\begin{aligned} P(e) &= \tfrac{1}{2}\,\text{Prob}\,(V_n > V_p) + \tfrac{1}{2}\,\text{Prob}\,(V_n < V_p) \\ &= \frac{1}{\sqrt{2\pi}\sigma_n} \int_{V_p}^{\infty} e^{-Vn^2/2\sigma_n^2}\, dVn \\ &= \tfrac{1}{2}\,\text{erfc}\,\frac{V_p}{\sqrt{2}\sigma_n} \end{aligned}\right\} \quad (2.3.1)$$

where σ is the rms value of the noise and erfc is the complementary error function. The probability of error, for the NRZ binary sequence, versus the peak signal to rms Gaussian noise (S/N) ratio is plotted in Fig. 2.6 as the curve labelled L=2. Above 15 dB the probability

of error decreases very rapidly with respect to small decreases in S/N ratio. This phenomenon is referred to as the threshold or cliff effect in digital transmission. A typical repeater section requires a probability of error in 10^8 symbols which refers to a S/N ratio of 16 dB.

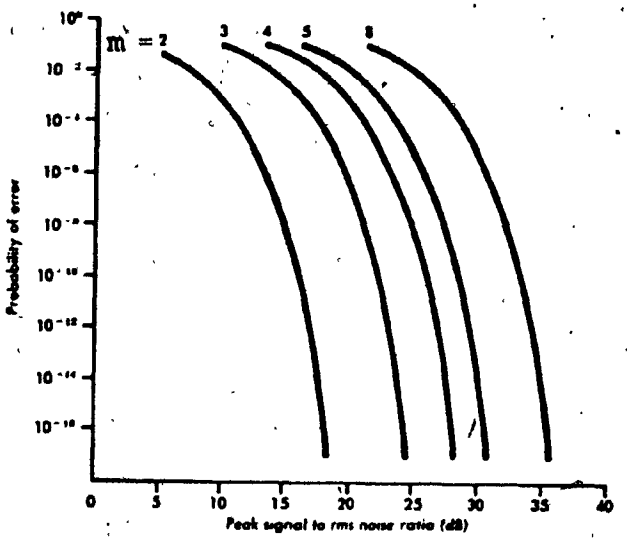

FIG. 2.6 Probability of error versus peak signal to rms gaussian noise for random m-level polar transmission.

Flexibility in the trade between S/N ratio and bandwidth (which is related to signalling rate in bauds) may be effected by using a multi-level transmission system. Multi-level is used to mean multiple decision thresholds which implies three or more transmitted levels. For an m-level PAM system, the probability of error is given by:

$$P(e) = \frac{L-1}{L} \operatorname{erfc}\left[\frac{Vp}{(L-1)\sqrt{2\sigma_n}}\right] \qquad (2.3.2)$$

Another parameter of importance is the bit energy (E_b) to noise density (N_o) ratio. The probability of error is then expressed as:

$$P(e) = f\ (E_b/N_o)$$

Equation 2.3.3. facilitates the comparison of measurements with theoretical predictions of various S/N requirements and their relation to E_b/N_o for multi-level digital transmission.

$$\frac{E_B}{N_o} = \frac{S}{N} \times \frac{BM}{BR} \qquad \text{or} \qquad \frac{E_b}{N_o} = \frac{S}{N} \times \frac{BM}{br} \qquad (2.3.3)$$

where

S = average Signal Power

N = mean noise power in the measured Noise Bandwidth (BM)

br = the bit rate bandwidth

E_b = Energy of one bit

E_B = Energy of one baud

BR = the baud rate bandwidth

BM = the measured noise bandwidth

It is assumed that the noise power spectrum is constant over all frequencies ("White Noise").

2.5 Error Rate with Non-Ideal Eyes

In digital communication, due to channel impairments, the various practical degradations shrink the eyes. The additional S/N requirement to maintain the error rate is a function of the amount of degradation and the number of levels.

The margin against error is reduced by the various degradations added to the waveform as it travels to the regenerator and by the imperfections in the decision process itself. The first of these decreases the size of the eye, while the second moves the crosshair relative to the boundaries of the eye. It is more useful, however, to account for the latter by holding the crosshairs fixed and shrinking the boundaries.

The degradations usually fall into two categories of amplitude and timing, corresponding to vertical and horizontal displacement. To obtain the shrunken eye, the amplitude degradations such as intersymbol interference, echoes, regenerator output variation and decision threshold uncertainties are summed. This sum is referred to as ΔA. The boundaries of the eye are then shifted vertically, as shown in Fig. 2.7 to account for these amplitude degradations. Next, the timing degradations such as static decision time misalignment and jitter are summed. This sum is referred to as ΔT. The boundaries of the eye are then displaced horizontally, as shown in the figure. Finally, the placement of the crosshairs is chosen

so as to maximize the vertical distance between its centre and the boundaries of the shrunken decision area. The only remaining degradation is noise, and to keep the probability of error unchanged from its value for the ideal system, the S/N ratio must be increased by:

$$\Delta S/N = 20 \log \frac{H}{h} \text{ dB} \qquad (2.4.1)$$

where H and h are the vertical openings of the ideal and degraded eye respectively, as illustrated in the figure.

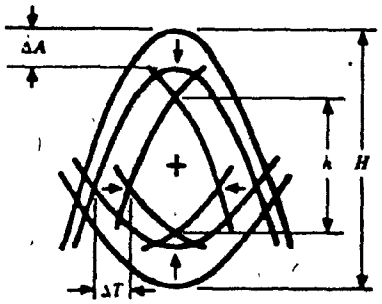

FIG. 2.7 SHRINKING THE EYE TO ACCOUNT FOR PRACTICAL DEGRADATIONS

Since the degradations are usually related to the maximum value of pulse rather than to the number of levels, it is useful to define a peak normalized eye degradation:

$$D = \frac{H-h}{V_p} \qquad (2.4.2)$$

Since $(m-1)H = 2V_p$, $\Delta S/N$ for an m-level eye can be expressed as:

$$\Delta S/N = -20 \log \left(1 - \frac{H-h}{H}\right)$$

$$= -20 \log \left(1 - \frac{D}{2}(m-1)\right) \qquad (2.4.3)$$

The relationship between S/N ratio eye degradation, and number of levels is shown in Fig. 2.8. The figure presents the S/N requirement for random polar m-ary transmission and a 10^{-10} error probability as a function of D.

For example, let D = 4. In this case, eight level transmission cannot be used since the eight level eye closes at D = 0.29. Five level transmission would be quite difficult, requiring an S/N ratio of 43 dB since the five level eye closes at D = 0.5. Three level transmission, however, would require only 25 dB.

An additional technique for evaluating degradations is the eye degradation plane. With ΔA and ΔT as coordinates, contours along which $\Delta S/N$ is a constant are given by a polar quarternary system in which pulses at the input to the regeneration have the cosine squared shape illustrated in Fig. 2.9. The combinations of ΔA and ΔT which completely close the eye are given by the curve labelled $\Delta S/N = \infty$ (Fig. 2.10).

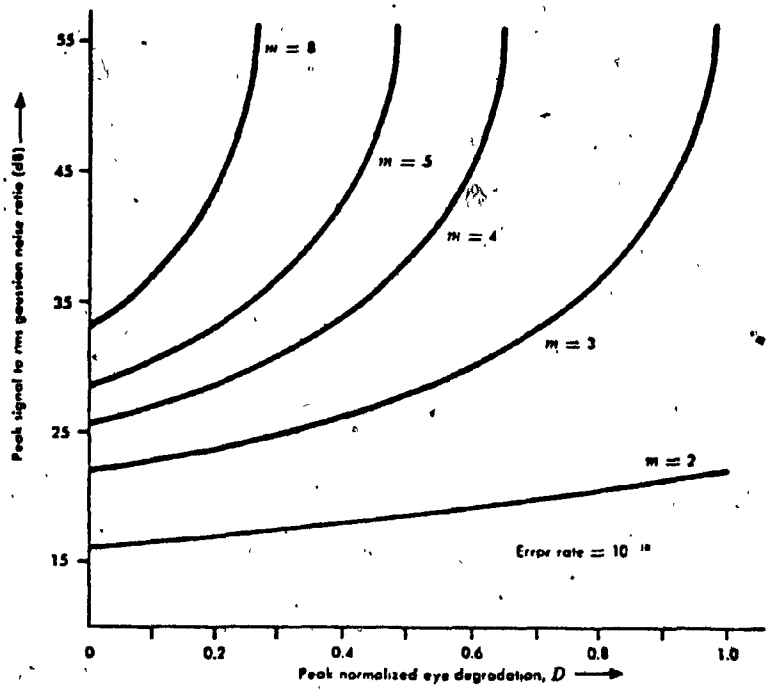

FIG. 2.8 SIGNAL-TO-NOISE REQUIREMENTS FOR m-LEVEL TRANSMISSION WITH DEGRADED EYES

$$p(t) = \begin{cases} P \cos^2 (\pi/2 \cdot t/T) & |t| \leq T \\ 0 & |t| > T \end{cases}$$

$P = (+1, 0, -1)$

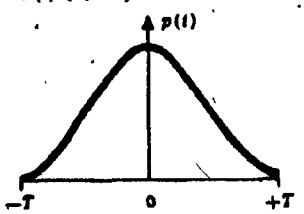

Pulse shapes for eye diagram

FIG. 2.9 RAISED COSINE SIGNAL EYE DIAGRAM

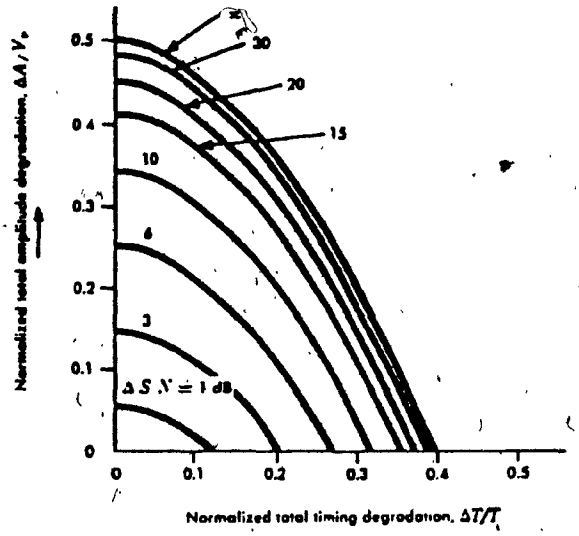

(a) Polar ternary

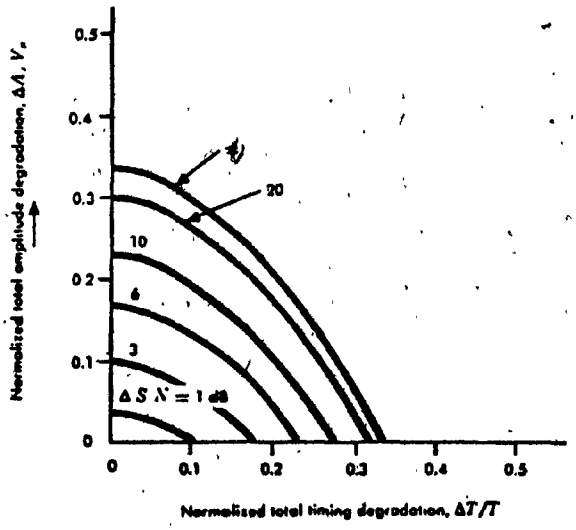

(b) Polar quaternary

FIG. 2.10 EYE DEGRADATION CONTOURS

CHAPTER 3

SURVEY OF MEASUREMENT TECHNIQUES IN DIGITAL TRANSMISSION

3.1 The Basic Digital System Problem

An important consideration in the design of any multi-user communication system is the ability to assess the performance of the operating system. The ultimate performance criterion is that all users are completely satisfied with the service they receive. For a large multiple user multi-service, the cost of a system that meets this criterion is prohibitive. Consequently, the system is designed to give certain prescribed traffic handling capabilities that meet most user needs. Thus a performance monitor should indicate if the system is giving the service it was designed to give. The ultimate monitor checks each system and tells whether the service was given properly. For some multi-national communication agencies, even if there were a system to gather all the data on each use, the cost of examining the data would be prohibitive. Thus performance monitoring must be restricted to an assessment of certain gross features of the system, features that are critical to good service (as designed).

With the sharp increases in digital communications that have occurred in the recent past and that are predicted to continue, must of the service requirements can be more easily handled by a time-division multiplex (TDM) system. More specifically, the information to be communicated is presented to the system as a sequence of binary digits. Different users send in their sequences at different rates, almost all of which are slower than the rate at which the system is capable of operating.

The user bit streams are converted to electrical waveforms and multiplexed into different time slots in the main communication channels. Since the electrical waveform is an encoding of binary digital pulses, this system of waveform generation and transmission is called pulse code modulation (PCM). The overall system is referred to by the acronym PCM/TDM. The specific task reported in this study was the investigation of performance monitors for PCM/TDM systems.

3.2 Basic Parameters

The basic operation of any multiplexed communications system is as follows:

First the user (subscriber) requests service so that he may communicate a specific type of information to one or more other users. The request may be for service on a more or less continuing basis (a dedicated line) or on a demand basis (switched service). When the request is granted, the user sends his information to a central office serving the desired receiver. There the information is demultiplexed and converted to information that the receiver can understand. Thus, for any user-to-user system the operation can be broken into two parts. The first problem is that of getting in and out of the system. The second problem is proper operation of the system. In this report, the first of these two problems is not discussed (the multiplexer problem) but major effort has been directed to monitoring system performance.

Once in the system, each message is a sequence of binary digits encoded in an electrical waveform. These waveforms are then sent over links through intermediate stations (nodes, offices) to their ultimate destination. The system will work properly if each link and each node works properly. At the node there are two problems. The first is that of determining where to send each message; (i.e. the routing information for each incoming message must be properly interpreted and responded to by proper transmission). The second is that of keeping up with the traffic flow.

The main trust of this study is the assessment of performance of individual links of a data communication system. The links considered in this study are radio links. That is, the basic digital waveform is used to modulate a radio frequency carrier. This modulated carrier is transmitted to a receiving station that removes the carrier and converts the modulation to a waveform representing a sequence of bits. The index of performance of such a link is the "bit error rate", that is, the percentage of bit errors between the original waveform and the final waveform of each link. Specifications of a reliable digital system require no more than one bit error in 10^7 bits on average. The terminology used for this situation is a "bit error rate less than 10^{-7} or a probability of an error of 10^{-7}".

3.3 Performance Monitoring Initial Considerations

In order to measure bit error rate directly at the

receiver, one must know the transmitted bit stream exactly. Obviously the receiver does not know exactly what is transmitted, for if it did, there would be no need for the transmission.

As stated before the BER is measured and is defined as

(1)

$$BER = \frac{Ne}{N_t} = \frac{Ne}{Bt_o} \qquad (3.3.1)$$

Where, N_e = number of bit errors in a time interval t_o; N_t = total number of transmitted bits in t_o; B = bit rate of the binary source; t_o = measuring time interval, i.e. error counting time.

The BER under a nonoperational (out-of-service) condition is measured with a "Pseudo Random Binary Sequence" (PRBS) generator and a BER analyzer. The BER analyzer compares, on a bit by bit basis, with the demodulated received bits with a stored replica of the transmitted sequence and computes the BER. A large number of commercially available BER analyzers exist on the market. In the above 1 Mb/Sec range the Hewlett Packard HP 1645, the Marconi .8460 and the Tantron BO are some frequently used instruments.

The main problem associated with simple out-of-service BER analysis is that it is not feasible to evaluate the performance of an operating in-service system carrying the unknown digital pulse stream of the customer. On-Line BER monitors make use of "a prior" knowledge of some characteristics of the received signal. The measurement duration and the error rate estimation for a short t_o might also cause a problem. For example, to

evaluate a $P(e) = 10^{-9}$ for a 1 Mb/S data stream, assuming that for a meaningful statistical estimate at lease 10 bit errors have to be counted, a measurement interval of $t_o = 10^4$ sec. (approximately 3 hours) is required. However, the measurement duration may have to be limited to less than one second because of some possible system requirements for immediate action (for instance in diversity or protection switching initiators).

On-line (in service) monitoring can be achieved with:

(1) Test sequence interleaving;

(2) Parity check coding;

(3) Code Violation detection;

(4) Psuedo-error detectors.

A brief description of the first three of these test methods follows.

Critical Parameters in the Digital Network

1. Introduction:

There are several parameters critical to the efficient operation of a communication network but they may be divided into two main categories - those of importance to the network user and those important to the network operator.

A typical global communication network is shown in Fig. 3.1 and serves to illustrate the different interests of the user and the operator. The user is interested in the end-to-end performance

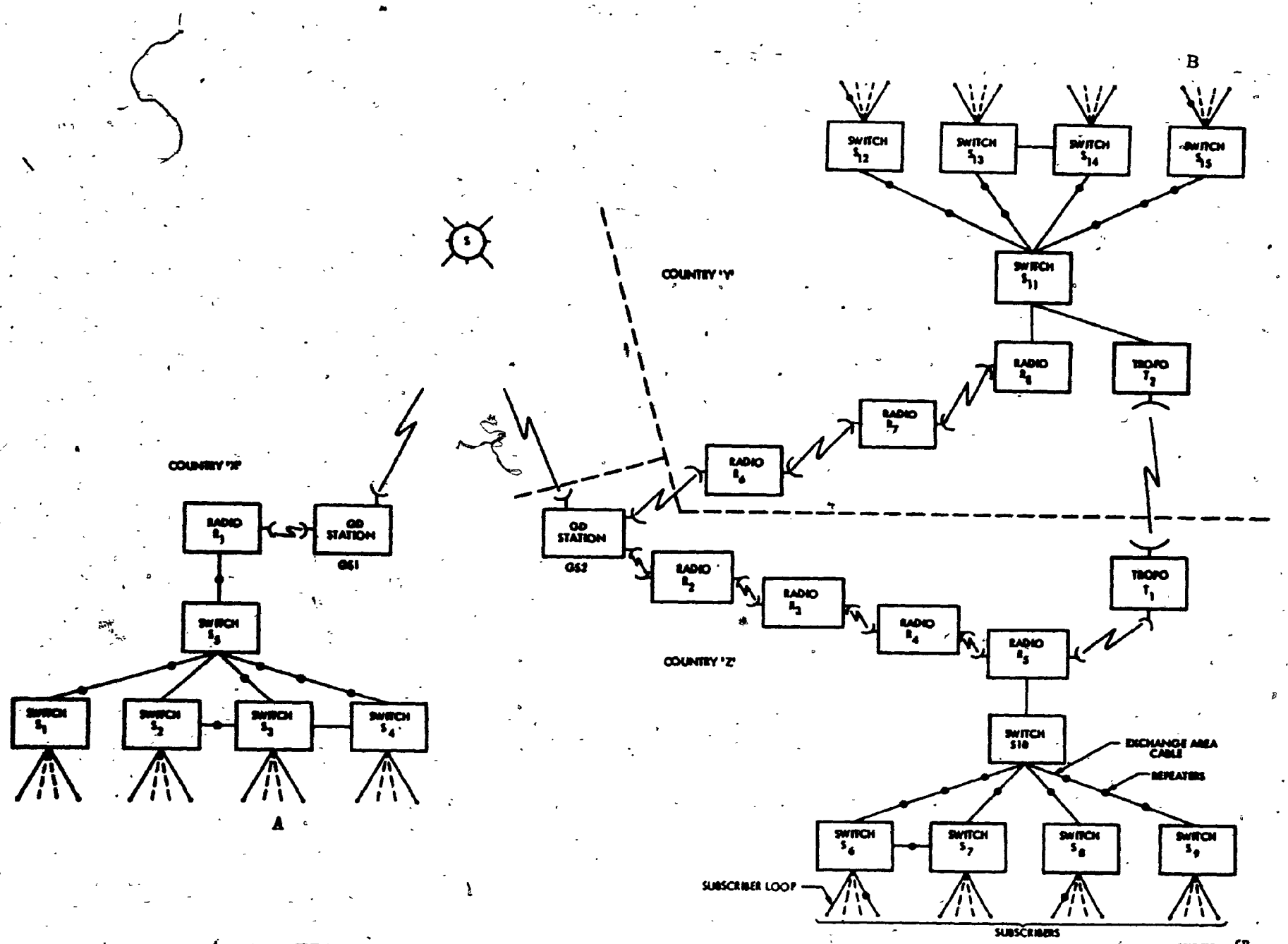

FIG. 3.1 GLOBAL COMMUNICATION SYSTEM MODEL

of such a network, say between A and B in Fig. 3.1; he is not interested in the performance of a particular hop, such as from radio R6 to radio R7, or of an individual piece of equipment such as the receiver in R1, or of the circuit routing. The operators, on the other hand, must consider the performance of each element in the network.

2. User Critical Parameters:

The network user is only interested in whether or not the network will faithfully transmit a message when required. He is, therefore, concerned with two criteria:

(1) Error rate (or digelity);

(2) Availability.

From his point of view the channel may be modelled as shown in Fig. 3.2 for digital transmission. The model envisages three possible receive states:

(a) Correct

(b) Incorrect

(c) Outage, or erasure

In the correct and incorrect states a bit is correctly or incorrectly detected whereas in the outage state the bit is lost entirely. Bits in the first two states reflect fidelity while

those in the third state reflect availability relative to the other two states. Voice equivalent definitions of these two states are also shown in Fig. 3.2.

FIG. 3.2 DIGITAL CHANNEL USER MODEL

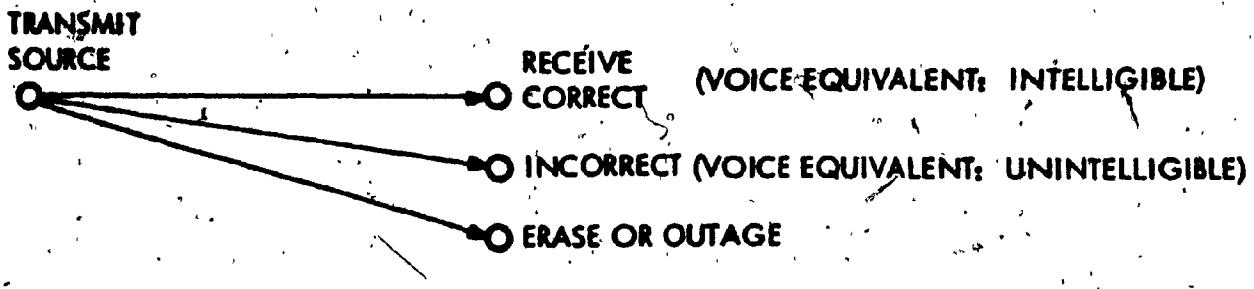

Error rate (number of incorrect bits over the sum of all bits) and availability (up time over total time) are the traditionally used measures of quality, but higher order statistics are also required. The latter include the probability distribution of error burst layers and down time.

a) Fidelity:

Fidelity is the end-to-end error rate but it is more than simply the average error rate (incorrect bits over total bits received) and must include various error burst or conditional error effects. Thus, given that the previous bits were incorrectly detected, the probability that the next bit will be incorrectly detected is also required. These various error statistics are of importance since different messages, modulation, and coding techniques differ in their ruggedness to various types of interference and error statistics. Thus, error correcting codes may be used to correct certain types of error.

b) Availability:

The error rate refers to brief failures of a system but availability refers to large outages. The classis definition of availability is:

$$A = \text{Up time/Total time}$$

but this gives no consideration to the lengths and frequency of

outages or to their time of occurrence which are important for some messages.

Operator Critical Parameters:

The above-mentioned performance parameters are also important to the network operator as they measure how well he is operating and maintaining the network and, hence, meeting his service obligations. These end-to-end parameters do not however assist in isolating faults in the network and for this many more parameters must be used and applied to elements in the network. A major disadvantage of digital transmission is that, unless an error is caused, degradation information is lost at each regenerative repeater. Errors causing recognizable code format violations are the only exception to this but even if in this case it is only possible to say that the degradation was large enough to cause the error. For example, if the signal received at a regenerative repeater is very close to its decision threshold, no indication will be evident at the receiving end, since the repeater will transmit a clean signal as shown in Fig. 3.3. Because of this phenomenon performance monitoring is required at each repeater. This monitoring capability will take two forms: One will be a qualitative monitor forming part of each repeater so that when an alarm threshold is exceeded an interrupt is generated which, in turn, initiates a more detailed qualtitative test performed by a processor via order wires at a remote location.

A digital transmission system may be considered to consist

FIG. 3.3 LOSS OF DEGRADATION INFORMATION IN A DIGITAL TRANSMISSION SYSTEM

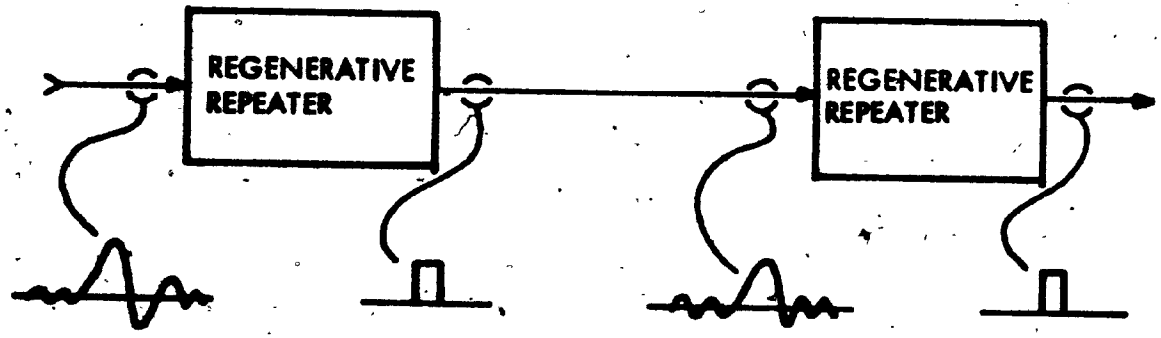

of up to three major groups of equipment: Multiplex, repeaters, and transmission media. Several important parameters should be monitored within each of these groups; these indicate, either directly or indirectly, the equipment's ability to provide reliable service.

(a) Multiplex Performance

i) Bit Error Rate: The easiest technique for monitoring multiplex (mux) BER is to compare the multiplex input and output. This quickly detects multiplex failure, but the BER introduced by the multiplex must be small - say, on order 10^{-11}.

ii) Phase Jitter: This is generated in every multiplex because staff and housekeeping bits are inserted with the bit stream at the transmitter and removed at the receiver. Fortunately, buffer memories in the mux receiver can be used to reduce jitter. The accumulation of low frequency jitter does, however, limit the number of mux's in tandum.

iii) Bit Integrity:

1) Loss of Sequence: Large noise-bursts such as lightening or jamming may cause a large block of errors and result in the loss of frame synchronization (synch). In most cases loss of frame synch in a higher order mux receiver will result in a loss of frame synch in all lower order mux receivers and in the PCM channel bank.

2) Stiff Indication Bit Errors: If the mux receiver incorrectly interprets a stiff indication signal because of an error in transmission, the output will contain one more or one less time slot which will upset the frame synch. The probability of such an occurrence is greatly reduced by using multi-bit codes for pulse stuffing; this allows errors to be corrected and the margin to be monitored.

3) Input Signal Quality: The input signal to a multiplex I/O BER monitor can be used to monitor the input signal quality; checks should include signal presence, level, and quality.

(b) Repeater Performance

i) Transmit: Four important transmit parameters should be monitored as follows:

1) Signal Level: The output power level should be above an alarm threshold set to ensure an adequate signal at the next repeater, and a warning level above the alarm threshold should also be provided for margin. In some equipment the output degrades with a steady trajectory, and in such cases the output level trajectory can be used for "*trend predictions*". (Fig. 3.4 and T - 3.1).

2) Output Waveshape: This is critical to

FIG. 3.4 **TREND PREDICTION**

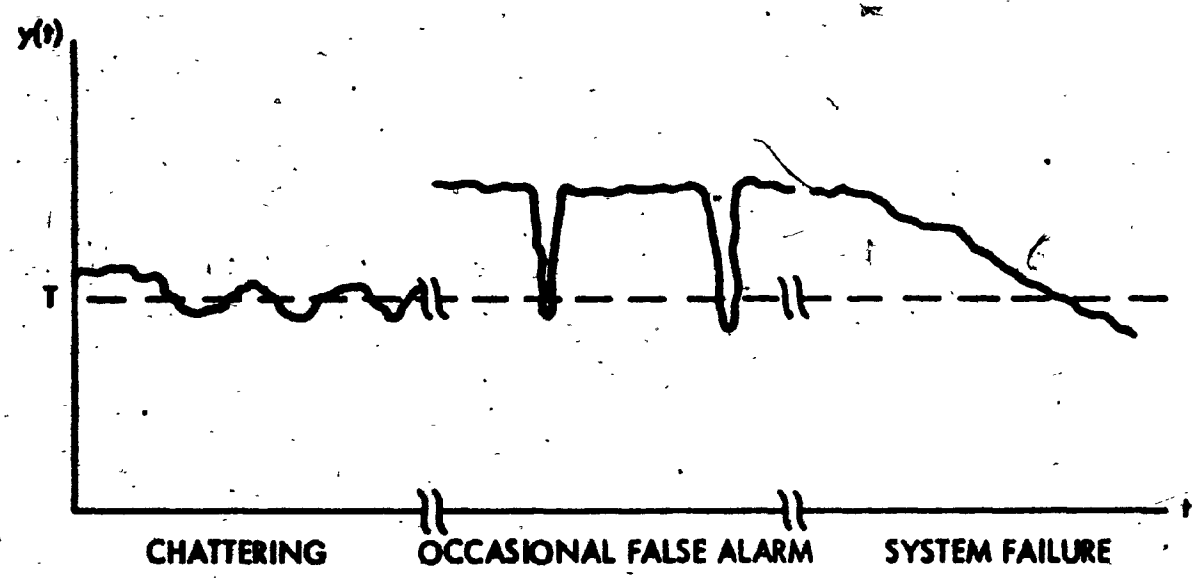

TABLE 3.1

TREND PREDICTION

FUNCTIONAL EXTRAPOLATION

$$X(t) = T(t) + S(t) + N(t)$$

TREND: $T(t) = a_0 + a_1 t + a_2 t^2 + \ldots$

CYCLIC FUNCTION: $S(t) = \sum_n a_n \cos n\omega t + b_n \sin n\omega t$

RANDOM FUNCTION: $N(t)$

transmission through a band limited channel and for low error rate detection at the next repeater. The measurement could be made in the time or frequency domains, but considering the limited alphabet time domain measurements would likely be most easily implemented.

3) Phase Jitter: Repeaters are the major cause of jitter which increases with the number of repeaters. It may be reduced by inserting a dijitterizer.

4) Error Rate: The errors produced by a repeater after detection must be small. The size of the error rate depends on the number of repeaters, for long-Band Systems the actual size of the error rate may typically be 10^{-12}. A bit by bit comparison is possible but is usually not required since the monitoring of other items effectively detects faults.

ii) Receiver: Any detection errors in the receiver are locked into the bit stream and consequently an estimate of receiver probability of error is of paramount importance. Even with correct detection any line degradations are sorted in the regeneration process, so estimates of both quality and error rate are required. Input signal parameters which should be monitored are as follows:

1) Signal Level: The signal plus noise

FIG. 3.5 ADAPTIVE CHANNEL ESTIMATOR

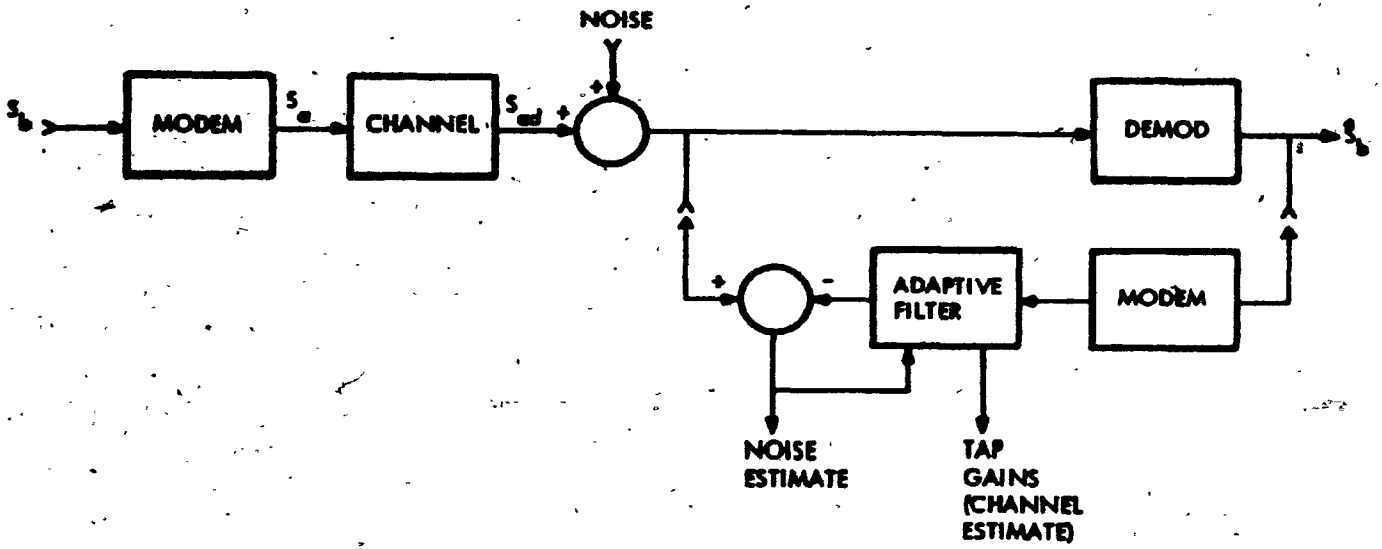

FIG. 3.6 TAP GAIN - FOURIER TRANSFORM RELATIONSHIP

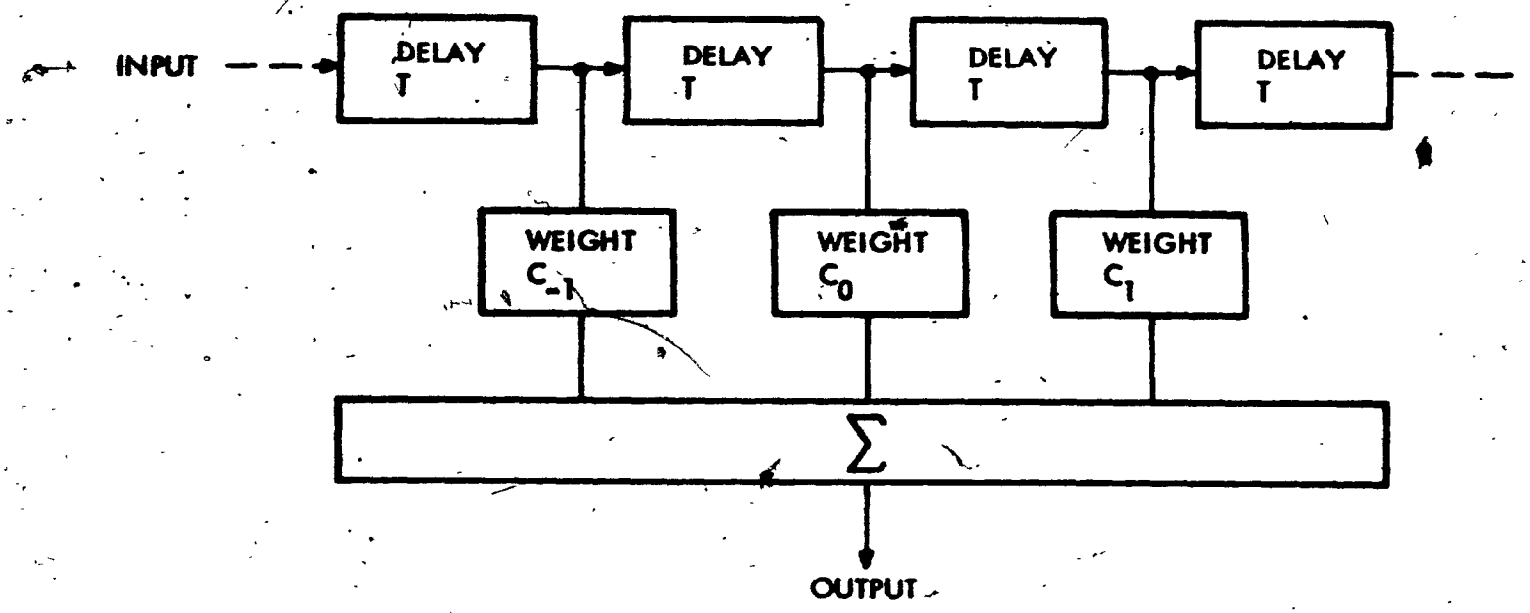

FILTER IMPULSE RESPONSE

$$h(t) = \sum_{n=-N}^{N} C_n \, \delta (t - nT)$$

FILTER FREQUENCY RESPONSE

$$H(\omega) = \sum_{n=-N}^{N} C_n e^{-jn\omega T}$$

THIS EQUATION IS PERIODIC (IN FREQUENCY) WITH PERIOD $f_0 = 1/T$

FIG. 3.7 BASEBAND PERFORMANCE OF ADAPTIVE CHANNEL ESTIMATOR

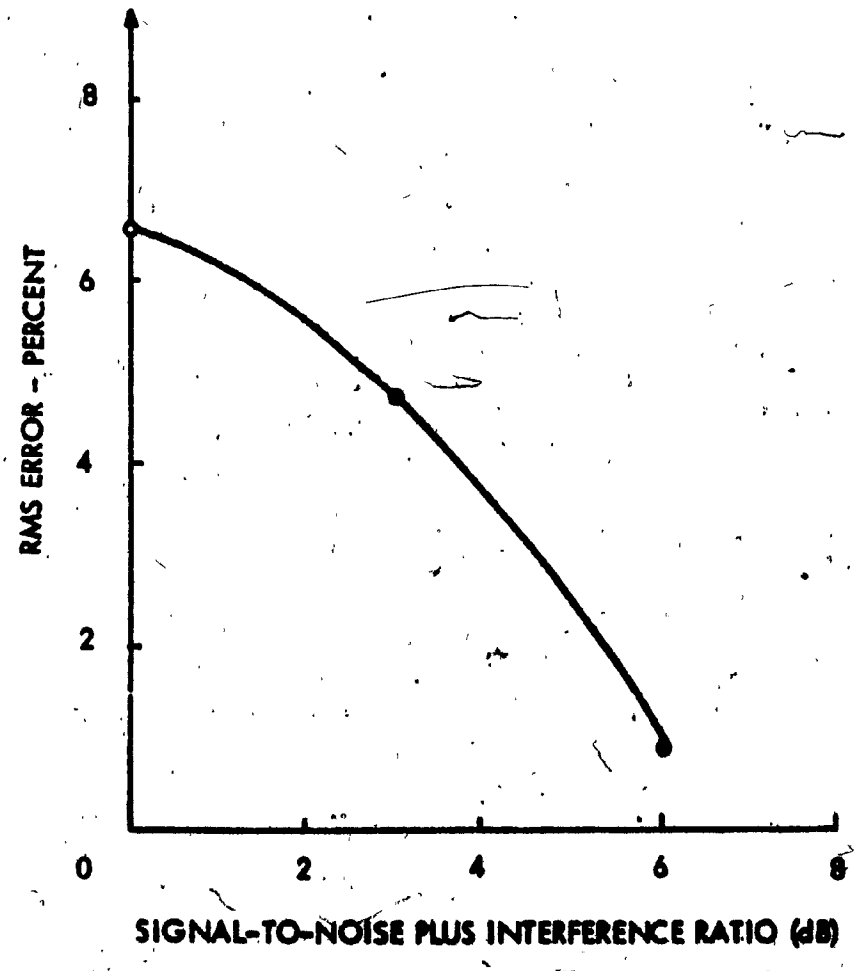

FIG. 3.8 RESPONSE OF ADAPTIVE CHANNEL ESTIMATOR

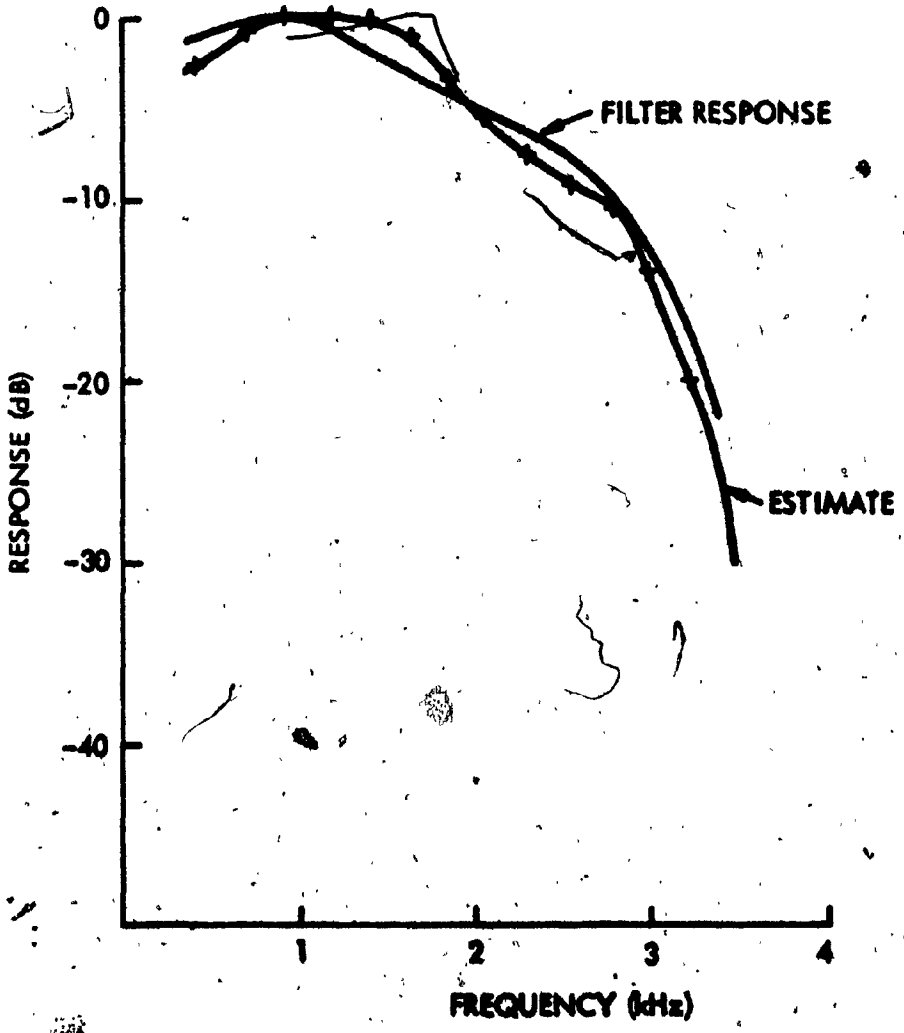

level is easily monitored, and under normal operating conditions this is sufficient. When it is insufficient, other measurements will indicate the high noise situation.

2) Distortion: Signal distortion is more difficult to monitor but "*adaptive channel estimator*" (Fig. 3.5 - 3.8) techniques are available to estimate the channel impulse or frequency response.

3) Noise: Noise may be monitored by two techniques. An out-of-band slot measurement is simple but has the disadvantage that the noise monitored is not that interfering with the signal. In-band noise can be measured with a device which separates the signal from the noise such as an adaptive channel estimator; once separated, the noise statistics can be analyzed.

4) Implementation: Detailed analysis of the signal received at each repeater is complex and costly. Consequently, a simple estimate of signal quality at each repeater is useful. This qualitative estimator will generate an interrupt if the alarm threshold is exceeded, and a more detailed estimate can then be made. The qualitative estimate should include the effects of received signal plus noise, noise impulses, and an estimate of distortion. Suitable techniques in this case are the psuedo-error eye pattern and DERE techniques. This qualitative

estimator could be a microprocessor which is economical to have at each repeater.

(c) Pressure Alarms

Cables and waveguides are pressurized to keep moisture out of them. Monitoring this pressure is useful because moisture can cause degradation, and also because low pressure indicates a break in the cable or waveguide. Hence, the pressure alarm is also a fault isolation device. Systems have been developed enabling the use of cable pressure to accurately locate breaks in buried cable.

4. Miscellaneous Parameters:

Parameters which do not directly affect communication system performance are included in this category. They do, however, have a long-term effect on general network performance.

(a) Configuration and Routing

The complete network configuration should be known at all times for technical control; this includes the general circuit configuration and the status of all equipment in the circuit. The availability of the standby equipment is an example of this. This information can be obtained by monitoring the position of the various switches which set up circuit and control standby equipment. Missage routing of each packet is of little importance to technical control due to the dynamic

nature of packet networks.

3.4 Error Rate Estimation by Counting Test Sequence Interleaving

At the transmitter of the digital radio-relay terminal, sample pulses are inserted into the information pulse stream at the rate of 1/N (N an integer number) times the clock rate as shown in Fig. 3.9. Conversely, at the receiver of the next relay, the sample pulses are extracted and their errors are counted.

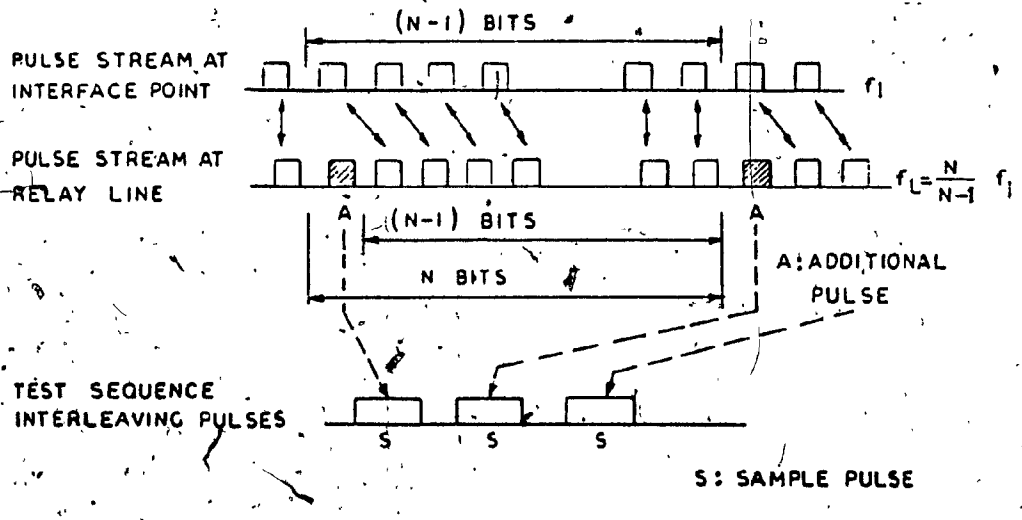

FIG. 3.9 TRANSFORMATION OF DIGITAL SIGNAL STRUCTURE BY ADDITIONAL PULSE INSERTION

The error rate of the on-line system is estimated from the count of sample pulse errors. In this method, the time taken to recognize a specific error rate condition is about N-times that required by counting the errors in all the transmitted pulses, such

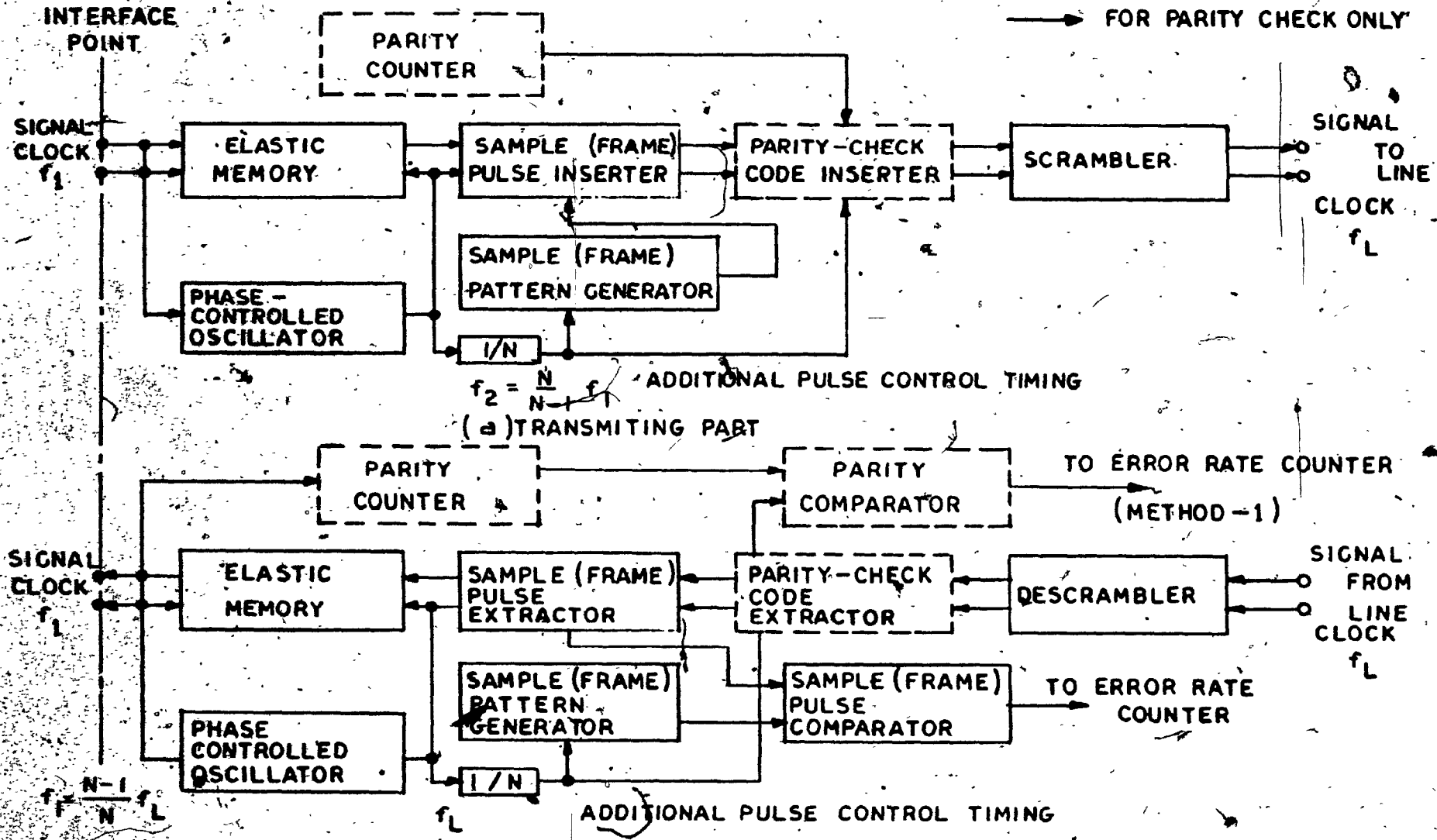

FIG. 3.10 RADIO-RELAY TERMINAL CIRCUIT DIAGRAM FOR ERROR RATE ESTIMATION

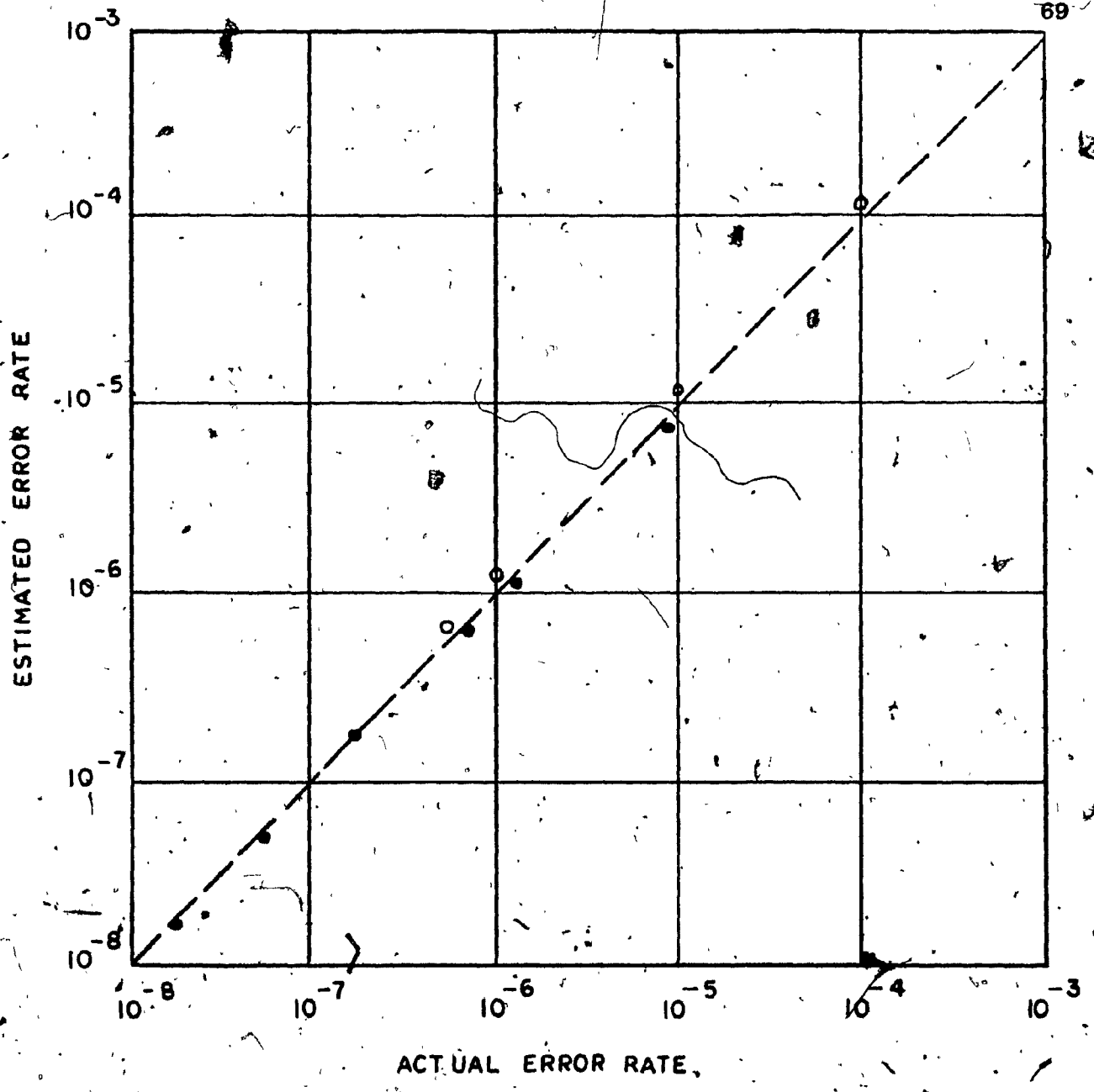

FIG. 3.11 COMPARISON OF ACTUAL AND ESTIMATED ERROR RATE, MEASURED IN EXPERIMENTAL SYSTEMS

as in non-operational (out-of-service) BER measurement.

The pulse repetition (clock) frequency of the digital signal is converted on transmission using a phase-controlled oscillator (Fig. 3.10), from f_1 to $f_1N/(N-1)$ or vice versa on receipt of the signal when the sample pulses are extracted. The data scrambler, shown in Fig. 3.10, enables transmission of pseudo-random binary sequence signals, even if there is neither signal nor clock-timing at the interface point of the transmitting terminal.

Fig. 3.11 shows the test results of this error rate estimation method when applied to the experimental 20 GHz 200Mb/Sec QPSK (400 Mb/Sec) transmission system { Ref. 5 }. In this experimental system, for example, an error rate of 10^{-4} is recognized by counting 8 bit errors in the sample pulses in about t_o = 100 m sec for parameter values of N = 511 bits and f_1 = 200 MHZ.

3.5 Error Rate Estimation by Using Parity-check Coding

At the transmitting part of the radio-relay terminal, marks (symbol) in the inerface digital signal are counted, and the number of marks in each frame, Fig. 3.12 is translated into an r-bits (modulo 2) parity-check code.

The parity-check codes and frame pulses are then additionally inserted into the digital signal, as shown in Fig. 3.12. Conversely, at the receiver, these additional pulses are extracted and each extracted parity-check code is compared with the one generated in the same manner at the transmitting terminal, as shown in Fig. 3.10.

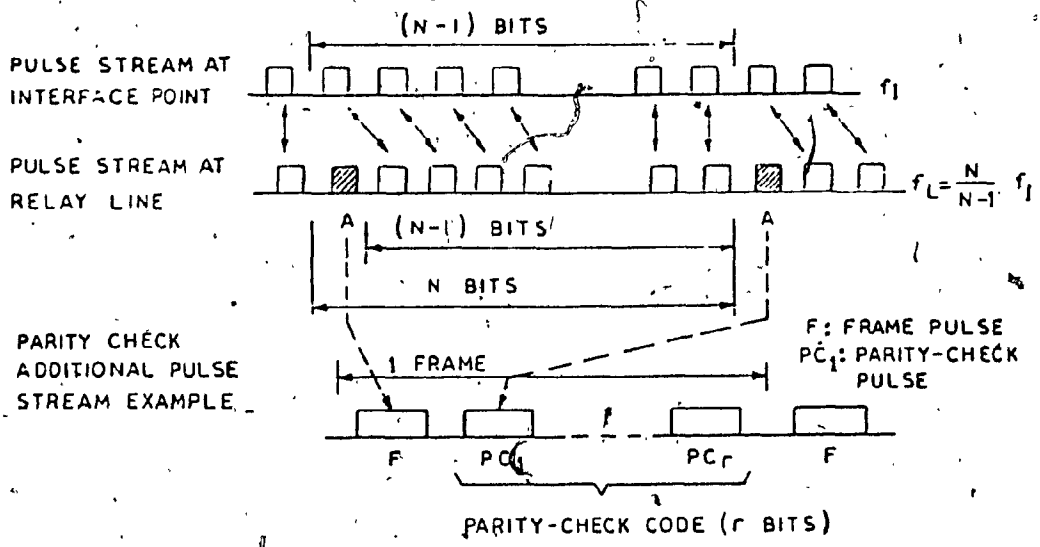

FIG. 3.12 TRANSFORMATION OF DIGITAL SIGNAL STRUCTURE BY ADDING PARITY CHECK PULSE

For a small error rate (below about 10^{-3}, for example), the number of deviations in the parity-check code comparison is approximately equal to the total number of errors in all the pulses in the digital signal. Therefore, the error rate of the radio-relay circuit is estimated by counting the number of deviations in the parity-code comparison as if it was measured by counting the errors in all the transmitted pulses.

Fig. 3.11 shows the test results of this error rate estimation method applied to the experimental 400 MB/Sec 4-QPSK (800 Mb/Sec) guided-millimeter-wave transmission system {Ref. 6}. In this experimental system, an error rate of 10^{-6} is recognized by counting 8 bit deviations in parity-check codes in about 10 m sec for parameters values of N = 256 bits, r = 2 bits (module 4) and f_1 = 400 MHZ.

3.6 Disadvantages of Sequence Interleaving and Parity-check Coding

As stated before one could make spot tests on bit error rate by interrupting the information flow every so often to transmit a test pattern of bits (sequence interleaving). This method is not very practical with bit error rates of 10^{-7} or less. Since a ten million bit test pattern would be required to obtain one error on the average, thus, a prohibitively long test pattern would be required to obtain a statistically significant measure of the error rate.

The second approach was to monitor the error rate by encoding the bits in error detecting code. The simplest such code is the addition of a parity-check bit after every N^{th} bit. By checking parity codes the receiver can detect if there was an odd number of errors in the proceeding (N-1) bits. If a parity-check is the only error detection scheme for a system operating at a bit error rate of 10^{-7}, a long time elapses between errors. If the system should degrade to a bit error rate of 10^{-6}, direct measure of parity errors are not sufficiently fast to be of use as indications of trouble.

Even if all errors were detected it would take several hundred million bits to obtain a reliable measure of degradation at 10^{-6}. This means that a large quantity of information would flow through the system with an unacceptable error rate before the monitor would indicate trouble.

For a system operating at a normal rate of 10^{-7} or less one should develop a degradation measurement system which reports trouble even though no errors have yet been made. This monitor should have an output that is monotonic with the bit error rate and sufficiently sensitive to give a reasonable indication of error rate changes near the normal range of system operation.

3.7 Code Violation Detection

Some signaling codes are intrinsically redundant. This intrinsic redundancy can be used very efficiently to detect line errors in a very short time. Bipolar codes and duobinary partial response coding have this property statics. Bipolar coding and its use in bit error rate monitoring was discussed in Chapter 1. The partial response technique has been used to allow channel "memory" to span over bit-time intervals. The technique was investigated and classified into 5 classes according to the features of channel "memory". Partial response signaling has been intensively studied and applied to practical data transmission for both low-speed and high-speed signal rates.

The partial response signal format, implemented by a digital low-pass filter, is shown in Fig. 3.13. Observing the waveform in

the figure the properties of a 3-level Class 1 partial response can be summarized as follows:

(1) The output of the decoder is 0 if the partial response waveform was at a top peak.

(2) The output is the opposite of the preceding bit if the partial waveform was at a middle level.

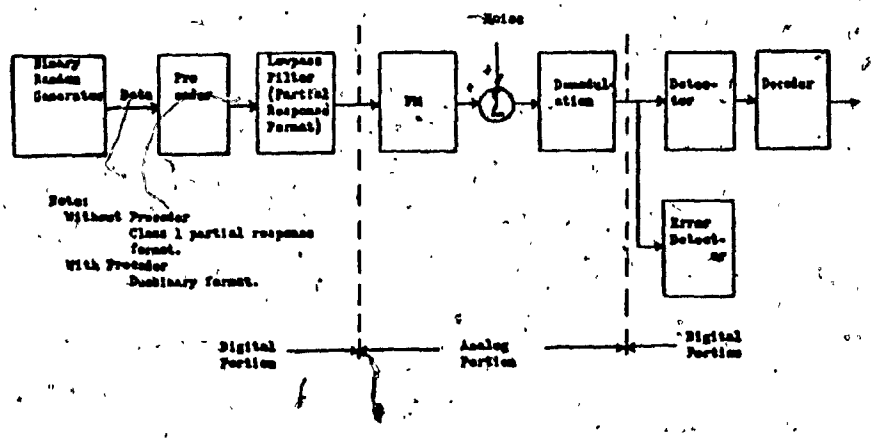

FIG. 3.13 BLOCK DIAGRAM OF HYBRID DUOBINARY PARTIAL RESPONSE TRANSMISSION SYSTEM WITH ERROR DETECTION SCHEME

In addition to these detection features there is an important format which can be used for detecting errors in the received signal. To describe the signal format a closely related coding, called Duobinary by A. Lender, will be introduced here.

Duobinary is simply formed by one extra encoding before the partial response process which can be expressed as $b_n = A_n \oplus A_{n-1}$ ($\oplus$ Modulo 2 addition).

The relationship between Class 1 partial response and duobinary is also shown in Fig. 3.14. Some interesting properties of duobinary can be stated as follows:

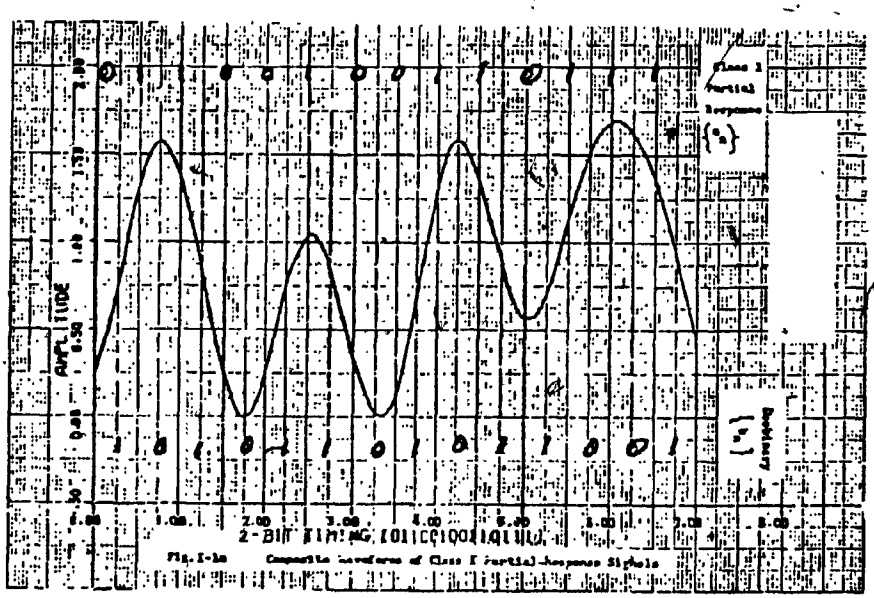

FIG. 3 14 COMPOSITE WAVEFORMS OF CLASS 1 PARTIAL RESPONSE SIGNALS

(1) Top and bottom peaks are for 0's while the middle levels are for 1's.

(2) Adjacent top (or bottom) peaks are separated by an odd number of 1's.

Composite wave forms as Class 1 Duobinary Partial Response Signaling and the associated eye pattern are shown in Figs. 3.14 and 3.15 respectively.

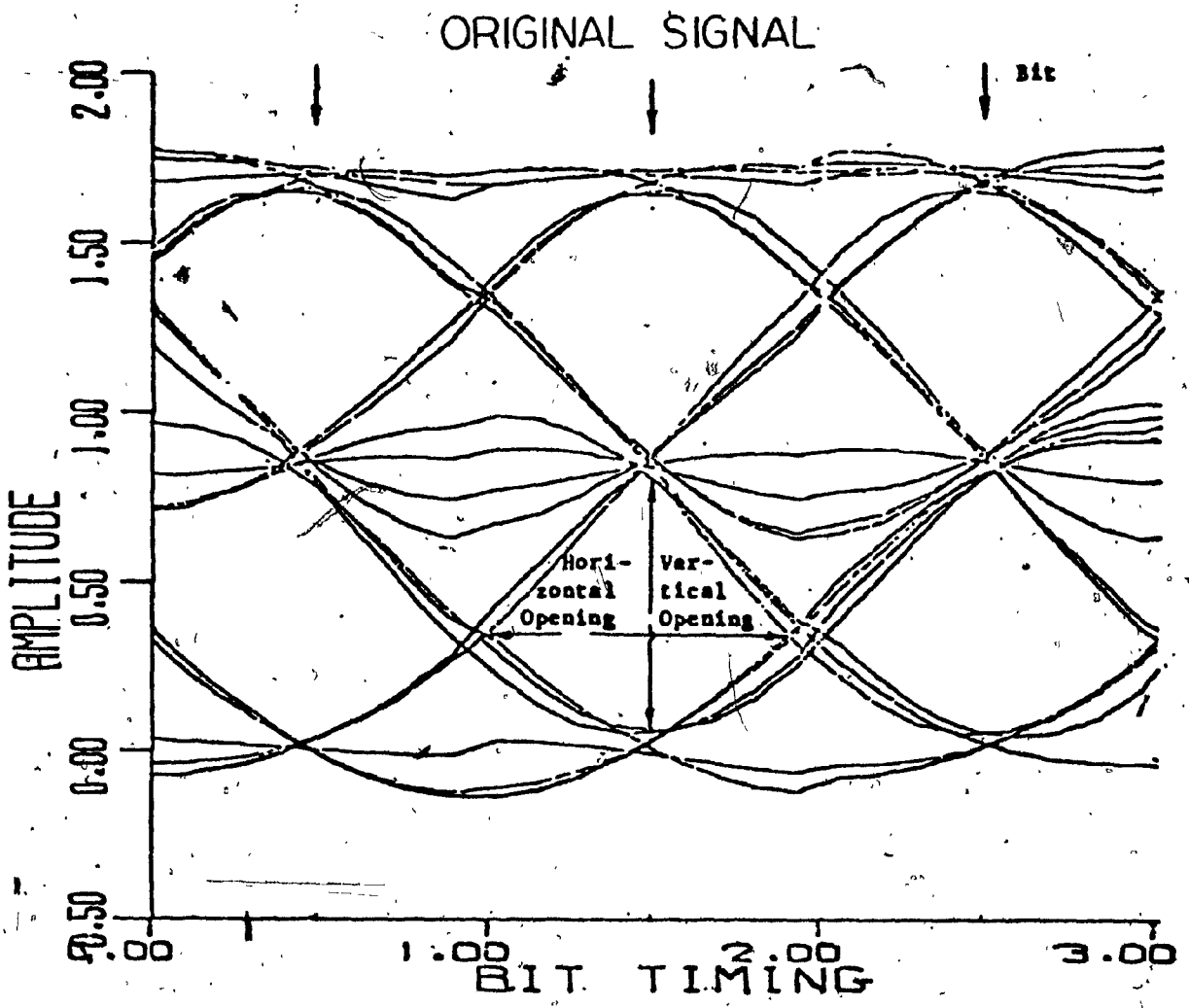

FIG. 3.15 PARTIAL RESPONSE SIGNAL EYE-PATTERN

3.8 Pseudoerror Fundamentals

This study will cover the operating principle of a Pseudo-error Monitor and also mathematical methods of synthesis for such monitors. The operating principle described here was originally given by Gooding {Ref. 7} and followed by J. Leon et al {Ref. 8}, and is extensively utilized in data communication networks. Past approaches to monitoring have included substantial emphasis on monitoring specific variables, such as the Signal-to-Noise Ratio and Insertion Loss. This approach is however better suited to analog than the digital system monitoring.

For digital systems, some means of monitoring bit error rate, which is a key variable, is desirable. Several of the methods described previously could be used to obtain an accurate bit error rate estimate at a receiver but they have the disadvantages of long evaluation time and interruption of the data traffic.

This study is concerned with the problem of monitoring methods based on a pseudoerror technique which avoids both of the disadvantages noted above. The method is based on an extrapolation technique using "pseudoerror" as defined by Gooding {Ref. 7 } for use in estimating error rates for adaptive FSK and PSK receivers operating over fading channels. Some statistical aspects of the method have been studied previously by Weinstein {Ref. 9 }

In an extension of Gooding's work, Leon { Ref. 8 } relates values of monitor variables, based on pseudoerror, to true bit error rates for general types of failure.

This study was intended to provide information on which to

computing P(e) and P(p) from Eq. (3.11.6) to (3.11.13) under a variety of conditions. Results were obtained for binary and quarternary, differential and coherent PSK systems.

Fig. 3.1 gives $f_\alpha(\alpha)$ for extreme conditions of CNR and CIR. The intent of these curves is to show the range of possible shapes for these density functions. Also indicated on the curves are the decision boundaries and typical boundaries for pseudoerror. Figs. 3.18 and 3.19 give P(e) and P(p) versus CNR for typical values of CIR. Fig. 3.18 applied for coherent and Fig. 3.19 for differential PSK. Note that for fixed CIR the P(p) and P(e) curves are essentially parallel for high CNR. The effect of the offset angle δ and P(p) is shown in Fig. 3.20 for quadriphase coherent PSK. The results are typical of the other cases studied. Curves of P(p) versus P(e) for fixed CIR are given in Fig. 3.21.

Contour plots of constant P(p) and P(e) as a function of CIR and CNR are given in Fig. 3.22.

Monte Carlo Study

A Nippon Electric Company QPSK receiver {Ref. 11}, shown schematically in Fig. 3.23 was modelled for a Monte Carlo type simulation study. The angle of the received signal was computed as a function of time so that a simulated on-line calculation of pseudoerror could be carried out. Values of δ equal to 10, 14, 18, 22, 26, 30, 34 and 38 degrees were used in the simulation.

A Monte Carlo simulation has the potential of incorporating any number of effects including nonlinearities. For the present

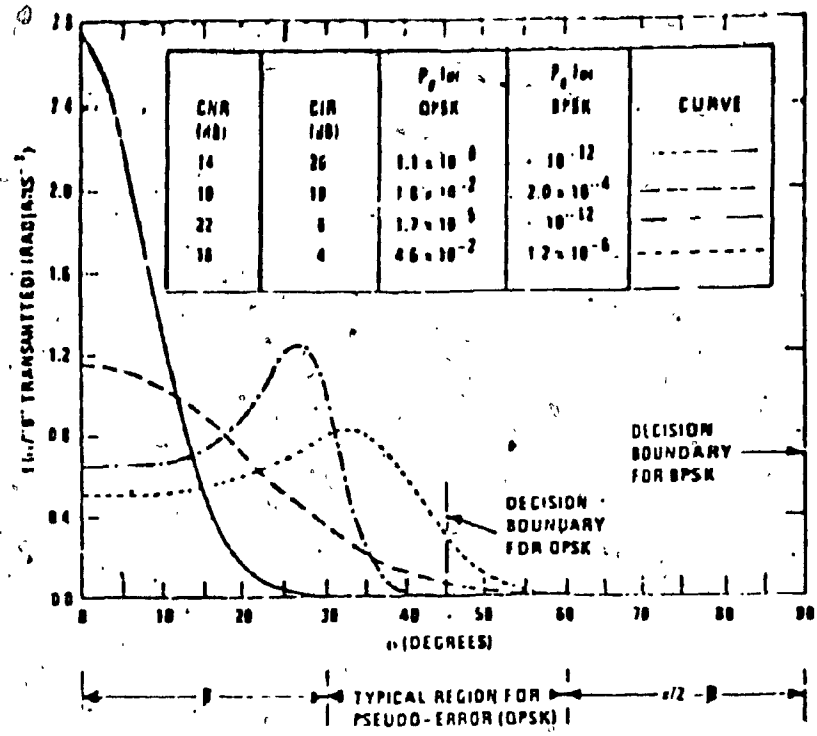

FIG. 3.17 REPRESENTATIVE PROBABILITY DENSITY FUNCTIONS FOR α WITH CNR AND CIR AS PARAMETERS

	CIR (dB)	β (°)	SYMBOL P_e	SYMBOL P_p
QPSK	8	35		■
	8		□	
	17	35		▲
	12		△	
BPSK	18	68		●
	18		○	
	38	68		▼
	38		▽	

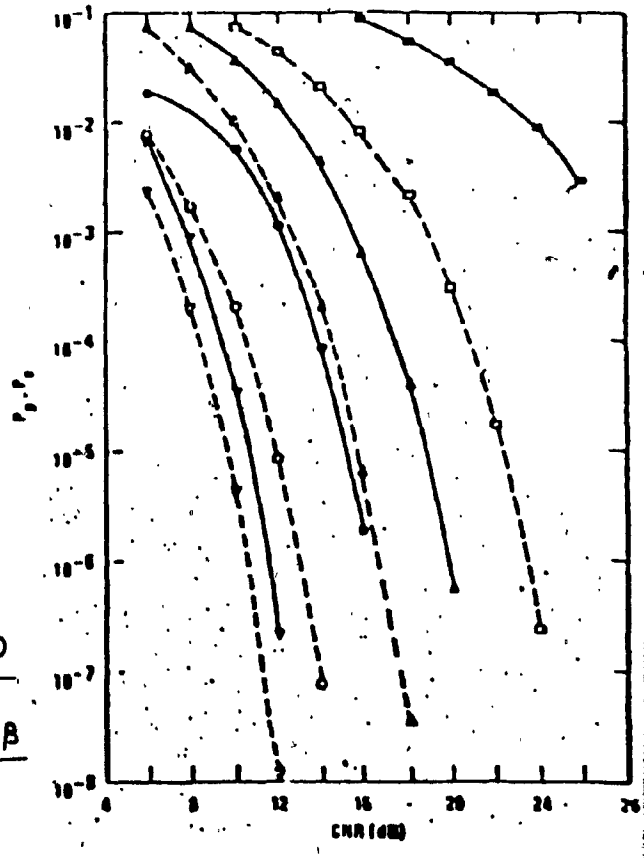

FIG. 3.18 P_e AND P_p COHERENT QPSK AND BPSK VERSUS CNR FOR FIXED β AND SEVERAL VALUES OF CIR

	CIR (dB)	β (°)	SYMBOL P_e	SYMBOL P_b
QPSK	18	35		■
	18		□	
	16	35		▲
	16		△	
BPSK	18	68		●
	18		○	
	30	68		▼
	30		▽	

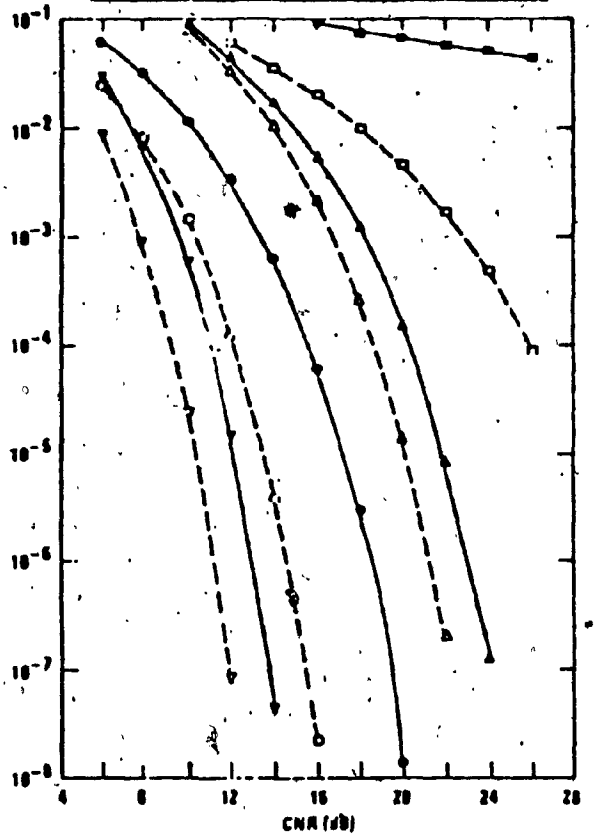

FIG. 3.19 P_e AND P_b FOR DIFFERENTIAL QPSK AND BPSK VERSUS CNR FOR FIXED β AND SEVERAL VALUES OF CIR.

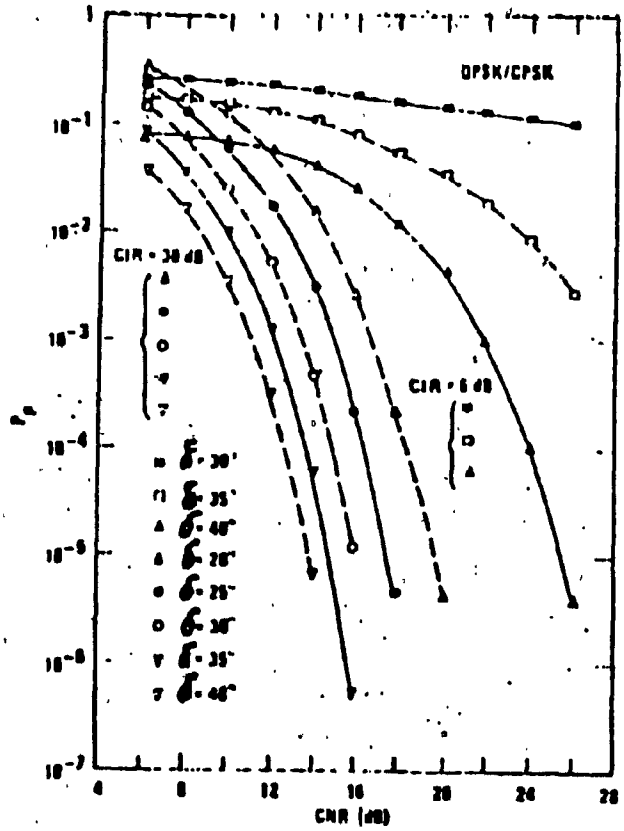

FIG. 3.20 P_b FOR COHERENT QPSK VERSUS CNR FOR SEVERAL VALUES OF δ AND CIR

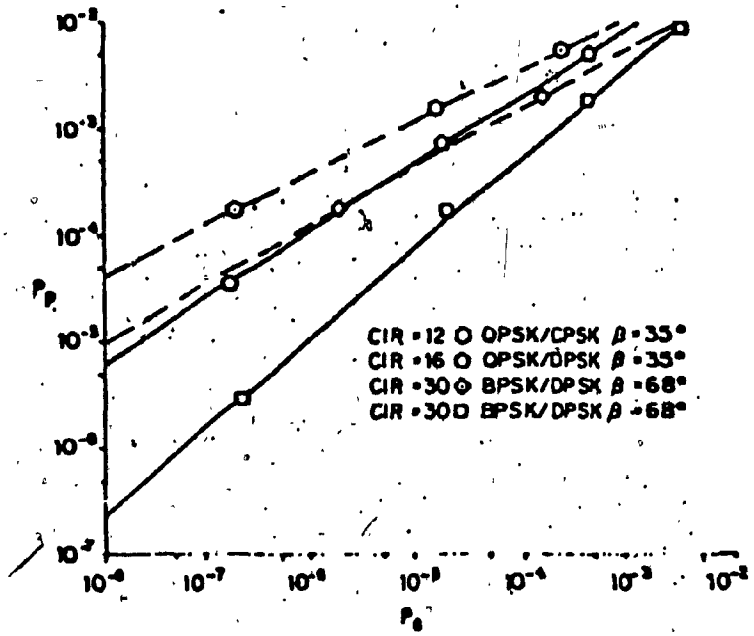

FIG. 3.21. P_e VERSUS P_p FOR COHERENT AND DIFFERENTIAL BPSK AND QPSK

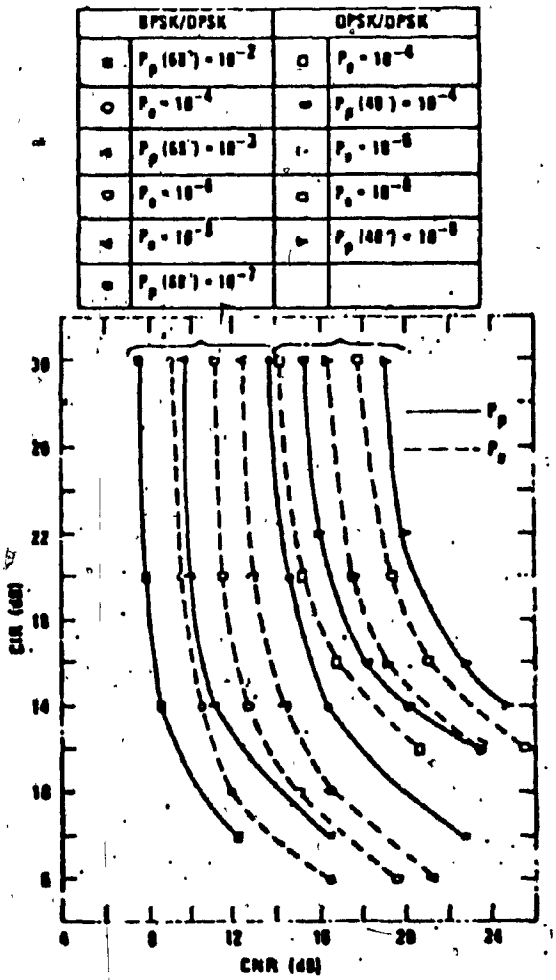

FIG. 3.22 CONSTANT CONTOURS OF P_e AND P_p FOR DIFFERENTIAL BPSK $\delta = 68°$ AND DIFFERENTIAL QPSK WITH $\delta = 40°$

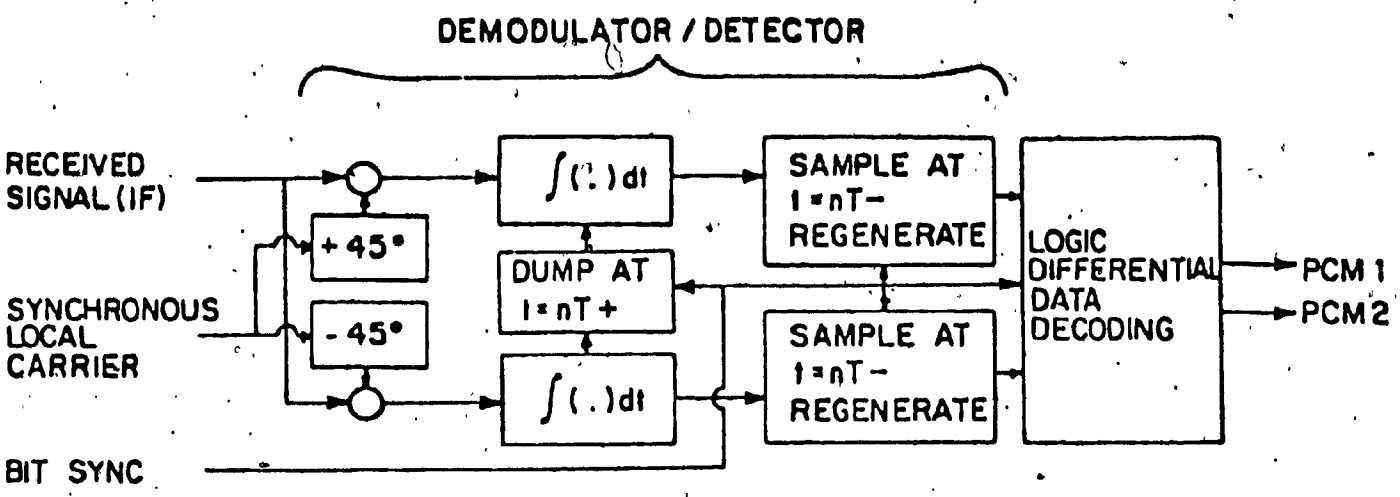

$$\text{IF SIGNAL} = m(t)C\cos(\omega_0 t + \theta) + n(t)$$

FIG. 3.23 NIPPON ELECTRIC COMPANY RECEIVER MODEL

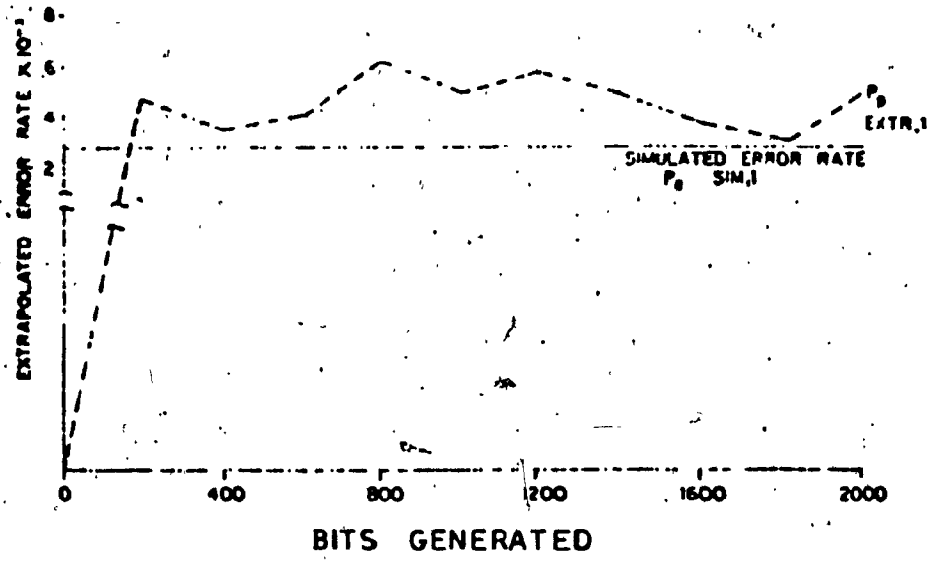

FIG. 3.24 SIMULATED ERROR RATE AND EXTRAPOLATED ERROR RATE (SIM, 1 AND EXTR, 1, RESPECTIVELY) AS A FUNCTION OF TIME WITH NO PHASE JITTER AND A SIGNAL-TO-NOISE RATIO OF 11dB.

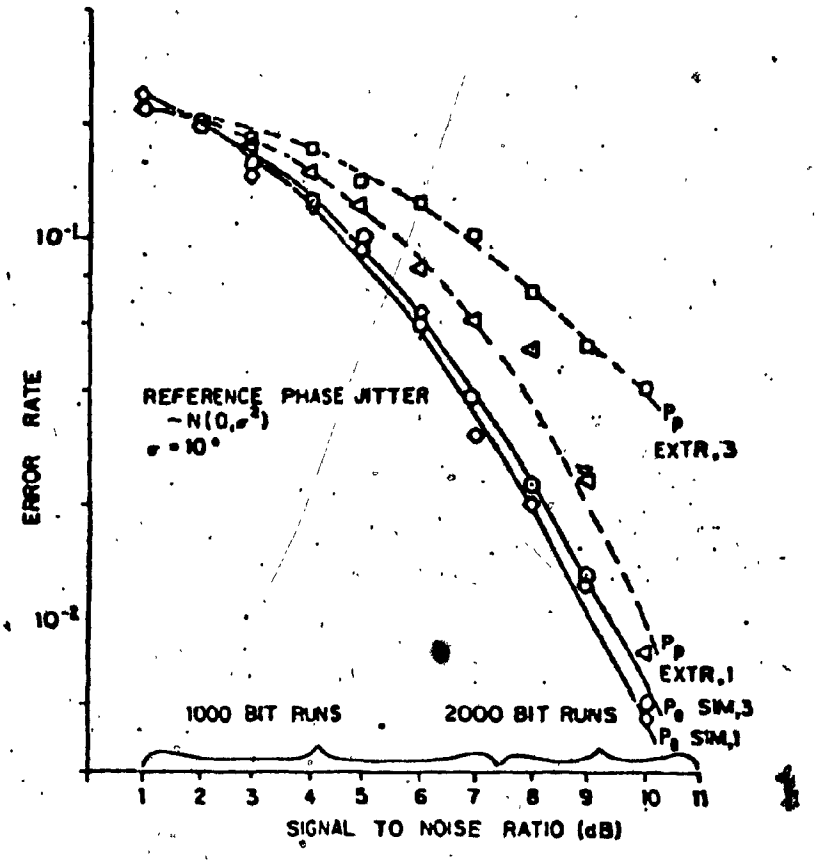

FIG. 3.25 SIMULATED ERROR RATE AND EXTRAPOLATED ERROR RATE AS A FUNCTION OF SIGNAL-TO-NOISE RATIO WITH NO PHASE JITTER (SIM, 1 AND EXTR, 1, RESPECTIVELY) AND WITH GAUSSIAN PHASE JITTER (SIM, 3 AND EXTR, 3, RESPECTIVELY).

study, Gaussian noise, reference phase jitter and frequency offset jitter were used as the sources of degradation.

Generally speaking, it was found that the Monte Carlo simulation program consumed considerable computer time. For each 2000 bits generated, the basic program without jitter offset effects ran for approximately 50 seconds on a CDC 6500 computer. At typical rates for computer time it costs approximately $4000 to locate a single error at error rates of 10^{-6}.

Because of this cost, Monte Carlo simulation studies were not carried out for error rates below 10^{-3}. Studies of P(p) for various values of δ at these error rates and higher were made with Gaussian noise degradation and the results were consistent with those obtained in the analytical-numerical study.

As representative output of the simulation study, Fig.3.24 gives a time history of Gooding's extrapolated estimate of true error rate, while Fig. 3.25 shows extrapolated error rate behaviour versus signal-to-noise ratio with and without phase jitter with true error rate for comparison. Note that the quality of the extrapolated estimate of true error rate is degraded by the presence of phase jitter.

3.12 Conclusions and Evaluation of Extrapolation Monitors

The analytical results as shown in the graphs above can be used as a performance monitor giving a continuous indication of P(e) or a highly quantized indicator. We refer to a continuous indication as a proportional monitor since P(p) is monatonically

related to P(e) for most degradations discussed above. (Gooding's estimate of true error rate could be used as a proportional monitor.) The quantized indicator would be a simple threshold with red and green, or red, yellow, green LED lights. Table 3.2 lists the desirable properties of the two types of indication. In a more recent report [12] the authors discussed the problem of extending the pseudoerror monitor concept to an indicator that constructs a histrogram of the angle of received signals. The simple monitor of this study is adequate for evaluating system performance with a minimum of hardware.

A final comment on hardware implementation of an extrapolation monitor seems appropriate. Three steps seem necessary for implementing any monitoring device based on pseudoerror, namely:

(1) Detection of pseudoerrors as they occur;

(2) estimation of pseudoerror probability by some type of relative frequency calculation; and

(3) calculation of a final monitor output as a function of estimated pseudoerror probability.

Although hardware implementations of the three steps listed above have not been a subject of this study, such implementations are not expected to be complicated or costly. The algorithm used

in the Monte Carlo study can be implemented in a straight forward fashion.

Step 1 requires an offset in the decision threshold of the PSK receiver;
Step 2 requires some sort of counter to indicate the cumulative number of pseudoerrors in a given period of time, and
Step 3 requires an implementation of some fixed functional relation to determine the monitor output.

Gooding [7] and Weinstein [12] both described relatively simple devices for estimating pseudoerror probability.

TABLE 3.2

DESIRABLE PROPERTIES OF MONITOR VARIABLES

Proportional	Quantized
1) Respond rapidly to degradations in system performance.	
2) Produce a detectable indication of all possible system failures and degradations.	
3) Monotone function of true error.	3) Unambiguously divide system states into a fixed set of conditions.
4) Single value function of true error.	4) Provide a margin or advanced indication of a change in condition.

CHAPTER 4

BASEBAND PSEUDOERROR CONCEPTS

4.1 Baseband Transmission

The system configuration for baseband transmission is one without a modulated channel, as shown in Fig. 4.1.

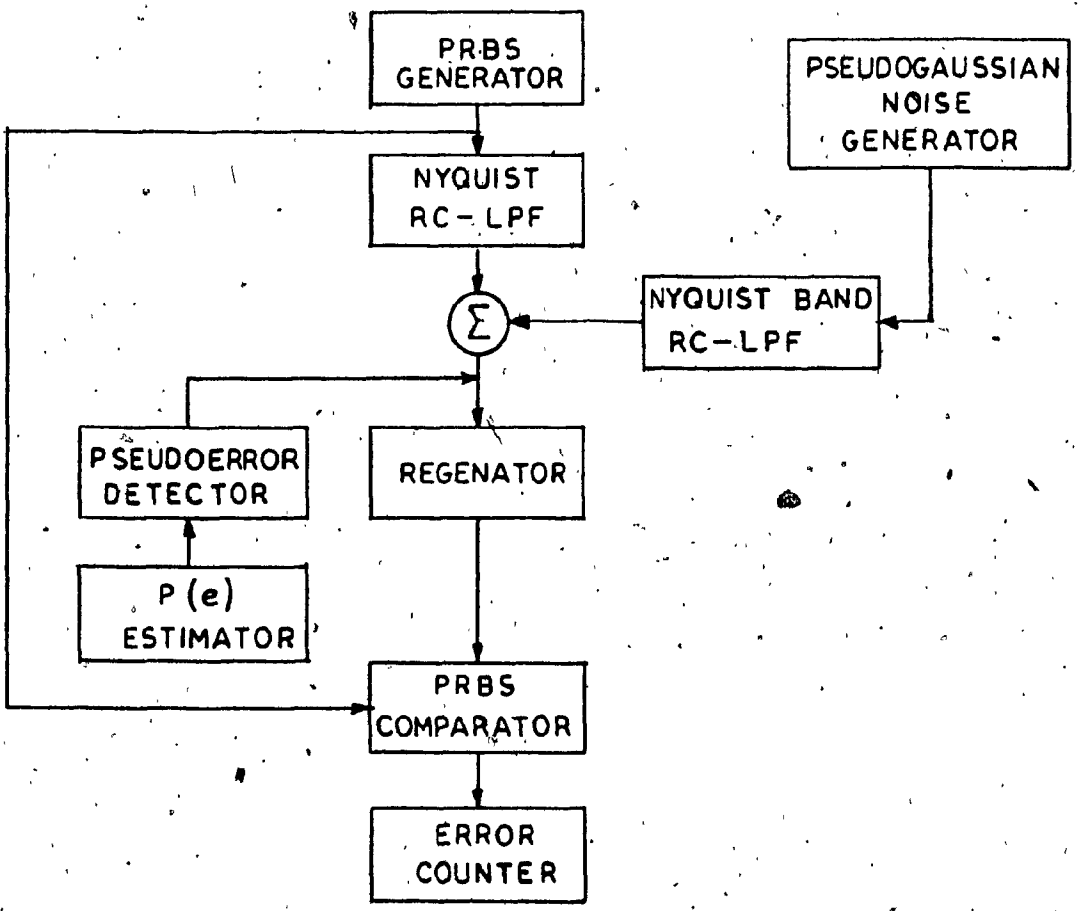

FIG. 4.1 FLOWCHART FOR BASEBAND TRANSMISSION

The baseband signal is mixed with Gaussian noise of Nyquist bandwidth. The Nyquist band filter is approximated by a first-order filter. The error rates of the baseband transmission with this noise for the NRZ signal are given in Fig. 2.6. The experimental error rate is compared with a theoretical error rate, which is derived under an optimum system without intersymbol interference. There is 1.2 db difference between these two error rates. The difference is attributed to the following:

(1) The simulated system is not an optimum system.

(2) The NRZ signal at the subject of the RC-Low-pass filter defenitively has some tails to interfere with the adjacent bits. (Evaluation of the effect of these intersymbol interferences on the error rate is rather difficult.)

(3) The Nyquist Low-pass filter for the noise is approximated by a simple first-order filter.

4.2 Pseudoerror Detector

For the baseband pseudoerror, P(p), detection a "secondary" pseudoerror processor device is connected in parallel with the main data path. The pseudoerror techniques used in parallel path is catagorized as following:

(1) Techniques based on detecting the peak of the composite signal (data plus noise existing within the "Pseudo-Error Zone" (PEZ) of the received baseband signal.

(2) Techniques intentionally increasing the error rate in the secondary (pseudoerror) path by degrading the performance of the latter.

In this chapter the basic concepts of on-line pseudo-error monitoring, and the theory of the various techniques will be presented. A number of pseudoerror implementation techniques, and their measured performance in additive Gaussian noise, non-Gaussian noise, interchannel-interference, and intersymbol interference environments, will be described and analyzed in the following chapters. Experimental results in these interference environments are also presented. The results (obtained using a coherent QPSK 1.544 M bit/S modem) clearly indicate that pseudo-error monitors can be gainfully employed in even more complex interference environments than referred to in the literature.

4.3 Composite Signal Peak Detection in Pseudo-Error Zone (PEZ)

In data transmission, the "eye pattern" has been used as a measure of channel characteristics. The quality of signal can be clearly shown in the eye pattern. Furthermore, proper sample timing (i) and slicing levels (ii) can be easily determined from the eye pattern.

(i) Sample timing is obtained at maximum eye opening.

(ii) Slicing level for AC coupled NRZ eye pattern is the zero crossing level (in this case zero volt).

The basic idea of composite signal peak detection within the PEZ can be understood by considering a simple discrete waveform corrupt by noise. Suppose that the signal waveform is a rectangular wave such that +V volts represents a binary "one" and -V represents a "zero" (AC-coupled NRZ). The binary number 00101 is shown in Fig. 4.2a as a dashed curve. A possible received signal corrupted by noise is shown by the solid curve. Note that in the first logic state, there is a short section where the received signal is actually positive. There are similar "wrong" sections in each of the two succeeding intervals. If the noise has a mean value of zero, the effect of the noise is reduced by averaging. Thus a decision as to whether the signal in a particular interval is a zero or a one is made by integrating the received signal over the interval of time

occupied by one bit. If, at the end of any interval the integrater output is positive, the receiver decides that a one was transmitted. If the integrator output is negative, then it decides a zero was transmitted. The integrator outputs for the signals of Fig. 4.2a, in this case all five bits, would be received correctly by "integrate-and-dump" circuitary.

In the example above it was assumed that the integrator resets at the trailing edge of each bit. Now, if the dumping time was off 20% as shown in Fig. 4.2c, then the signal in the third interval, which should be a one would be detected as a zero. Thus the factors which contribute to errors include both noise and timing errors in the received signal.

When the signal-to-noise ratio is very high and properly conditioned, and the timing is precise, then the detector output at the decision instant (dump or reset instant) will be +V for a "one" and -V for a "zero". The effect of noise, timing errors, and poor signal amplitude conditioning, is to make the outputs ΔV instead of V. The factor Δ represents the effect of noise and can in principle, take on any value. In the case of a timing error $\Delta < 1$, and also in the case of a loss of signal gain, or fading of the signal, when Δ is near zero the system makes an error.

If the transition from proper system operation ($\Delta \sim 1$) to operation with frequent errors ($\Delta << 1$) is a gradual one, then we can detect errors by observing the values of Δ. For each error detection there is a distinct Δ value. When there are essentially no errors, the values of Δ will always be bounded well away from zero. When there are many errors, there will be even more cases where Δ is near zero.

We assume that noise conditions that make Δ very negative are extremely rare.

The monitor scheme investigated in detail in the subsequent sections of this report was set to a threshold value of Δ, say $\Delta = 0.5$ as shown in Figs. 4.3a and 4.3b. Whenever Δ is less than this threshold, we say a pseudoerror has occurred. Heuristically this pseudoerror rate is greater than the error rate and monotonically related to the actual error rate.

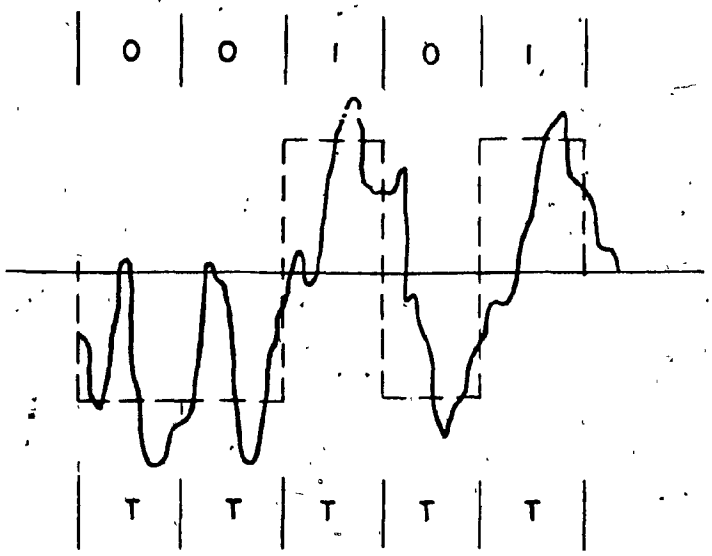

FIG. 4.2a SIGNAL OF 00101

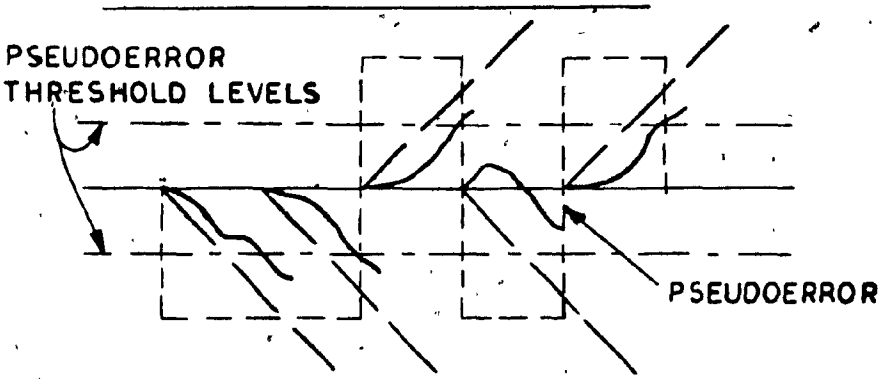

FIG. 4.2b DETECTOR OUTPUT

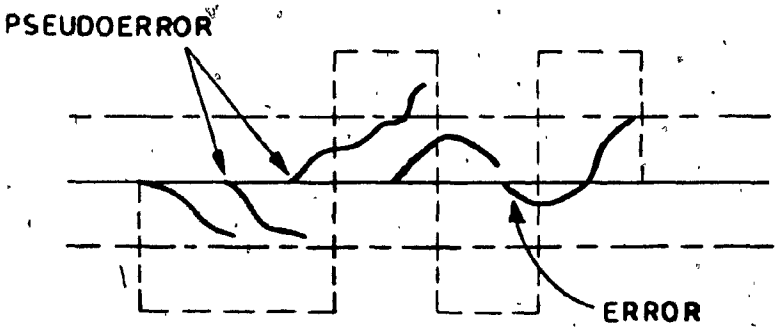

FIG. 4.2c DETECTOR OUTPUT WITH TIMING ERROR

4.4 Two-level Pseudoerror Zone (PEZ)

In this technique for detecting the peak of a composite signal within the PEZ, a new decision zone replaces the "one" and "zero" decision level used to detect the received signal. This new decision zone is called the pseudoerror zone and all received signals falling in this zone are pseudoerrors.

The objective is to find a relationship between the pseudo-error and the actual error rates given that pseudoerrors occur much faster (say 100 to 1000 times) than the actual errors.

The error and pseudoerror zones are easily seen in terms of probability density functions. Figure 4.3a shows the probability density function of a binary baseband NRZ data sequence with noise added. The decision threshold is VT/τ. (Note 1) All received signals greater than $\frac{VT}{\tau}$ are detected as V and all those less than VT/τ as -V. Fig. 4.3b shows the decomposition of P(V) into its component distributions, so that the probability of an error, given that +V or -V was transmitted, can be seen; for example, the cross-hatched area is the probability of error given that a +V was transmitted. Furthermore, if Va is received it is more likely that

Note 1. The probability density of the noise sample no(T) is Gaussian and hence appears as in Fig. 4.4. Suppose that during some bit interval the input signal voltage is held at, say -V, then, at the sample voltage $So(T) = -VT/\tau$. while the noise sample is no(T). If no(T) is positive and larger in magnitude than VT/τ, the total sample voltage $Vo(t) = So(T) + no(T)$ will be positive. Such a sample voltage will result in an error, and the probability of such a misinterpretation, that is the probability that $no(T) > \frac{VT}{\tau}$, is given by the shaded area of the zone in Fig. 4.4. The PEZ limits are also shown in Fig. 4.4.

FIG. 4.3 a

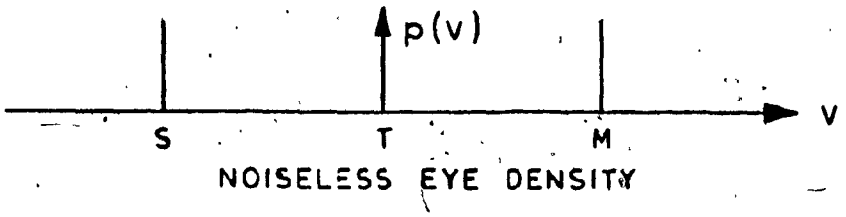

NOISELESS EYE DENSITY

FIG. 4.3 b

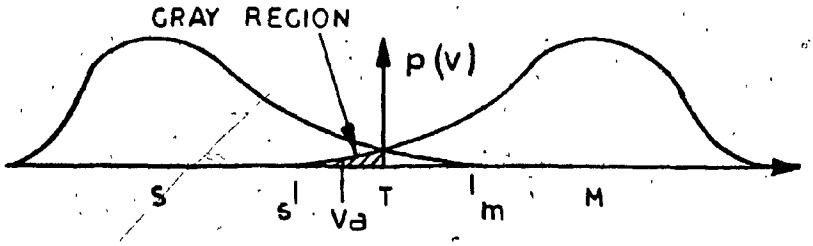

NOISY EYE DENSITY

PROBABILITY OF ERROR GIVEN THAT +V WAS TRANSMITTED

FIG. 4.3 c

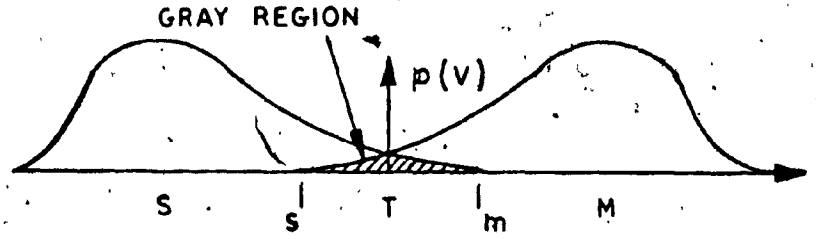

NOISY EYE DENSITY

a -V was transmitted and it is decided that a -V was transmitted, but it is still possible to decide that a +V was transmitted instead. Thus when the signal peak appears near the decision threshold its correct detection is in doubt.

Fig. 4.4c defines the cross-hatched zone as the pseudoerror zone, and as can be seen from Fig. 4.4b, a received signal in this zone has a high probability of being incorrectly detected. Any signal in this zone is considered a pseudo error. Since the pseudo errors occur more frequently than real errors, the pseudoerror rate is an amplification of the true error rate. This comprises an error amplification technique.

Derivation of the probability of two-level PEZ, for a baseband two-level PAM system in a Gaussian noise environment, together with the statistics of the number of pseudoerrors are derived in the following sections.

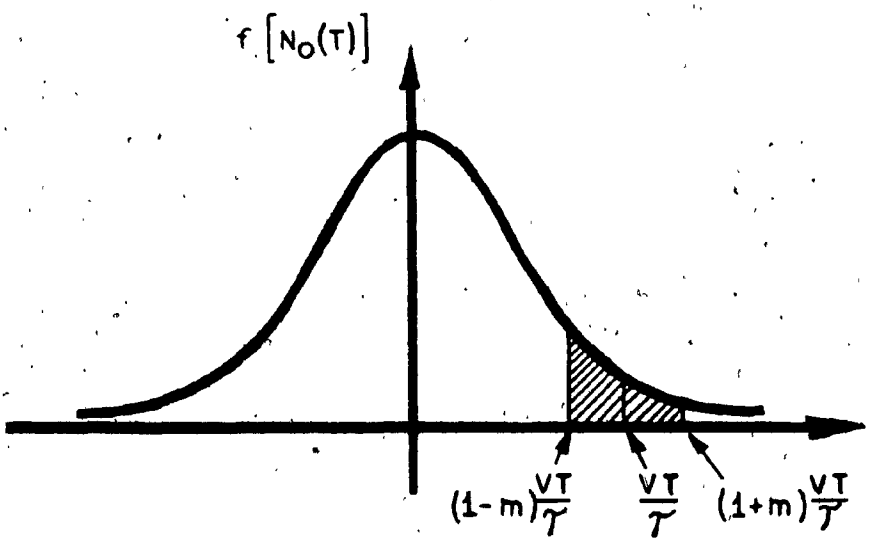

FIG. 4.4 THE NORMAL PROBABILITY OF THE NOISE SAMPLE $N_0(T)$ AND PSEUDOERROR REGIONS

4.5 Derivation of Probability of Two-level PEZ

In this section the equation for the probability of pseudo-error, P(p), in an "Additive White Gaussian Noise" (AWGN) environment will be derived. The final equation for the binary baseband system having the PEZ will also be established.

The probability of error of a baseband PAM system is given by { Ref.13 }

$$P(e) = (1-\frac{1}{L})\ Pr\ (|n|>d) \qquad (4.5.1)$$

where L is the number of baseband transmission levels and Pr stands for the probability distribution function.

For White Gaussian Noise (WGN), this expression becomes

$$P(e) = 2(1-\frac{1}{L})\ Q\left[\frac{d}{\sigma}\right] \qquad (4.5.2)$$

where

$$Q(x) = \frac{1}{\sqrt{2\pi}} \int_{x}^{\infty} \exp -t^2/2\ dt \qquad (4.5.3)$$

and d is the difference between the actual level of the received signal and the nearest decision threshold, σ^2 is the total mean power of the WGN at the comparator input, n_o is the value of the noise at the sampling instant.

A similar situation to that of the baseband PAM system described above exists in coherent modulation schemes as shown in

Fig. 4.5. At the receiver input (A) the noise bandwidth is relatively wide in comparison with the bandwidth of the receiver Band-pass filter (BPF). Following the BPF, at (B), this noise has a flat power spectrum. After the demodulator, at (C) the power spectrum density of the noise remains the same as at (B). The limited bandwidth of the WGN at (C) is further filtered by the received Low Pass Filter (LPF). This filter does not modify the probability density function (Pdf) of the Gaussian noise; however it further limits the bandwidth at (D). At the input of the comparator (a threshold detector) a signal with added band-limited WGN is received. The detector is then followed by a sampling device.

The mathematical model of the system is shown in Fig. 4.6. C(w) is used to band-limit the WGN which has a uniform power spectral density $\frac{\eta}{2}$. The input symbols (A_n) are assumed to have two equally speced levels of equal probability (L = 2); symbols occuring at different times are independent. The time duration of each symbol is T. Based on the above conditions P(e) can be expressed as:

$$P(e) = \frac{1}{2} \Pr \left[|n| > d \right]. \qquad (4.5.4)$$

Suppose that noise n(t) is applied to the input of the RC-LPF, {R(ω)}, at the time t = 0 then the noise power at the output of the LPF {R(ω)} at t = T is given by , {Ref.15}

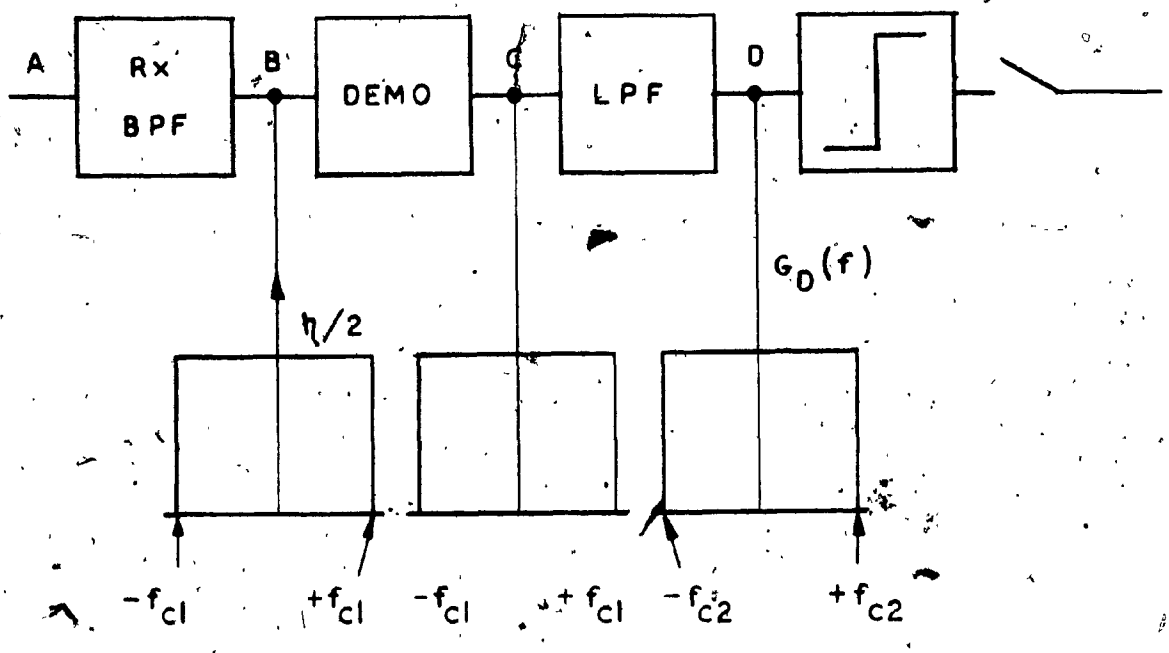

FIG. 4.5 SIMPLIFIED MODEL FOR TWO LEVEL RECEIVER

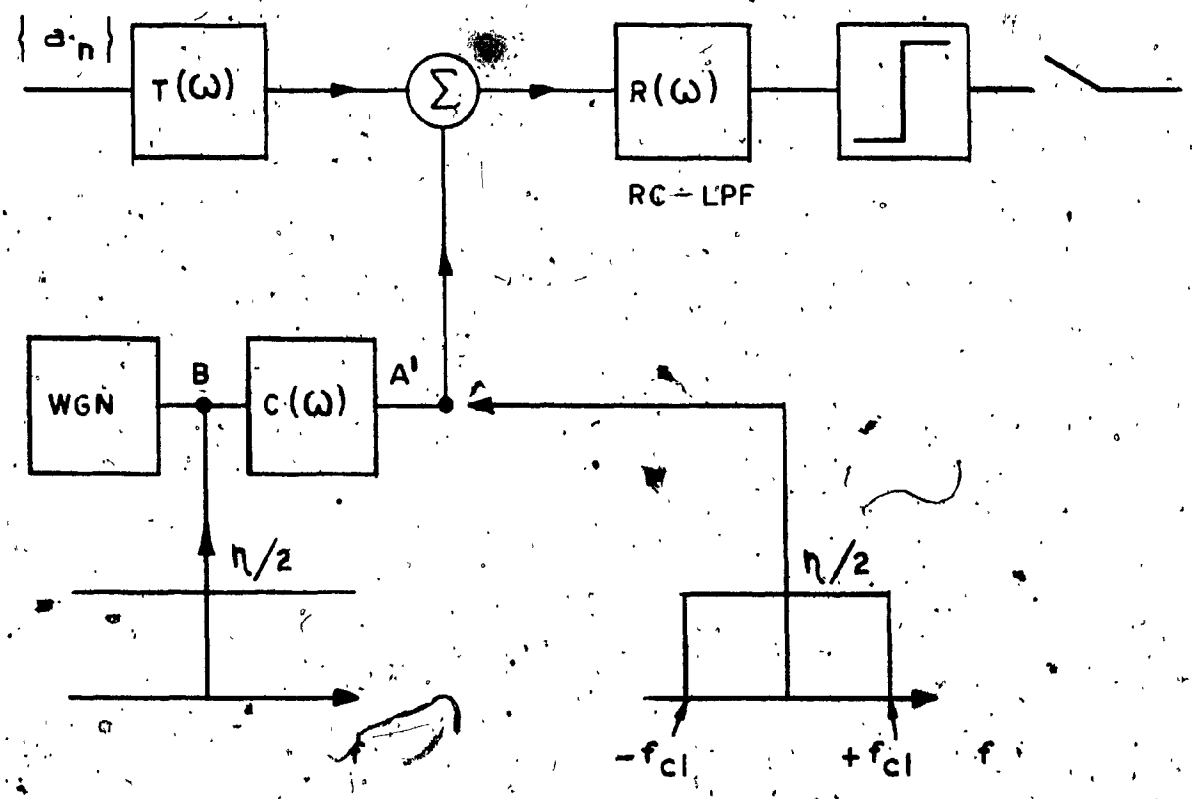

FIG. 4.6 MATHEMATICAL MODEL FOR TWO LEVEL TRANSMISSION SYSTEM

$$\overline{No^2(T)} = \frac{\eta T}{2\tau 2} \qquad (4.5.5)$$

where T is the signal bit duration and τ is the time constant ($\tau = 1/RC$) of the LPF. The signal amplitude at time t = T, at the output of the LPF is given by

$$\delta o(T) = \frac{VT}{\tau} \qquad (4.5.6)$$

where V is the peak signal amplitude at (A). By replacing the threshold comparator by a PEZ circuit, the pseudoerror of the on-line signal will be obtained (Fig. 4.7). The function of PEZ is to detect the value of the composite signal peaks within the PEZ. At the sampling instant it is important to determine the probability of occurance of these peaks. From this the probability of pseudoerror {P(p)} can be calculated for a two-level Non-Return to Zero (NRZ) random binary sequence with added band-limited WGN.

The probability density of the noise No(T) (Fig. 4.4) at the output of the LPF at (B) is given by:

$$P\ \ No(T) = \frac{1}{\sigma_0\sqrt{2\pi}} e^{-No(T)/2\sigma_o^2} \qquad (4.5.7)$$

where the variance σ_0^2 of the noise after passage through the first order LPF, is given by {Ref. 15}

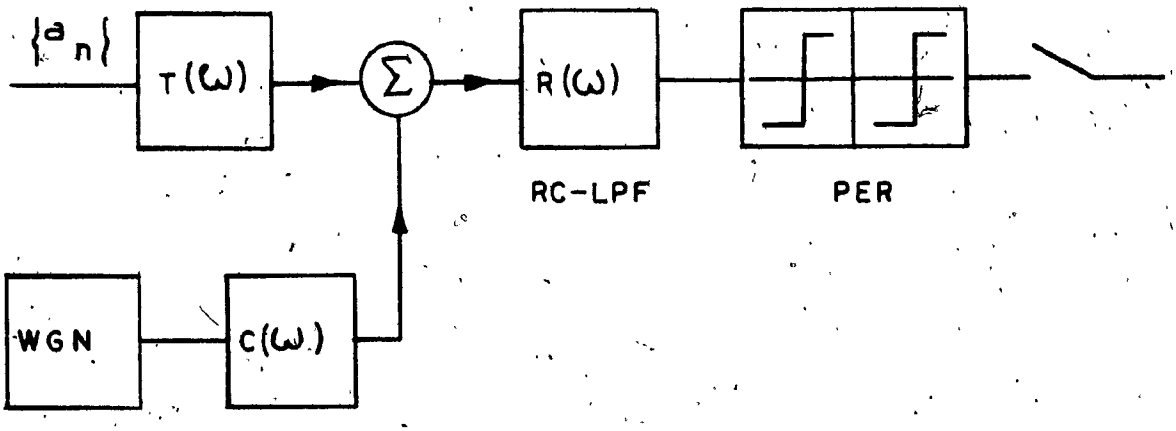

FIG. 4.7 MATHEMATICAL MODEL FOR MONITORING THE PSEUDOERROR RATE

$$\sigma_o^2 = \overline{N_o^2(T)} = \nu T/2\tau^2 \qquad (4.5.8)$$

P(p) then is defined by the area under the normal probability density curve of Fig. 4.4. from $(1 - \Delta)d$ to $(1 + \Delta)d$ where Δ indicated the arbitrary decision level in terms of signal amplitude V, and $d = \frac{VT}{\tau}$ is the typical received level at the regenerator. Δ, is fixed for a given PEZ such that $o < \Delta < 1$; then P(p) is given by

$$P(p) = \frac{1}{\sqrt{2\pi}\sigma_o} \int_{(1-\Delta)\frac{VT}{\tau}}^{(1+\Delta)\frac{VT}{\tau}} \exp -No^2(T)/2\sigma_o^2 \; . \; dNo(T) \qquad (4.5.9)$$

while the probability of the true error P(p) is given by

$$P(e) = \frac{1}{\sqrt{2\pi}\sigma_o} \int_{\frac{VT}{\tau}}^{\infty} \exp -No^2(T)/2\sigma_o^2 \; . \; dNo(T) \qquad (4.5.10)$$

By definition, the normal probability distribution is given by,

$$P(x) = \int_{-\infty}^{x} Z(t)dt \qquad (4.5.11)$$

where

$$Z(t) = \frac{1}{\sqrt{2\pi}} \; e^{-t^2/2}$$

so from equations (4.5.9) and (4.5.11)

$$P(p) = P\{(1+\Delta)\sqrt{\frac{2V^2T}{\eta}}\} - P\{(1-\Delta)\sqrt{\frac{2V^2T}{\eta}}\} \qquad (4.5.12)$$

and hence,

$$P(p) = P\{(1+\Delta)\sqrt{\frac{2E_s}{\eta}}\} - P\{(1-\Delta)\sqrt{\frac{2E_s}{\eta}}\} \qquad (4.5.13)$$

in which

$$E_s = V^2T$$

is the signal energy per bit. Fig. (4.8) shows plots of P(p) versus $\frac{Es}{\eta}$ as obtained from equation (4.5.13) for $\Delta = 0.8$, $\Delta = 0.9$ and $\Delta = 0.95$ using a standard table of areas under the normal probability curve.

4.6 Pseudoerror Versus Error Rate in Gaussian Noise Environment

The mathematical model of a two-level pseudo error technique in a Gaussian noise environment was derived in Section 4.4. The pseudo-error Zone (PEZ) was defined and any detected received signal in this zone was called a pseudoerror. Since the PEZ is defined such that pseudo-errors occur more frequently than real errors, the pseudoerror rate is an amplification of the error rate.

R. O. Brown {Ref.16} derived some of the statistical properties for the basic pseudo-error amplification technique which can be also

FIG. 4.8 PROBABILITY OF ERROR $P_{(e)}$ AND PROBABILITY OF PSEUDO ERROR $P_{(p)}$ FOR SEVERAL VALUES OF PSEUDO ERROR REGION SIZE Δ.

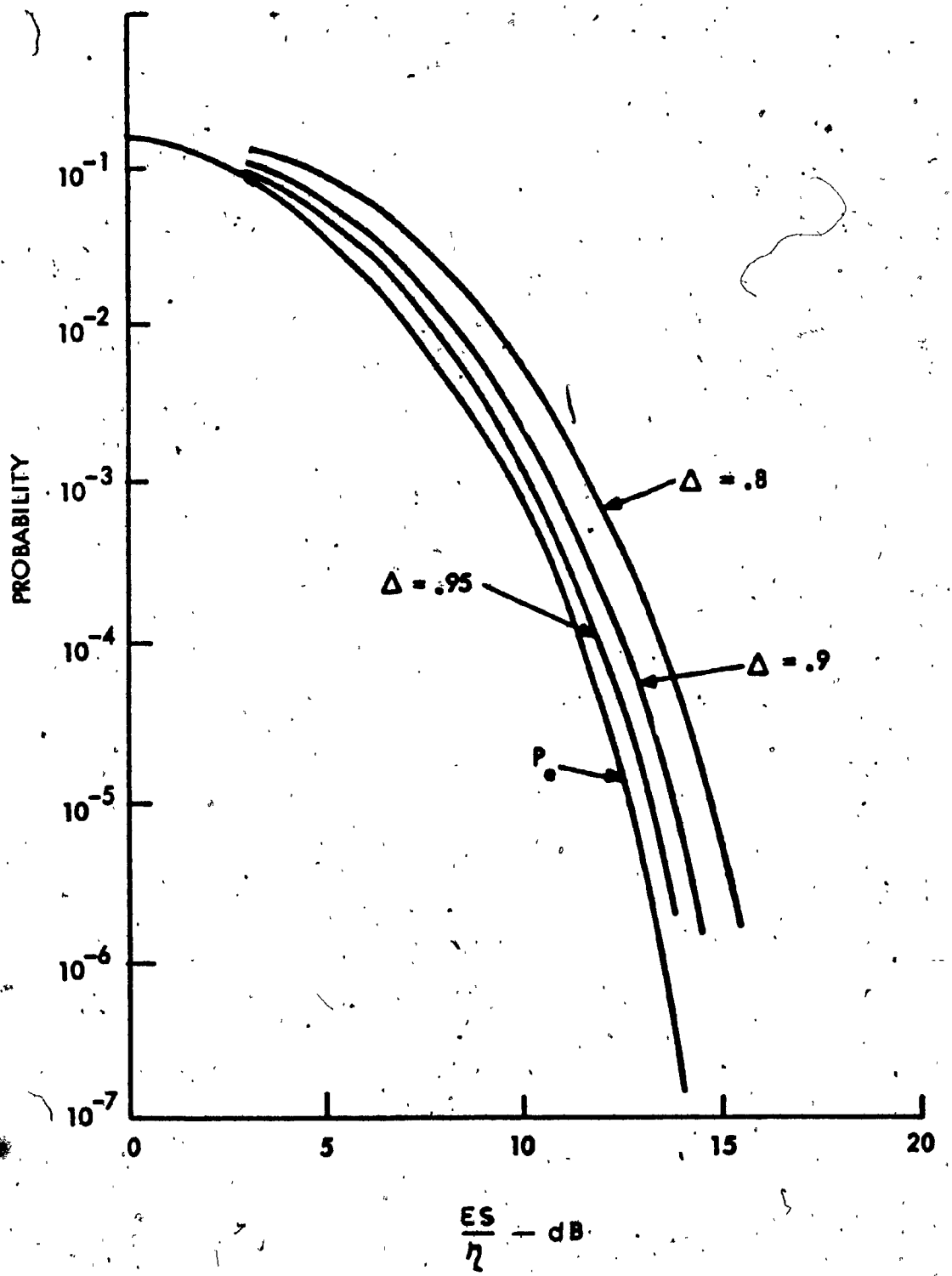

applied to other error amplification techniques.

For simplicity consider the differences between a typical received signal and the decision threshold as ±d ($d = VT/\tau$) as having an equal probability of occurence, and the noise to be Gaussian $N(o,\sigma)$. The decision threshold is zero volts at the receiver regenerator. Suitable modifications can be made to the results found here for other cases.

The probability of an error for a two-level PAM signal is given by (4.5.2). The result for L = 2 is

$$P(e) = Q\left(\frac{d}{\sigma}\right) \qquad (4.6.1)$$

Where $Q\left(\frac{d}{\sigma}\right)$ is defined by equation (4.5.3)

For simplicity define $\Phi(x)$ as

$$\Phi(x) = \frac{1}{\sqrt{2\pi}} \int_o^x \exp -t^2/2.dt \qquad (4.6.2)$$

hence,

$$P(e) = Q(n) = \frac{1}{2} - \Phi(x) \qquad (4.6.3)$$

The probability that +d or -d is incorrectly detected is $\frac{1}{2}P(e)$. Similarly the probability of correctly detecting a bit is

$$P(c) = 1 - P(e) = \frac{1}{2} + \Phi\left(\frac{d}{\sigma}\right) \qquad (4.6.4)$$

while the probability of correctly detecting +d or -d is $\frac{1}{2}P(c)$ and the probability of a pseudoerror is

$$P(p) = \int_a^b f(x) \, . \, dx \qquad (4.6.5)$$

If the boundaries of the pseudoerror zone (ℓ_a & ℓ_b) are such that $\ell_a = \ell_b = \ell$ as for a symetric distribution, the probability of a pseudo-error becomes approximately

$$P(p) = \frac{1}{\sqrt{2\pi}\sigma} \int_{-\ell}^{+\ell} \exp\{-(x+d)^2/2\sigma^2\} \, .dx$$

$$= \Phi(\frac{d+\ell}{\sigma}) - \Phi(\frac{d-\ell}{\sigma}) \qquad (4.6.6)$$

For typical values of ℓ and d, this can be further approximated by

$$P(p) \sim \frac{1}{2} - \Phi(\frac{d-\ell}{\sigma}) \qquad (4.6.7)$$

The value of P(p) is high for the tail of the probability curve beyond the PEZ. Fig. 4.8 shows the probabilities P(e) and P(p) as a function of Δ where Δ is defined as

$$\Delta = \frac{d-\ell}{d} \qquad (4.6.7a)$$

Next, define the error amplification A(e) as the ratio of the pseudo-error rate to the true error rate:

$$A(e) = \frac{P(p)}{P(e)} \qquad (4.6.8)$$

In the present case, with appropriately large arguments

$$P(p) \simeq \frac{\sigma}{\sqrt{2\pi}} \cdot \frac{\exp\{-(d-\ell)^2/2\sigma^2\}}{(d-\ell)} \qquad (4.6.9)$$

and

$$P(e) \simeq \frac{\sigma}{\sqrt{2\pi}} \cdot \frac{\exp\{-d^2/2\sigma^2\}}{d} \qquad (4.6.10)$$

and

$$A(e) = \frac{d}{d-\ell} \exp\{-(\ell^2-2d\ell)/2\sigma^2\} \qquad (4.6.11)$$

Since d is usually significantly greater than ℓ

$$A(e) \simeq \exp\{d.\ell/\sigma^2\} \qquad (4.6.12$$

or

$$A(e) = 10 \log_{10} \exp\{d.\ell/\sigma^2\}$$

$$= 4.3\, d\ell/\sigma^2 \text{ dB} \qquad (4.6.13)$$

Since, in this approximate relationship, A(e) is a monotonic function of the product "d.ℓ", "d.ℓ" can be used as an approximate indicator of the error amplification. Equation 4.6.12 is an exponential relationship wherein approximations have been made in the exponent and its accuracy is therefore frequently in question. For precise results more exact relationships such as equation 4.6.11 should be used. Equation 4.6.12 is useful for obtaining a rough estimate of the gain as a function of ℓ and d.

4.7 Statistics of the Number of Pseudo Error Observations

If P(p) is estimated by averaging the number of pseudoerrors observed in n observations, it becomes a random variable. The probability function of the number of pseudoerrors h in n observations is given by the binomial distribution {Ref. 16}.

$$P(\chi=h) = \binom{n}{h} P(p)^{h} (1 - P(p))^{n-h} \qquad (4.7.1)$$

For large n this distribution reduces to the Gaussian

$$P(\chi=h) = N\left[P(p), P(p).\{1-P(p)\}\right]$$

Consequently, $P(\hat{p}) = h-n$ becomes

$$P(\hat{p}) = N\left[P(p), P(p)\left\{\frac{1-P(p)}{n}\right\}\right]$$

In many cases $1-P(p) \approx 1$ so that the density of $P(\hat{p})$ becomes $N\left[P(p), \frac{P(p)}{n}\right]$.

For $P_{(\hat{p})}$ to be in the range $P(p) \pm \delta P(p)$ with probability Y, the required number of observation n is found from

$$Y = \frac{1}{\sqrt{2\pi}} \int_{\delta\sqrt{n.P(p)}}^{\delta\sqrt{n.P(p)}} \exp\{-z^2/2\} .dz \qquad (4.7.2)$$

For example, for Y = 0.95 (95% confidence):

$$\delta\sqrt{n.P(p)} = 1.96$$

$$n.P(p) = \frac{3.8416}{\delta^2}$$

Fig. 4.9 shows this result as a function of δ for 90, 95 and 99 percent confidence levels and that the confidence limits depend on the value of P(p).

Fig. 4.9 is useful for testing the state of the system against a known standard. For example, given a system operating in a Gaussian noise environment with SNR = 10dB with a two-level pseudo-error monitor with $\Delta = 0.8$ we have from Fig. 4.9 $P(p)=7 \times 10^{-3}$ and and $P(e)=9 \times 10^{-4}$. For 95% confidence that P(p) is accurate to $\pm$ 20%, n= 100/P(p) = 14.3 Kilobits must be observed. Conversely, suppose 14.3 Kilobits are observed with the same monitor in a system when the standard SNR is 10 dB ($P(p) = 7 \times 10^{-3}$) then if h = 200 observations are made and $\delta = 0.2$ is selected it can be concluded, based on a 95% confidence test, that a rare event has been observed

and that the system is not operating with a SNR = 10dB.

Similarly, if h = 115 with a 95% confidence of being within 20% of the true value it can be accepted that the system is operating with SNR = 10dB.

In general it was shown by Brown {Ref. 16} that the minimum acceptable value of h is about 10. In this case, the true P(e) is within ± 50% of P(p) and the confidence coefficient is about 90%. If the gradient of a typical P(e) = f(CNR) curve is taken into account, then this estimate may be considered very accurate (equivalent to 0.3dB variation) in the carrier-to-noise ratio (CNR).

4.8 Width of Confidence Interval for a Given Confidence Level

When the monitor only monitors h (the number of pseudoerrors) and n (the number of bits observed) with no other information being known, upper and lower confidence limits on the estimate of $P(p) = \frac{h}{n}$ may be found by the following technique of Hald {Ref. 17}.

The upper and lower limits $P_{(pu)}$ and $P_{(p\ell)}$ are

$$P_{(pu)} = \frac{f_1 \cdot F_{1-P_1}(F_1-f_2)}{f_2+f_1 \cdot F_{1-P_1}(f_1 \cdot f_2)} \qquad (4.8.1)$$

where

f_1 = 2(h+1)

f_2 = 2(n-h)

P_1 = Probability that h/n is greater than P(pu)

$F(\ )$ = The F-distribution

FIG. 4.9 NUMBER OF OBSERVATIONS REQUIRED FOR GIVEN CONFIDENCE IN THE ESTIMATE OF P_p

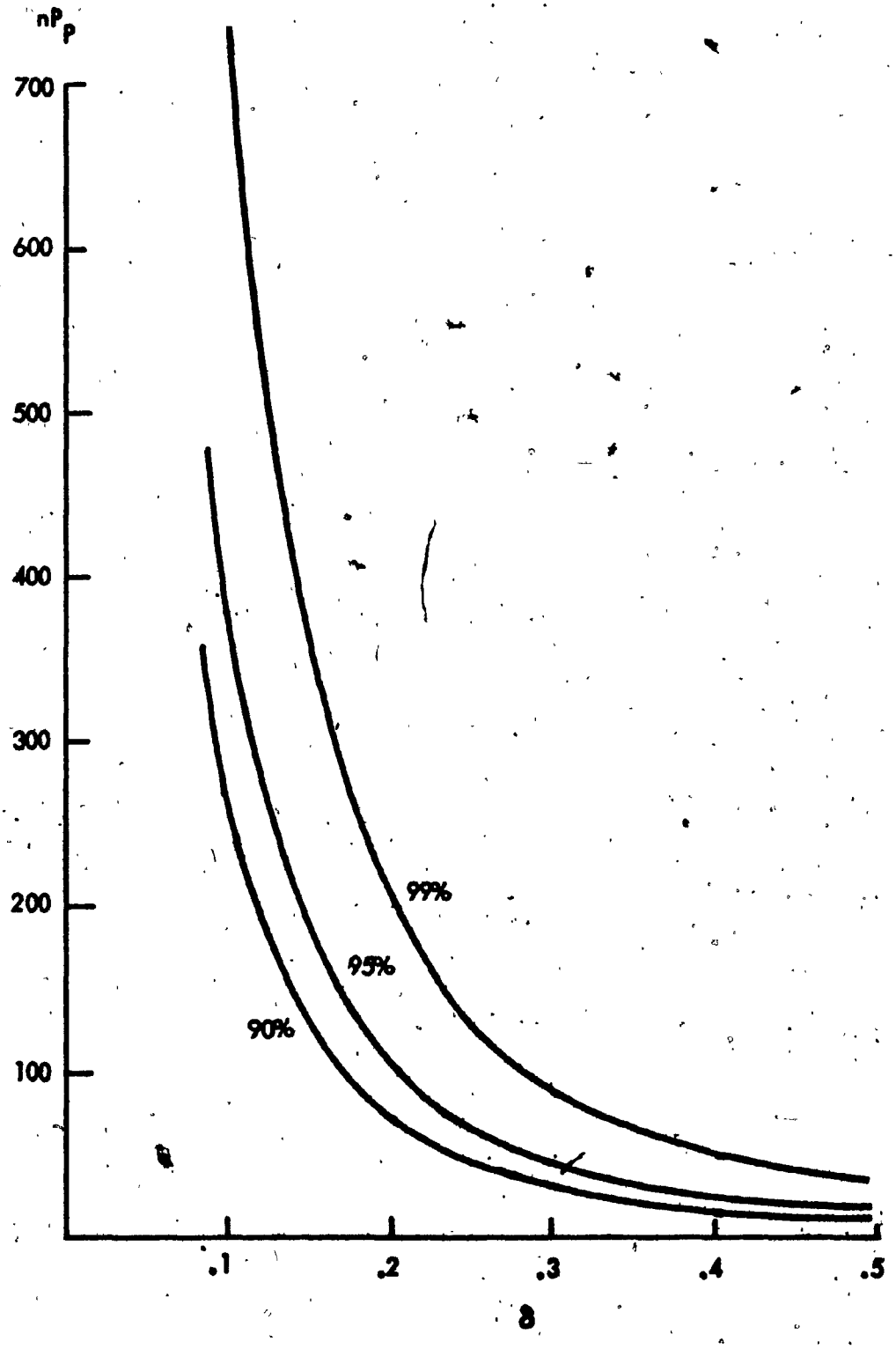

$$P(p\ell) = \frac{f'_2}{f'_2 + f'_1 \cdot F_{p2}(f'_1, f'_2)} \qquad (4.8.2)$$

where

$f'_1 = 2(n-h+1)$

$f'_2 = 2h$

P2 = Probability that h/n is greater than P ($p\ell$)

In the present case n is typically large, of the order of 1000 or more, while h is small, typically less than 100. For such cases Brown {Ref. 16} used two χ^2 distributions to approximate the F-distribution Thus:

$$Fp(f_1, \infty) = \frac{\chi^2_{p(f1)}}{f_1} \qquad (4.8.3)$$

$$Fp(\infty, f2) = \frac{f_2}{\chi^2_{(1-p)f2}} \qquad (4.8.4)$$

Substituting these results into the confidence limits:

$$P(pu) = \frac{1}{1 + \frac{2(n-h)}{\chi^2_{(1-p_1)}\left[2(h+1)\right]}} \qquad (4.8.5)$$

$$P(p) = \frac{\chi^2_{1-P_2}(2h)}{2n-2h+2+\chi^2_{1-P_2}(2h)} \qquad (4.8.6)$$

For example, suppose 10,000 bits are observed containing 10 pseudo-errors $\{P(p)=10^{-3}\}$ then for 95% confidence, the upper and lower limits on P(p) are:

$$P(pu) = \frac{1}{1+\frac{2(10.000-10)}{\chi^2_{1-0.025}\left[2(10+1)\right]}} \qquad (4.8.7)$$

and

$$P(p\ell) = \frac{\chi^2_{1-0.975}\left[2.(10)\right]}{2.(10,000)+2.(10)+2+\chi^2_{1-0.975}\left[2.(10)\right]} \qquad (4.8.8)$$

From standard tables of the χ^2-distribution: $P_{(pu)} = .00184$ and $P_{(p\ell)} = .00048$ for the 95% confidence limits on the estimate of $P_{(p)} = .001$ of interest is the width of the confidence level, i.e.:

$$r = \frac{P(pu) - P(p\ell)}{P(pu)} \qquad (4.8.9)$$

for small values of r. By substituting equations (4.8.5) and (4.7.6) into (4.8.9) a set of curves can be obtained which allow one to determine the width of the confidence interval for a given confidence level

knowing n and h.

4.9 Application to Multilevel Systems

Results obtained by use of the equations in section 4.4 through 4.8 are distribution-free and hence are applicable to a signal with any type of distortion. For a 4-Phase PSK system with signal levels $(\pm 1, \pm 1)$, the decision thresholds and pseudoerror zones are shown in Fig. 4.10. In this case the number of pseudoerrors is the total number of received signals in all of the pseudoerror zones.

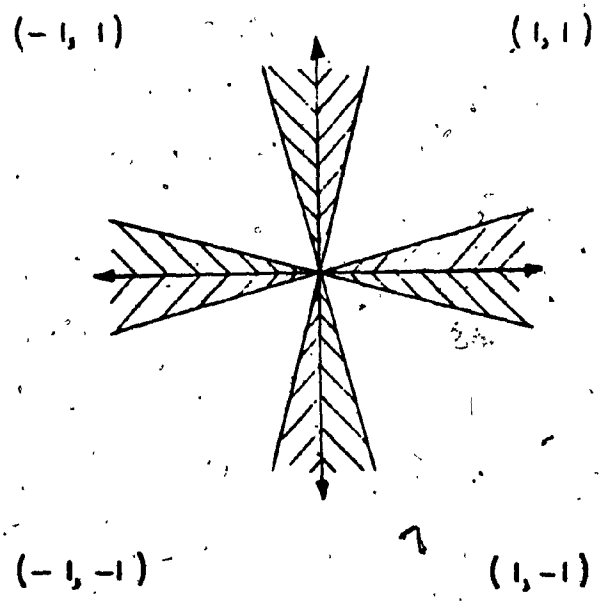

FIG. 4.10 4 PHASE-PSK WITH PSEUDOERROR REGIONS

4.10 Multi-Zone Pseudo-Error Monitor

In the previous sections, the operating principles of two-level PEZ (Fig. 4.11) and the statistical method of synthesis were studied. The following sections will cover the operating principles of the Multi-Zone Pseudo-Error Monitor (MZP) as well as the mathematical model for synthesising such a monitor. The operating principle described here begins by considering an eye pattern -- a tool which is extensively utilized in data communication monitoring systems.

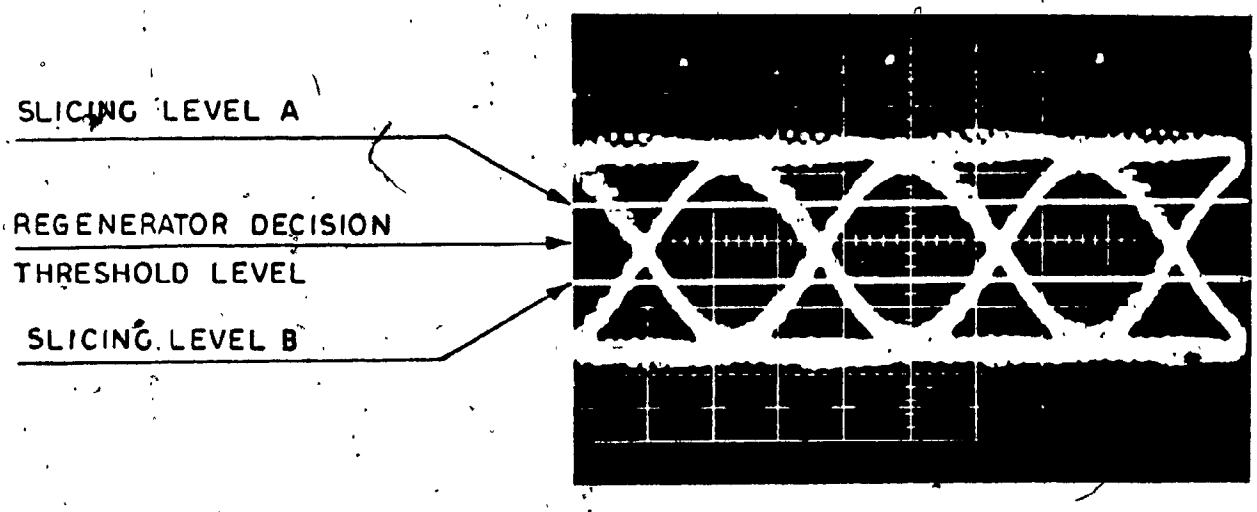

FIG. 4.11 EYE DIAGRAM AND 2—PEZ

Consider the eye diagram shown in Fig. 4.12. The eye-opening of Fig. 4.12 is divided into 2p zones, and for simplicity the slicing levels of equal distance. A typical positive demodulated signal peak at the receiver representing logic "one" is sliced into p equally spaced zones above the decision threshold. Similarly, a

negative voltage representing logic "zero" is sliced into p equally spaced zones below the threshold. By slicing the incoming one's and zero's into p zones, 2p zones are constructed in the eye opening. Any zone in the positive portion of the eye is associated with a symmetrically located zone in the negative part of the eye, and both zones have the same monitoring statistical properties. The number of zones may vary depending on the system requirements and the accuracy of the monitor.

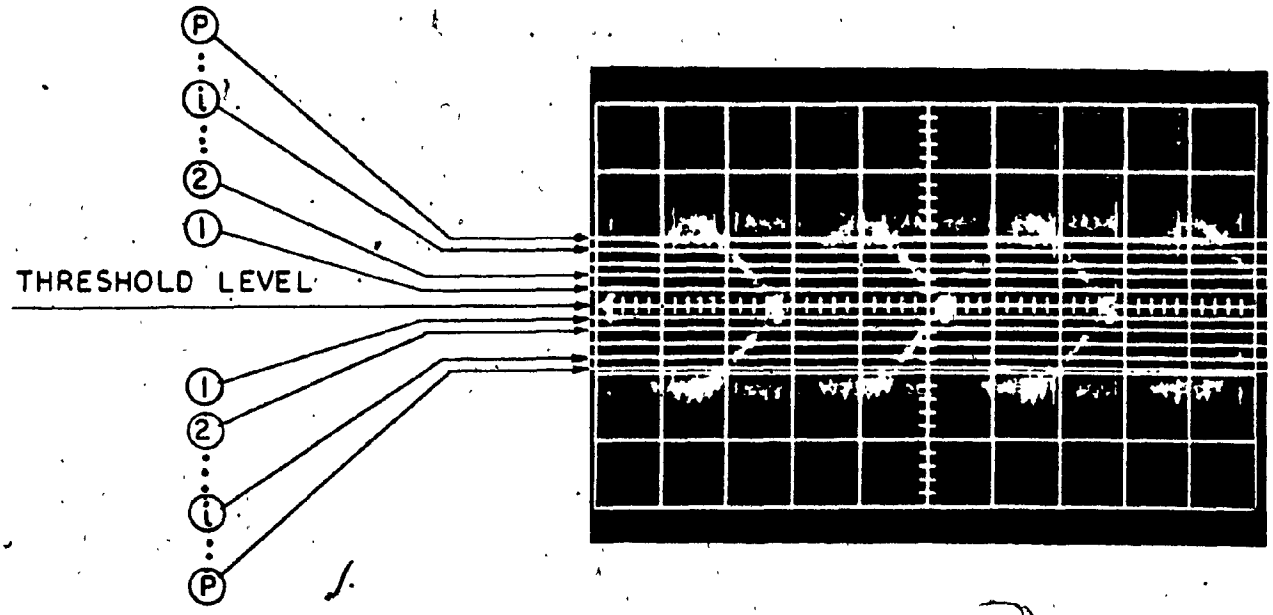

FIG. 4.12 TWO LEVEL EYE PATTERN AND MULTIZONE SLICING LEVELS

The function of the MZP monitor differs from the two-level PEZ. It is based on the detection of the demodulated signal peak within one of the zones at the sampling instant.

Considering a transmitted bit, this bit is sampled at its maximum peak in order to be regenerated. The MZP's function is to sample each received bit (positive or negative) at the instant of

regeneration and detect in which one of the zones it is located.

In this study whenever a zone, say the i^{th} zone, is referred to, the i^{th} zones above and below the threshold are referred to.

For "n" number of tested bits the occurences of composite peaks in each of the zones are counted. The number counted in each of the various zones will give a good statistical estimate of the performance of the transmission system.

The output processor of the MZP monitor can be preprogrammed in different ways depending on the application and the accuracy of the monitor. One can set the MZP to detect the zone with the maximum count in "n" observations. In such a case the MZP will activate a Light Emitting Diode (LED) associated with the zone which observes the maximum count of the sampled de-modulated signal existing in that particular zone. Obviously this type of MZP monitoring system will have "p" number of LEDs which will monitor and give a good indication of the BER and the signal-to-noise ratio of the system.

The second alternative is to consider the number of peaks detected in the other zones. For this purpose there will be p number of digital displays and one must estimate the BER by referring to a statistical chart which will provide the necessary information. A simple preprogrammed digital circuit can also be built into the MZP in order to automatically provide the BER estimate from the zone counts. It must also be noted that if the i^{th} counter (i=0,1,...p-1) displays "n" the count of the composite peak in the i^{th} zone, from n observations, the following equality is valid.

$$\sum_{i=o}^{p-1} ni = n \qquad (4.10.1)$$

The third alternative is to assign to each of the zones a certain threshold counting level based on a selected probability level so that the corresponding LED is activated if the count exceeds the threshold. The BER estimate is obtained from the probabilities associated with the LED's activated at the end of each test period. Note that it is unlikely that non-adjacent LED's will be activated in this type of procedure.

Thus, MZP monitoring is the key to evaluate received composite data. It also has the capability of evaluating the signal peak at the instant when the regenerator makes its decision (time synchronized with the regenerator). For a given confidence limit, BER evaluation of a communication system by using MZP monitoring technique requires less observation bits (n) than 2-PEZ or other pseudoerror techniques.

4.11 The MZP Monitoring in Gaussian Noise Environment

In a Gaussian noise environment, any increase in the noise power will be reflected in an increase in the standard deviation, σ_o, of the noise probability density function (pdf). The density function of scrambled data (logic one and logic zero with an equal probability of occurrence) plus added WGN is shown in Fig. 4.13. Fig. 4.14 also illustrates the MZP zones and the slicing levels.

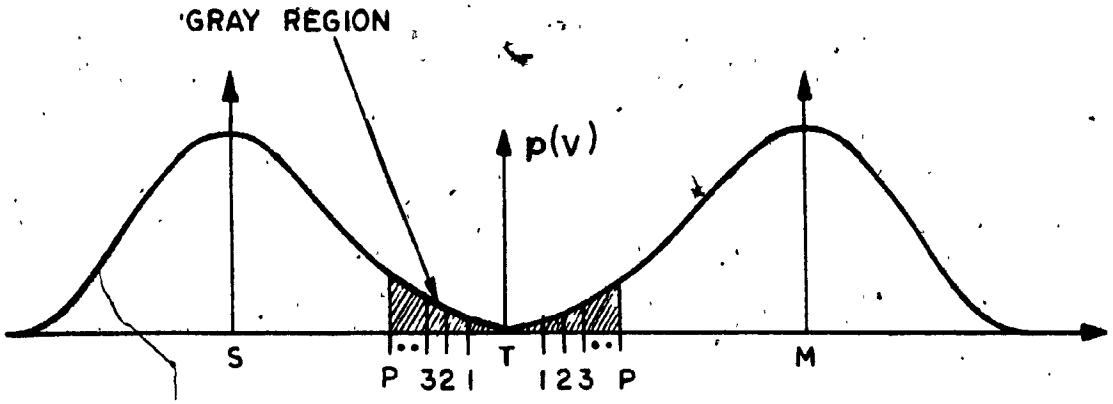

NOISY EYE DENSITY

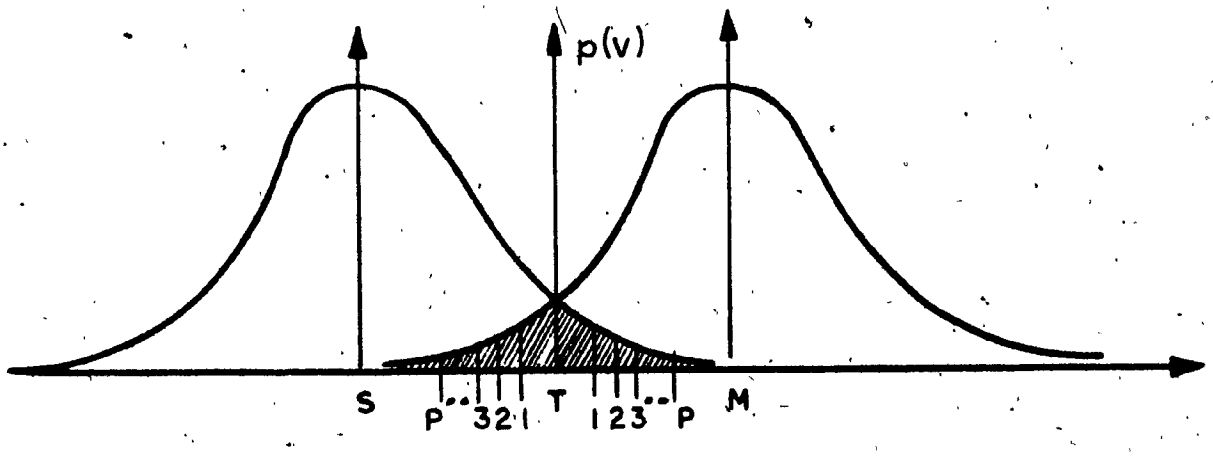

FIG. 4.13 LOGICS "1" AND "0" PLUS WGN WITH DIFFERENT σ

Since the area under the probability density function is unity, the Pdf decreases in amplitude as the noise power increases; it also increases in width so that the density decreases around the mean value. Conversely the density around the mean value increases when the noise power decreases.

The above statement can be understood by considering the eye diagram of a binary digit with added WGN as in Fig. 4.14.

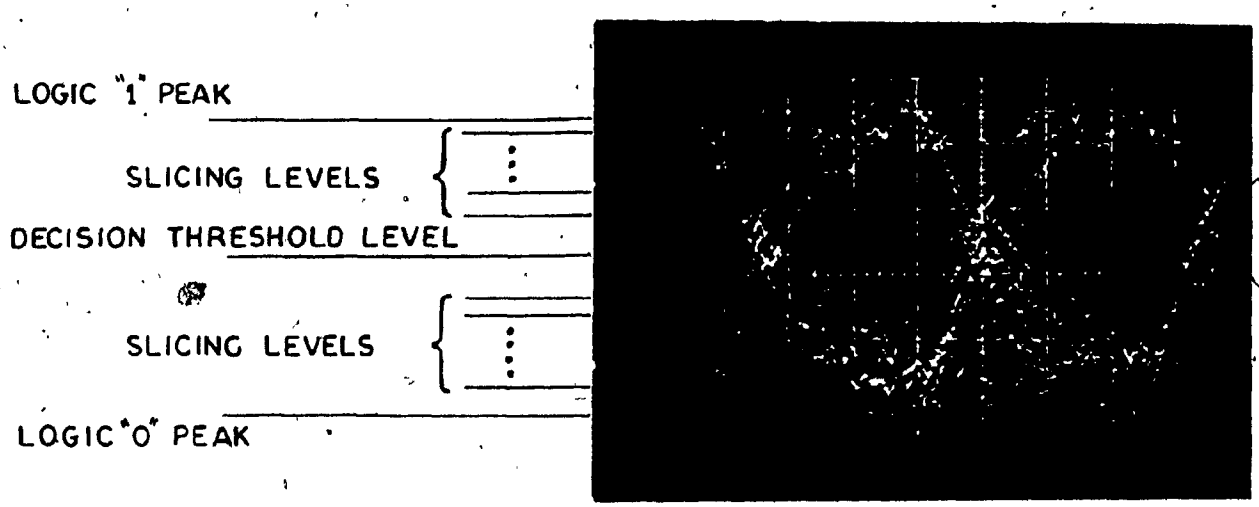

FIG.4.14 EYE DIAGRAM WITH ADDED WHITE GUASSIAN NOISE AND MZP LEVELS

For a low noise environment the probability density of the noise peaks existing inside the zones close to the data peak level is higher than in the zones near the regenerator decision level. Conversely for a higher noise power the probability density of noise occurring around the decision level becomes higher.

In the following section we will evaluate some statistical

properties of MZP zones in terms of the probability of occurrence of signal peaks versus the signal-to-noise ratio or energy per bit to noise power density.

4.12 Derivation of MZP in a Gaussian Noise Environment

The mathematical model of the system is shown in Fig. 4.6. C(w) is used to band-limit the WGN which has a uniform power spectral density over the entire Frequency range, $\frac{\eta}{2}$.

Previously it was stated that the probability density of the noise power, No(T), at the output of the LPF (at A in Fig. 4.6), is given by:

$$P\{No(T)\} = \frac{1}{\sigma_o\sqrt{2\pi}} \exp -No(T)/2\sigma_o^2 \qquad (4.12.1)$$

where the variance of the noise at the output of a first order RC-LPF is given by:

$$\sigma_o^2 = No^2(T) = \eta T/2\tau^2 \qquad (4.12.2)$$

The probability of occurrence of the composite signal peak inside a given zone $P_{MZP}(e)$, is defined by the area under the normal probability density curve of Fig. 4.1 from $\left[1-(p-i)\Delta\right] VT/\tau$ to $\left[1-(p-i-1)\Delta\right] VT/\tau$ plus the area from $\left[1+(p-i-1)\Delta\right]VT/\tau$ to $\left[1+(p-i)\Delta\right] VT/\tau$ where:

$2p$ = number of slicing levels

$\Delta = \frac{1}{p+1}$ (for the case of equiwidth zones)

V = NRZ data peak amplitude

T = Time duration of a single bit or period of the sampling instant

τ = LPF time constant

i = 0, 1, 2,...p-1 (see Fig. 4.12)

$\frac{VT}{\tau}$ = typical received signal level.

The following integrals are derived in order to obtain $P_{MZP}(e)$ for an individual zone.

$$P_{MZP}(e) = \frac{1}{\sqrt{2\pi}\sigma_o} \int_{\left[1-(p-i)\Delta\right]VT/\tau}^{\left[1-(p-i-1)\Delta\right]VT/\tau} \exp\{-N_o^2(T)/2\sigma_o^2\}.dN_o(T)$$

$$+ \frac{1}{\sqrt{2\pi}\sigma_o} \int_{\left[1+(p-i-1)\Delta\right]VT/\tau}^{\left[1+(p-i)\Delta\right]VT/\tau} \exp\{-N_o^2(T)/2\sigma_o^2\}.dN_o(T) \qquad (4.12.3)$$

The probability of the true error is given by equation (4.5.10). By definition, the normal probability distribution is given by equation (4.5.11).

From equation (4.5.11), and for $\Delta = 1(P+1)$ equation (4.12.3) becomes:

$$P_{MZP}(e) = P\{\frac{(1+i)\sqrt{2V^2T/\eta}}{(p+1)}\} - P\{\frac{(2+i)\sqrt{2V^2T/\eta}}{(p+1)}\}$$

$$+ P\{\frac{(2p-i)\sqrt{2V^2T/\eta}}{(p+1)}\} - P\{\frac{(2p-i+1)\sqrt{2V^2T/\eta}}{(p+1)}\} \qquad (4.12.4)$$

and hence

$$P_{MZP}(e) = P\{\frac{1+i}{1+p}\sqrt{\frac{2E_s}{\tau\eta}}\} - P\{\frac{2+i}{1+p}\sqrt{\frac{2E_s}{\tau\eta}}\}$$

$$+ P\{\frac{2p-i}{p+1}\sqrt{\frac{2E_s}{\tau\eta}}\} - P\{\frac{2p-i+1}{p+1}\sqrt{\frac{2E_s}{\tau\eta}}\} \qquad (4.12.5)$$

in which $E_s = \frac{V^2T}{\tau}$ is the signal energy per bit.

The $P_{MPZ}(e)$ equation in terms of Δ for equidistant slicing levels is given as follows:

$$P_{MZR}(e) = P\{\Delta(1+i)\sqrt{\frac{2E_s}{\eta}}\} - P\{\Delta(2+i)\sqrt{\frac{2E_s}{\eta}}\}$$

$$+ P\{[2-(2+i)\Delta]\sqrt{\frac{2E_s}{\eta}}\} - P\{[2-(1+i)\Delta]\sqrt{\frac{2E_s}{\eta}}\} \qquad (4.12.6)$$

From equations (4.12.4) through (4.12.6) and a table of the ordinates of the normal probability distribution, one could obtain

a set of probability curves for the existance of signal peaks within each MZP zone versus the S/N or $\frac{E_s}{\eta}$. This set of curves can then be used to derive an estimate of the BER.

Forms of equations (4.12.4) to (4.12.6) can also be obtained for other types of distribution functions and hence the concept is applicable to signals with any type of distortion.

4.13 Error Rate Amplification by Degrading the Performance in a Parallel Path

The basic idea of the techniques presented in this section is to connect a "secondary" decision device that is parallel with the main data path. This secondary path has intentionally-degraded performance. The output sequence of this path has an error rate much greater than the unknown error rate of the main receiver. This amplified error rate is specified by taking the main receiver output data as a reference and counting the number of mis-matches with respect to the secondary output data stream. Every mis-match is called a pseudoerror. Pseudoerrors occur more frequently than true errors in the main data path, and thus the pseudoerror rate $P(p)$ is higher than the true error rate.

The controlled degradation of the secondary path may be obtained by modifying the eye diagram sampling instant with respect to the optimal one. Alternatively, in the secondary path, the post-detection low-pass filter might have a wider band (greater fc than optimal) than the post-detection filter in the main demodulator. Thus, more noise appears in the secondary pseudoerror path than

in the main data path due to the larger bandwidth. Another alternative is that, the post-detection low-pass filter might have a narrower band than the optimal post-detection filter in the main demodulator. In this filter with smaller cutoff frequency, more intersymbol-interference is introduced than in the main path due to the smaller bandwidth thereby increasing the error rate of the parallel path.

In the following sections the controlled degradation of the parallel path, (implementation of sampling offset, increase in noise power, and introduction of intersymbol-interference in the signal) is discussed in more detail.

4.14 Error Rate Amplification By Introducing Sampling Offset

Considering that a binary-encoded PCM base band signal consists of a time sequence of voltage levels +V or -V, suppose, as is always the case with the types of noise we consider, that the noise voltage has a probability density which is entirely symmetrical with respect to zero volts, then the probability that the noise has increased the sample value is the same as the probability that the noise has decreased the sample value. It then seems entirely reasonable that we can do no better than to assume that if the sample value is negative the transmitted level was -V. It is, of course, possible that at the sampling time the noise voltage may be of a magnitude larger than V and of a polarity opposite to the polarity assigned to the transmitted bit. In this case error will occur as indicated in Fig. 4.15.

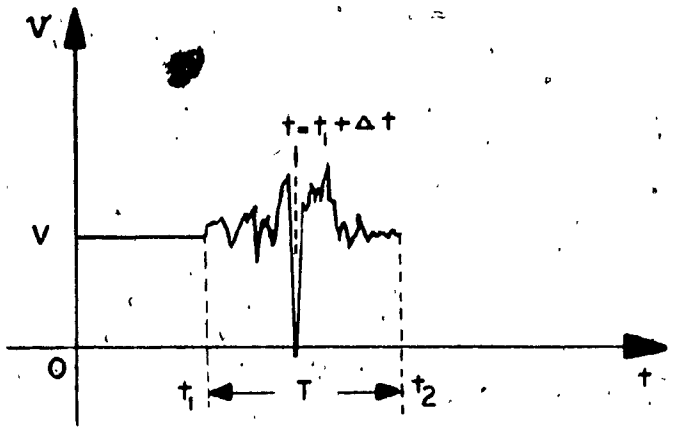

FIG.4.15 ILLUSTRATION THAT NOISE MAY CAUSE AN ERROR IN THE DETERMINATION OF A TRANSMITTED VOLTAGE LEVEL

The probability of error is reduced by processing the received signal plus noise in such a manner that we are then able to find a sample time where the sample voltage due to the signal is emphasized relative to the sample voltage due to the noise. Such a processor regenerator samples the receiving bit at the maximum peak (maximum eye opening), and the operation of the regenerator during each bit interval is independent of the waveform during past and future bit intervals.

Suppose a delay (Δt) is made on the timing of the sampling instant at the secondary path, thereby the probability of error is increased due to the fact that the superimposed noise peak has a greater probability of taking a magnitude larger than V and of a polarity opposite to the polarity assigned to the transmitted bit. Therefore, the bit error rate is increased in the secondary path due to the time offset of the sampling instant. Hence, an error amplification is created by this technique. There exists a direct relation between increase/decrease of error amplification and

sampling offset Δt.

Derivation of the probability of pseudo-error (error amplification due to sampling offset) can be obtained by considering an eye opening and the effect of the sampling offset on the performance of the parallel path. Fig. 4.16 illustrates a typical eye diagram and the main regenerator sampling instant (at maximum eye opening) along with the parallel path sampling instant (at Δt sec from the optimal timing). (Due to the fact that there is a volt difference on the signal amplitude at t and $t_o+\Delta t$, we could say that the error amplification is caused due to signal degradation, in other words, a decrease in signal to noise ratio of the parallel path.) Thus the degradation in the parallel path is very close to 20 log $2\Delta V$dB and the error amplification in the parallel path can be obtained from S/N versus P(e) curve of the system.

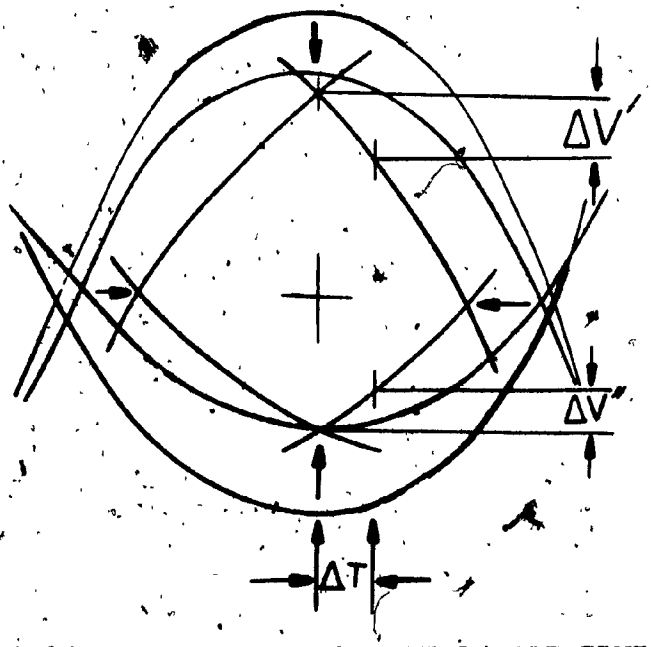

FIG. 4.16 OPTIMUM AND OFFSET SAMPLE TIMING AND THE EQUIVALENT AMPLITUDE DEGRADATION ($\Delta V'+\Delta V''=\Delta V$)

This method is also used in this study to estimate the performance of a data communication system. Experimental results obtained from this type of pseudo-error system is given in the following sections.

4.15 Error Amplification by Introducing More Noise in Parallel Path

The secondary path, has a degraded performance due to the fact that the post detection LPF has a wider band than the post-detection filter in the main demodulator. In this secondary pseudo-error path, more noise will appear than in the main path due to the larger bandwidth. The output sequence of this path has an error rate much greater than the unknown error rate of the main receiver. As was mentioned before, this amplified error rate is obtained by taking the main receiver output data as a reference and counting the number of mis-matches with respect to the secondary output data stream. Every mis-match is a pseudo-error.

4.16 Error Amplification by Introducing Intersymbol-Interference (ISI)

Intersymbol-Interference (ISI) enhancement in the secondary path may be obtained by introducing a narrower band LPF than the post detection filter in the parallel path. Due to intersymbol-interference the performance of the secondary path is degraded. Therefore, a large amount of BER is achieved.

The process of detecting the pseudo-error remains the same as the other technique described before.

In addition, it should be pointed out that each of the methods described in sections 4.13 to 4.15 have some disadvantage: The use of more noise may not be possible since the noise available may be restricted by bandpass filters in the system, the use of the sampling point offset method of introducing degradation can be jitter-sensitive and the shape of P(p) versus Eb/No curve may be less than ideal at the same error rates if ISI degradation is used.

In order to overcome the problems variations in the methods described are possible. For example, a pseudo detection path may be created containing its own PSK demodulation path and its own bandpass filter. Such an approach would permit the pseudo demodulator design to be independent of any constraints imposed by the traffic path bandpass filter.

CHAPTER 5

IMPLEMENTATION OF PSEUDOERROR MONITORING TECHNIQUES FOR PSK TRANSMISSION SYSTEM

5.1 Design and Evaluation of a Pseudoerror Monitoring For PSK Transmission System

The theory described in the previous chapters will now be applied to an example in data transmission system. Attention will be focused in particular PSK implementations because of PSK's utility, generality and the ease by which the concepts can be directly applied to baseband transmission systems. It is also well known that coherent binary and four-phase PSK system performance can be theoretically analyzed in an equivalent baseband configuration. For this reason our theoretical baseband model presented in the previous section directly applies to PSK systems.

5.2 Principle of Operation Data Above Voice (DAV)

Radio relay systems carrying FDM voice or video traffic using frequency modulation can be used to carry an additional digital signal up to several megabits in capacity. The data transmission system used to implement for the pseudo-error concept is termed Data Above Voice/Video (DAV/DAVID) and employs a QPSK carrier above the top baseband frequency of the existing analog traffic in a part of the baseband not normally used for FDM transmission. DAV equipment carries 1.544 Mb/s and is also used on cable systems and is suitable for satellite communication systems.

In DAV the 1.544 Mb/s or 2048 Kb/s bipolar digital signal is converted to a four-phase coherent PSK modulated signal and combined with the FDM baseband. In the case of a 960 channel FDM baseband, the QPSK signal is located at 5.0 MHz. For this use any continuity

pilot and noise measuring slot must be above 6MHZ. For other system channel capacity, different frequencies for the QPSK carrier and pilot would be more appropriate to provide the most efficient system.

At the receiver side the QPSK signal is separated from the FDM baseband and demodulated to provide a bipolar output. The FDM baseband is filtered to remove the QPSK signal.

For all DAV measurements a Quarternary Coherent PSK modem designed by RCA Limited was employed. This modem forms the most essential part of the RCA-9502 DAV-DAVID System. The block diagram of the receiver section is shown in Fig. 5.1.

The transmitter performs essentially the inverse signal processing functions from that of the receiver and therefore is not shown here.

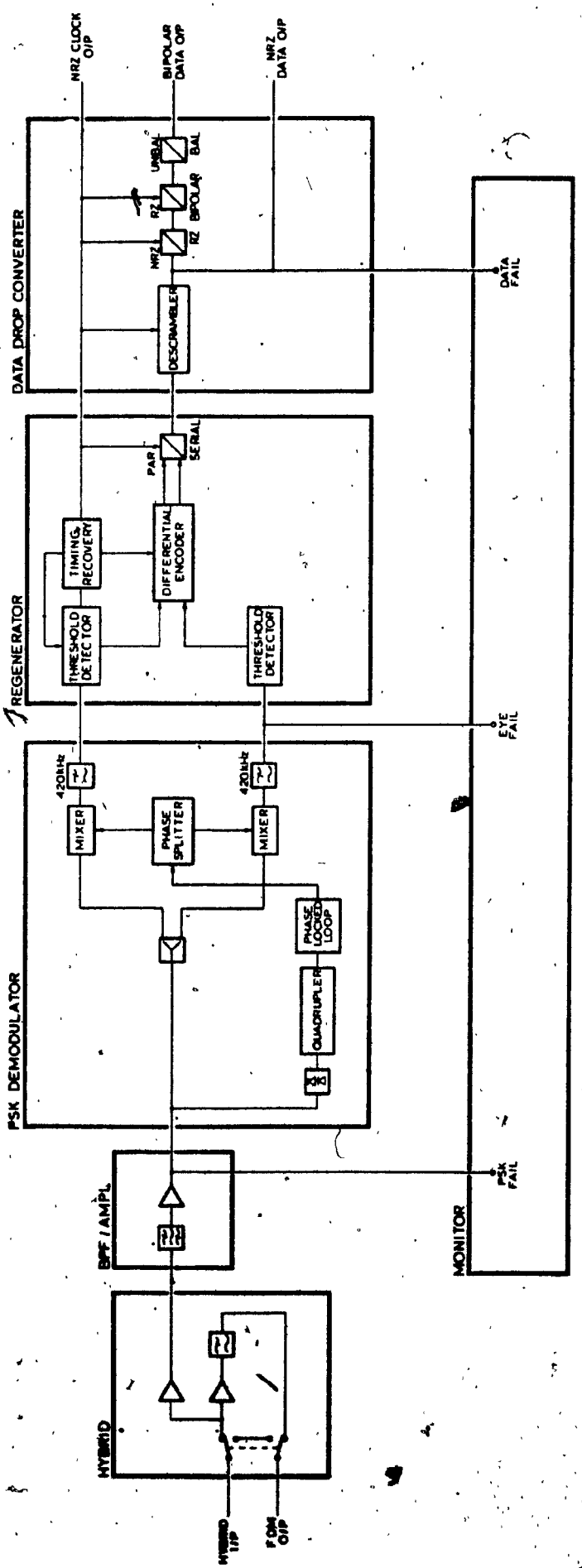

FIG. 5:1 FUNCTIONAL BLOCK DIAGRAM OF DAV RECEIVER

5.3 Pseudo-Error Monitor Circuit Description

In this section the general principle of operation of a Pseudo Error Monitor implemented with digital techniques is given.

Five different pseudo-error monitors implementing various techniques were completely designed and evaluated. The first one designated 2-PEZ, where the 2 preceding PEZ represents the number of slicing levels (one pseudo-error zone). The second was Multi-Zone Pseudoerror Monitor (MZP). Of this model an operational prototype unit was assembled and tested, the number of pseudo-error zones for this monitor were four for each logic level. The third monitor was a combination of the three error amplification units described before (noise addition (Fig.5.2); sampling point offset (Fig. 5.3) and intersymbol interference enhancement (Fig.5.2). These monitors were operational at 1.544 Mb/Sec.

The block diagram of a two-level PEZ is shown in Fig. 5.4. The buffer amplifier

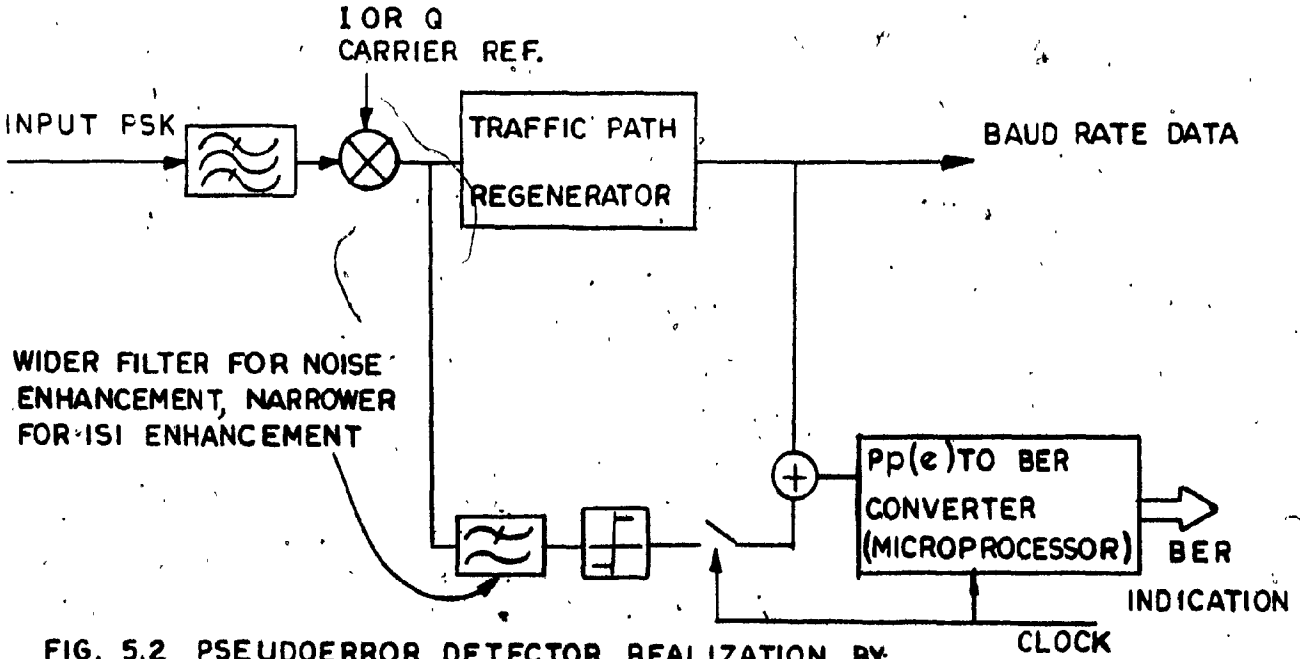

FIG. 5.2 PSEUDOERROR DETECTOR REALIZATION BY FILTER MODIFICATION

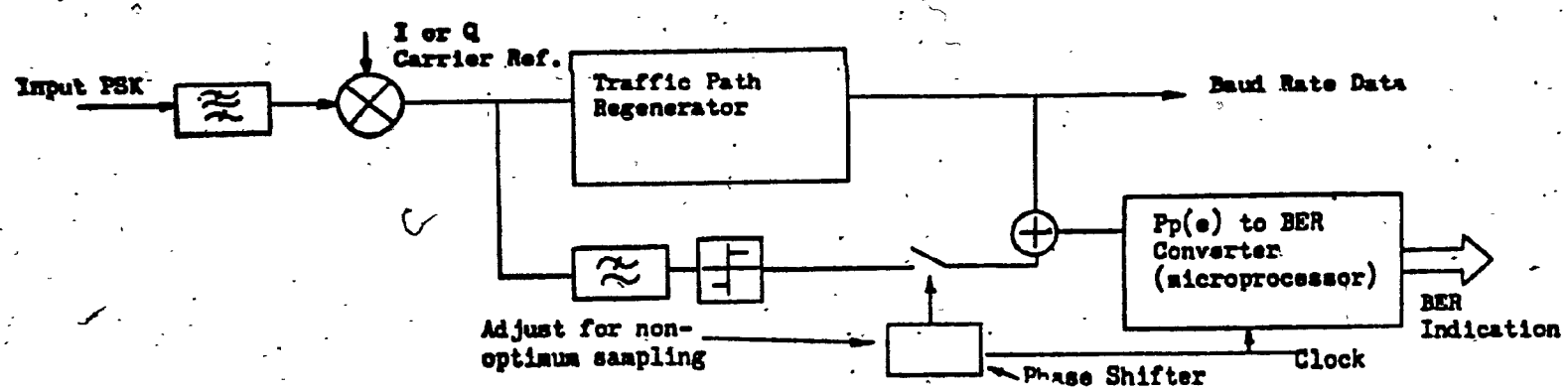

FIG. 5.3 PHASE OFFSET METHOD OF PSEUDOERROR DETECTOR IMPLEMENTATION

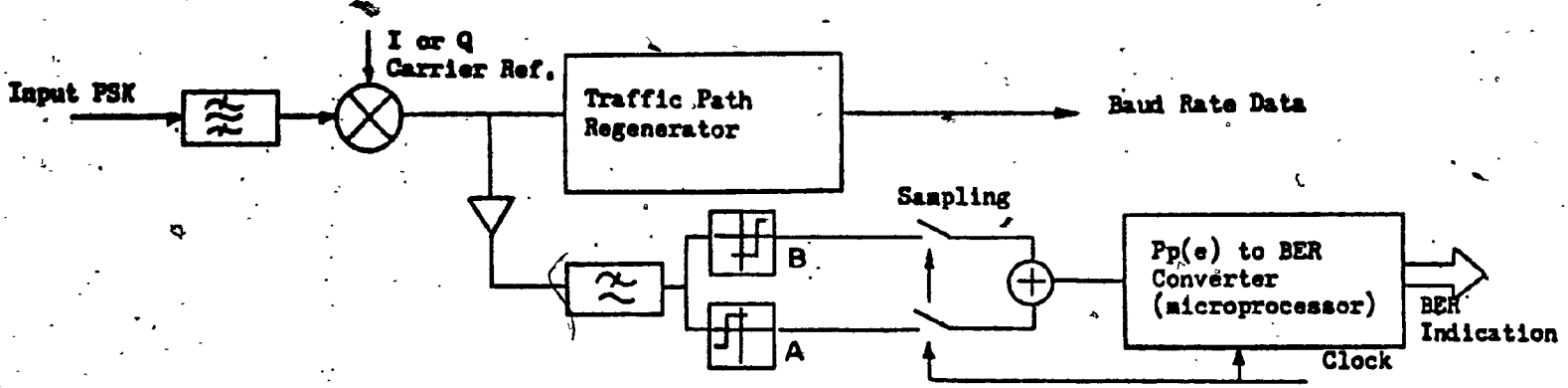

FIG. 5.4 DOUBLE THRESHOLD PSEUDOERROR DETECTOR REALIZATION

maintains a high bridge impedance to isolate the modem from the 2-PEZ monitor. The high input impendance and unity gain property of this amplifier maintains the exact replica of the demodulated signal to the input of 2-PEZ without any effect on the main data traffic.

The two threshold comparators in the diagram are set equi-spaced above and below the nominal level of the modem's threshold comparator.

The internal clock from modem bit timing recovery circuit is 1/2 times faster than data bit rate ($\frac{1.544}{2}$ Mb/Sec).

This clock is used for two purposes:

(1) To sample the composite signal peak at the maximum eye opening. This operation is performed through a J-K flip, flop where the output and the inverted output from the threshold comparator is fed to K and J inputs of the flip, flop respectively. At each clock pulse leading edge transition, the content of J-K is transferred to Q output of the flip, flop.

(2) To drive the P(p) to BER logic converter.

The output from the building block A has more probability of detecting negative pulses incorrectly whereas, the output from the building block B has more probability of detecting positive pulses incorrectly. Threshold comparator of Block A detects peaks of the composite signals with regard to reference level A, see Fig.(4.11). The comparator of block A will detect the composite signal peaks below A as a negative pulse (logic state zero), whereas the threshold comparator B will detect the same signal positive (logic one) as long as it falls in the pseudoerror zone, therefore, the two signals will have opposite polarity. Detected signal peaks above the level A will have positive polarity (logic state one) at the output of both treshold comparators and similarly the signal peaks selected below the level B will have negative (logic state zero) for both threshold comparators. Therefore the combined operations of sampling the signal peaks, determining the state of logic through both comparators independently and the modulo two addition of the two outputs from the threshold comparator will result in random binary pulses representing the number of composite peaks within the pseudo-error zone. Finally the last of these building blocks is a pre-programmed logic circuit or a microprocessor which converts the number of pseudoerrors to the true error rate.

The circuit diagram for the two-level PEZ is given in Fig. 5.5. This circuit having a total of 33 components was implemented using "Emitter Coupling Logic" (ECL) integrated circuits to take advantage of this relatively high speed logic family in comparison with the other families.

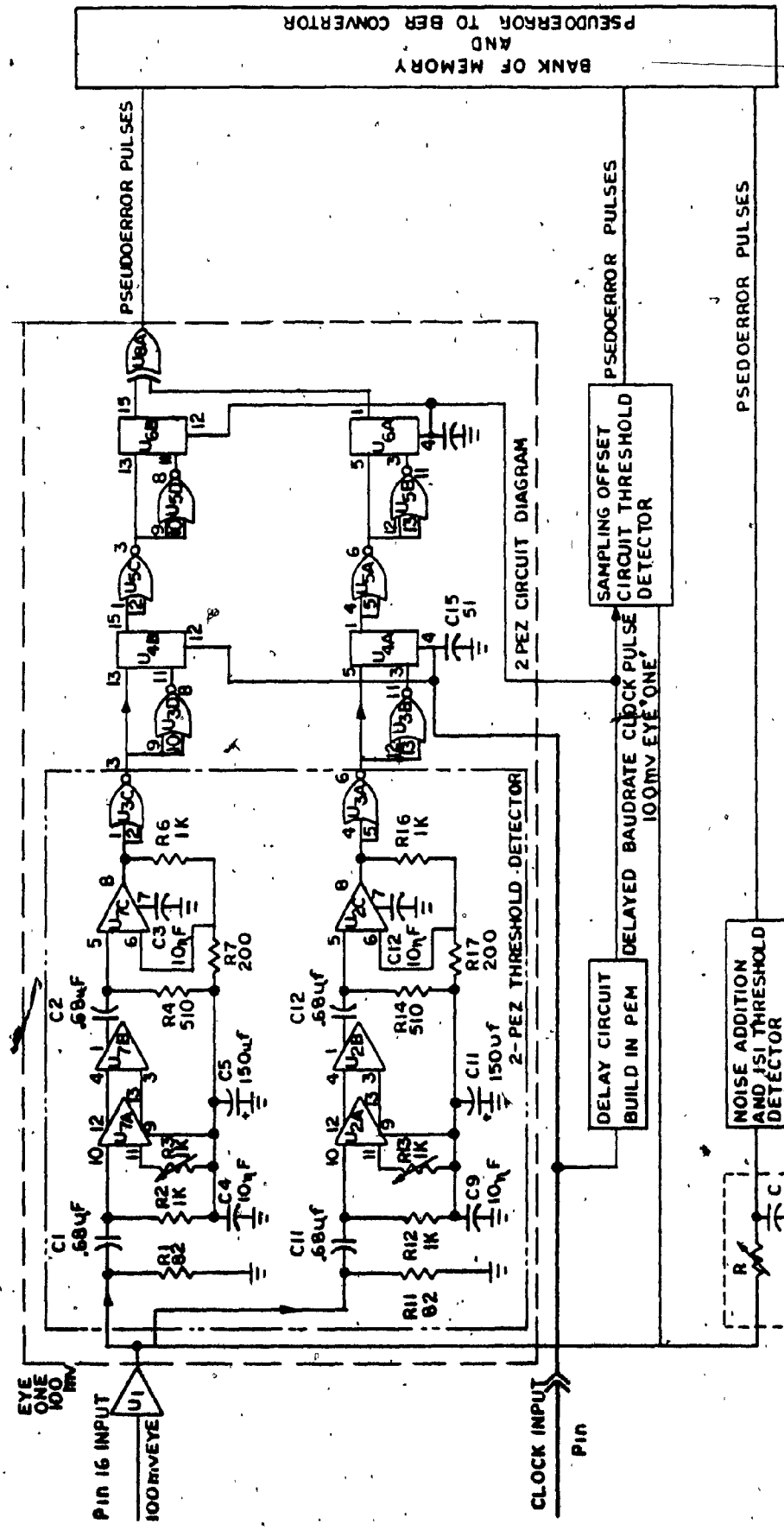

FIG. 5.5 CIRCUIT DIAGRAM OF 2PEZ AND GENERAL DIAGRAM OF PEM CIRCUIT

5.4 Principle Operation of MZP Monitor

Having established the general principle of operation of the 2-PEZ monitor, a brief survey of the principle operation for the MZP monitor is given.

The block diagram of MZP is given in Fig. 5.6.

This monitor was implemented using ECL logic devices due to relatively high bit rate of the modem.

The general principle operation of the MZP is similar to 2-PEZ, it differs in principle with the number of threshold levels, implementing equal number of threshold detectors. The "exclusive or" logic device combines the two adjacent threshold outputs which will result in a random pulse stream indicating the number of composite signal peaks detected in the zone between two levels.

Finally the outputs from the exclusive or logic devices can be either fed to a microprocessor, a preprogrammed logic device or a digital counter circuit with a predetermined counted threshold level, to activate the corresponding LEDS determining the estimate of the BER of the system.

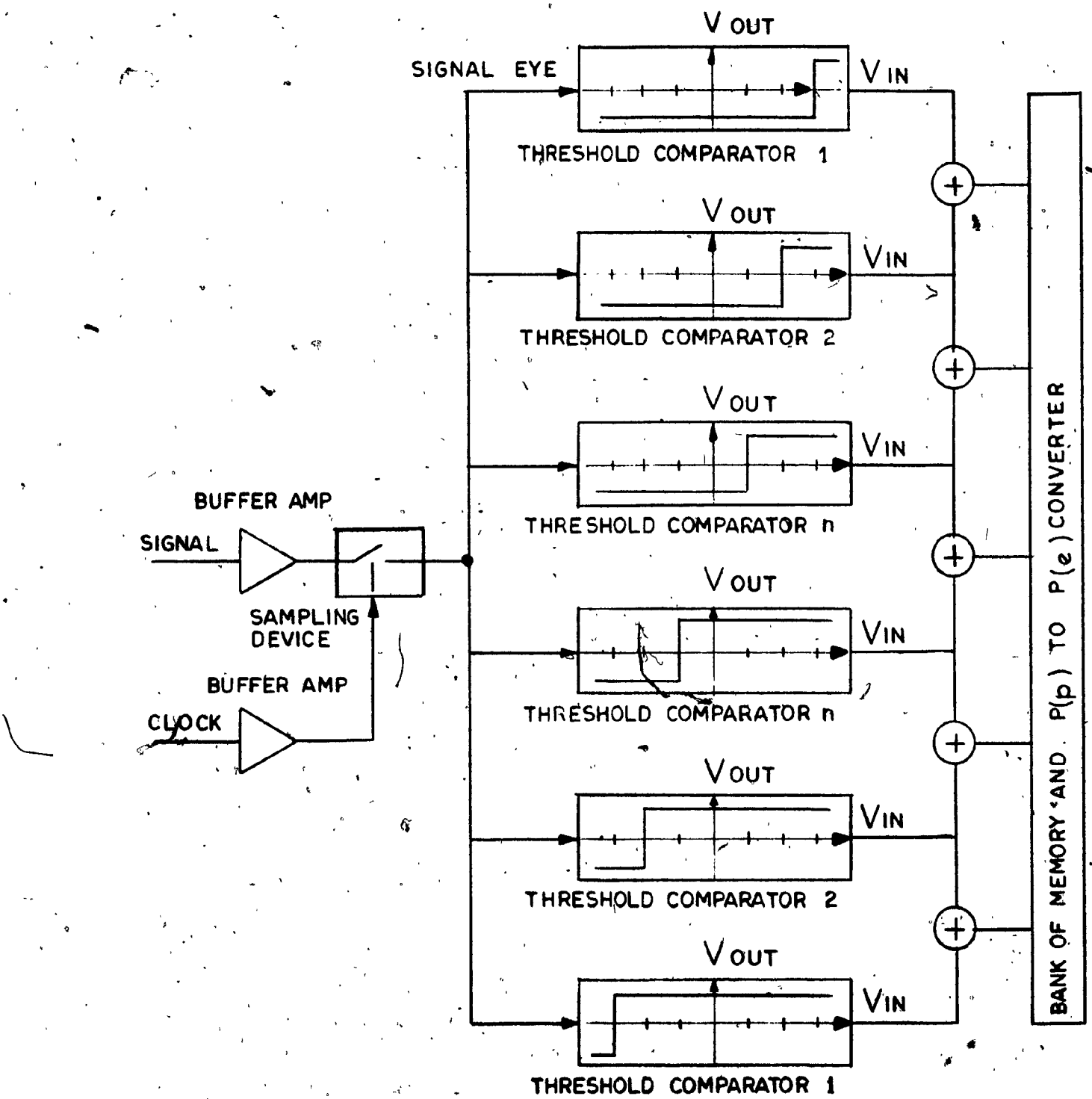

FIG. 5.6 · BLOCK DIAGRAM OF MZP MONITORING SYSTEM

5.5 Noise Addition, Intersymbol Interference (ISI) Enhancement and Sampling Offset Implementation Technology

Circuit components used for pseudo-error detection path implementing, noise addition, intersymbol interference (ISI) enhancement and sampling offset, are generally the same type as used for the modem traffic path. Figs. 5.2 and 5.3 illustrate the block diagrams of the three implementation techniques.

As stated before for the case of noise addition, more noise power in comparison with the receiver noise power is introduced due to the fact that the LPF of the pseudo-error path has a wider equivalent noise bandwidth than the postdetection LPF of the modem receiver (Fig. 5.2). Conversely, by maintaining an LPF in pseudo-error path, with a smaller cut-off frequency than the LPF of the main data path, the eye diagram opening becomes smaller due to the fact that ISI of the pseudo-error path is greater than the main data path (Fig. 5.2). In the case of sampling offset the regenerator part of the pseudo-error section remains the same as the main data regenerator, except the sampling time (*clock*) is offset from the maximum eye opening position with a delay circuit which can be simply implemented with a variable resistor, a capacitator and a flip flop. The triggering time of the flip flop is varied with the variation of the rising and falling time of the variable R-C in conjection to the strobing pins of the flip flop. This maintains a time delay relation between the input output of the flip flop.

The other ingredients are the buffer amplifier to isolate the pseudo-error path from the modem traffic path and the P(p) to

BER converter. The latter device is able to identify the BER corresponding to the number of pseudo-error counts received in the measurement time T_m over the entire BER range of interest. The first element in its construction is generally a counter acting as a totalizer. Simple digital or hybrid circuitry may then be used to process the counts and produce a BER estimate. Of particular note, for some applications, is the utility of a microprocessor since its programming and storage can contain very accurate information on the P(p) to BER relationship.

5.6 Physical Description and Circuit Diagram

(a) Functional Description

The Pseudo-Error Monitor unit is used with a DAV and/or DAVID hybrid series. This unit is also capable of monitoring the BER of any other digital modems. The unit may be used at terminals or through repeaters. The unit is used to monitor the modem BER and may control the switching and diversity terminals throughout the communication system. The unit also generates alarm logic outputs for use in associated circuits.

(b) General

The PEM card is mounted in an RCA-M-600 receiver base-band amplifier and alarm shelf. The 100 millivolt baseband eye ("eye 1" or "eye 2") from either one of the 420 KHZ (cut-off frequency) LPF enters the unit at Pin 6 (Input), buffered by U_1. U_1 is a unity gain high input impedance (greater than 10^7 ohm) with a low

output impedance of approximately 10 Ohms. The signal output from U_1 is directly connected to four pseudo-error generator circuits. The signal amplitude remains the same (100 m volts) at the inputs of PEM circuits because of the low output impedance of U_1.

The first one of the four PEMs is a 2-PEZ circuitry basically consisting of two differential amplifiers U_2 and U_3, variable resistors, and J-K flip flops.

The signal is applied to U_2 throughout R_{11} and C_{11} and R_{12}. The variable resistor R_{13} sets the drive level (one of the two levels of 2-PEZ) of the differential amplifier U_{2B} (Pin 3 and 4). Single output at pin 1 of U_{2B} is connected through C_{12} to one of the dual inputs at pin 5 of U_{2C}. The gain and stability of the differential amplifier connected in tandom in order to form the threshold detector is established by the signal feedback from the output (pin 8) through R_{16}, R_{17} to pin 9 of U_{2A}. The output from U_{2C} at pin 8 is connected through U_{3A} and U_{3B} to J-K flip flop dual inputs (U_{4A}). The function of U_{3A} and U_{3B} is basically to shape the output signal from U_{2C} in a proper rectangular ECL level. The clock signal enters the card at pin 16 and is fed to pin 4 of U_{4A}. U_{4A} samples the threshold differential amplifier at the point where the maximum eye opening is located, i.e. it is synchronized with the modem regeneration clock timing circuit. The data output from U_{4A} is then fed to U_{6A} (J-K flip flop) through U_{5A} and U_{5B}. The timing clock of U_{6A} is provided from the clock delay circuitry built in the PEM unit in order to synchronize all the pseudo-errors generated by the pseudo-error generators in the PEM Unit.

The second circuit connected to the output of U_1 is similar to the circuit described before. The function of this circuit is similar to the one described before with an identical circuit description. The only difference of this circuit from the former is that the comparator drive variable resistance is tuned in such a way that the second decision level is the mirror image of the first comparator decision level, from the modem regenerator decision level.

The output from U_{7C} is then applied to the dual input of U_{4B} (pin 13 and 11) through U_{3C} and U_{3D}. The clock rate of the modem receiver is used to trigger U_{4B} (J-K flip flop) at maximum eye opening. U_{4B} is used as a sampling device. The random binary sequence data at the output of U_{4B} is then applied to U_{6B} through U_{5C} and U_{5D}. U_{6B} is triggered by the delay clock from the delay circuitry which maintains the sampling offset circuitry within the PEM unit. The latter shifting process on data is due to the fact that the pseudo-error pulses from 2-PEZ and other sources of pseudo-error should be time-synchronized with the output pseudo-error pulses using sampling offset technique.

Finally the random data from the outputs of U_{6A} and U_{6B} which do not carry the same information, due to the fact that the threshold levels were offset, are applied to the dual inputs of an "Exclusive Or" logic gate, U_{8A}. The random pulses at the output of U_{8A} indicate the number of mis-matches of the data at the dual input of U_{8A}. The number of pseudo-error pulses in an observation (test period) achieved from this technique indicate the number of

composite signal peaks within the PEZ. Finally these pulses are applied in P(p) and P(e) logic circuit.

The third of the four outputs from U_1 is applied to the input of a pseudo-error generator circuit based on offsetting the time of the sampling device. The threshold detector circuit (U_9) will remain the same as the modem regenerator threshold detector. The output signal from U_9 is applied to the dual input of U_{10A} (J-K flip flop) which is triggered by the delayed clock rate with respect to the modem clock rate. The delay on the clock rate is performed by a dual input flip flop (U_{11}) and a variable R-C circuit. The delay circuit operates according to the variable time constant of the R-C, i.e. the flip flop will register the clock until its $\bar{Q}$ output arrives to the flip flop triggering level, (feeds back through R-C to its other output) then releases the registered clock to its output. As stated before the output clock is delayed according to the input clock of U_{11}. The output data from U_{10}, which consists of a higher error rate in comparison with the main data, is applied to one of the dual inputs of U_{8B} for comparison with the receiver main traffic data. In order to avoid any interruption from PEM to the receiver main data traffic, a duplicate of the receiver regenerator is built in the PEM unit. The output from this unit is delayed through U_{10B} (J-K flip flop) and applied to the other input of U_{8B}. U_{8B} generate pulses, namely pseudo-error pulses, according to the mismatches of the signals from U_{10A} and U_{10B}. Finally the pseudo-error pulses are applied to P(p) to P(e) logic circuits.

The last one of the signal outputs from U_1 was applied to a

receiver conventional regenerator (built-in the unit) through a R-C LPF with a cut-off frequency much less than the cut-off frequency of the receiver LPF. The R-C LPF degrades the eye pattern by introducing more intersymbol interference (ISI). Obsiously the output from the latter regenerator has more error rate due to the eye closure of the signal in this path.

Finally the output data from the ISI circuit is compared with the main data, generated in the unit, through U_{8C} (exclusive or logic gate). The output from U_{8C} is delayed and applied to P(e) to P(p) logic circuits.

In order to achieve a pseudo-error rate based on decreasing the signal to noise ratio of the pseudo-error path, a LPF with broader cut-off frequency band than the receiver post-detection LPF is developed. The signal in this case is taken before the receiver post-detection LPF and applied to the pseudo-error LPF. The remaining process is similar to the ISI circuit and finally the pseudo-error rate is delayed and applied to P(p) to P(e) logic device.

This monitor having a total of 95 components was implemented using ECL integrated circuits to take advantage of its relatively medium speed in comparison with other families.

The IC's numbers, resistance and capacitance values are given in Table 5.1.

As stated before, the P(p) to P(e) logic device can be either a simple analog or digital counter or it may be a sophisticated microprocessor circuit, depending on the system requirement and applications. For this reason it has never gone beyond the stage

of prototype. For the same reason no P(p) to P(e) was permanently added to PEM, although the measurements were taken using external counters to accumulate count of pseudo-errors during the test periods. A double sided printed circuit artwork for the PEM was prepared as it is shown in Figs. 5.7 and 5.8.

The final assembled version of PEM is shown in Fig. 5.9. Notice that all output signals are accessible through the PEM front panel BNC connectors. Provision was made to have these signals on the rear plugboard via finger pins (Fig. 5.7).

Finally, Fig. 5.8 also shows the PEM components layout which will facilitate the PEM assembling procedure.

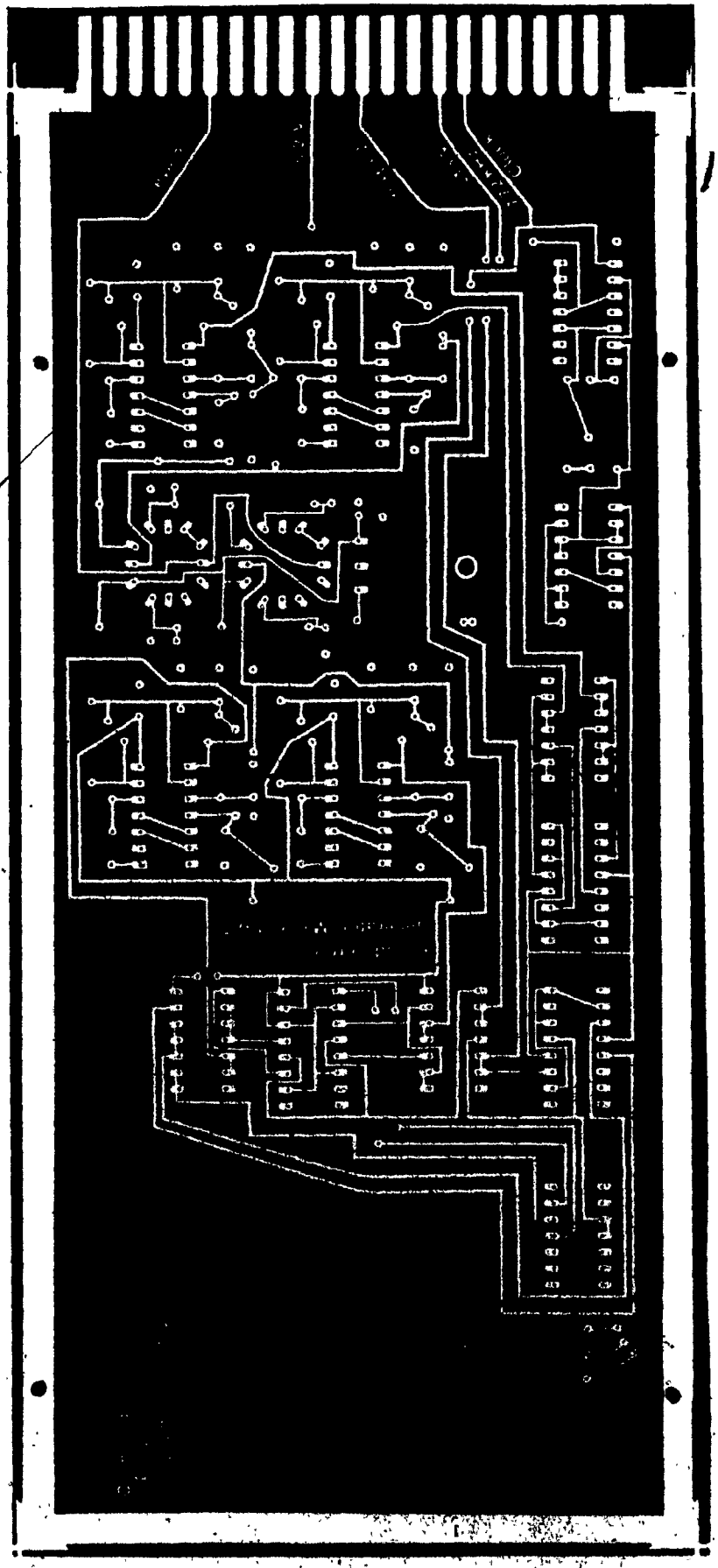

FIG. 5.7 PEM PRINTED CIRCUIT DIAGRAM

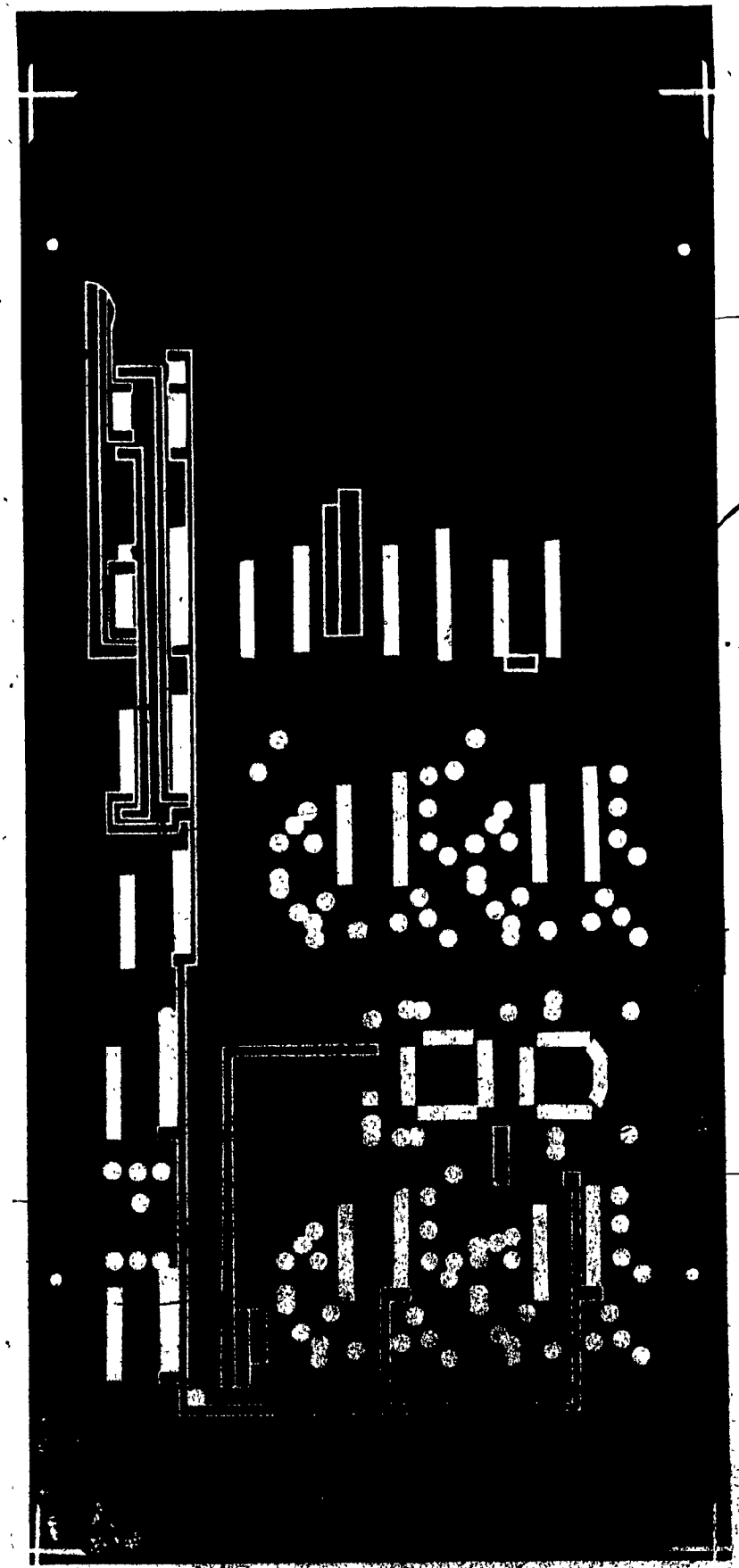

FIG. 5.8 PEM COMPONENTS LAYOUT

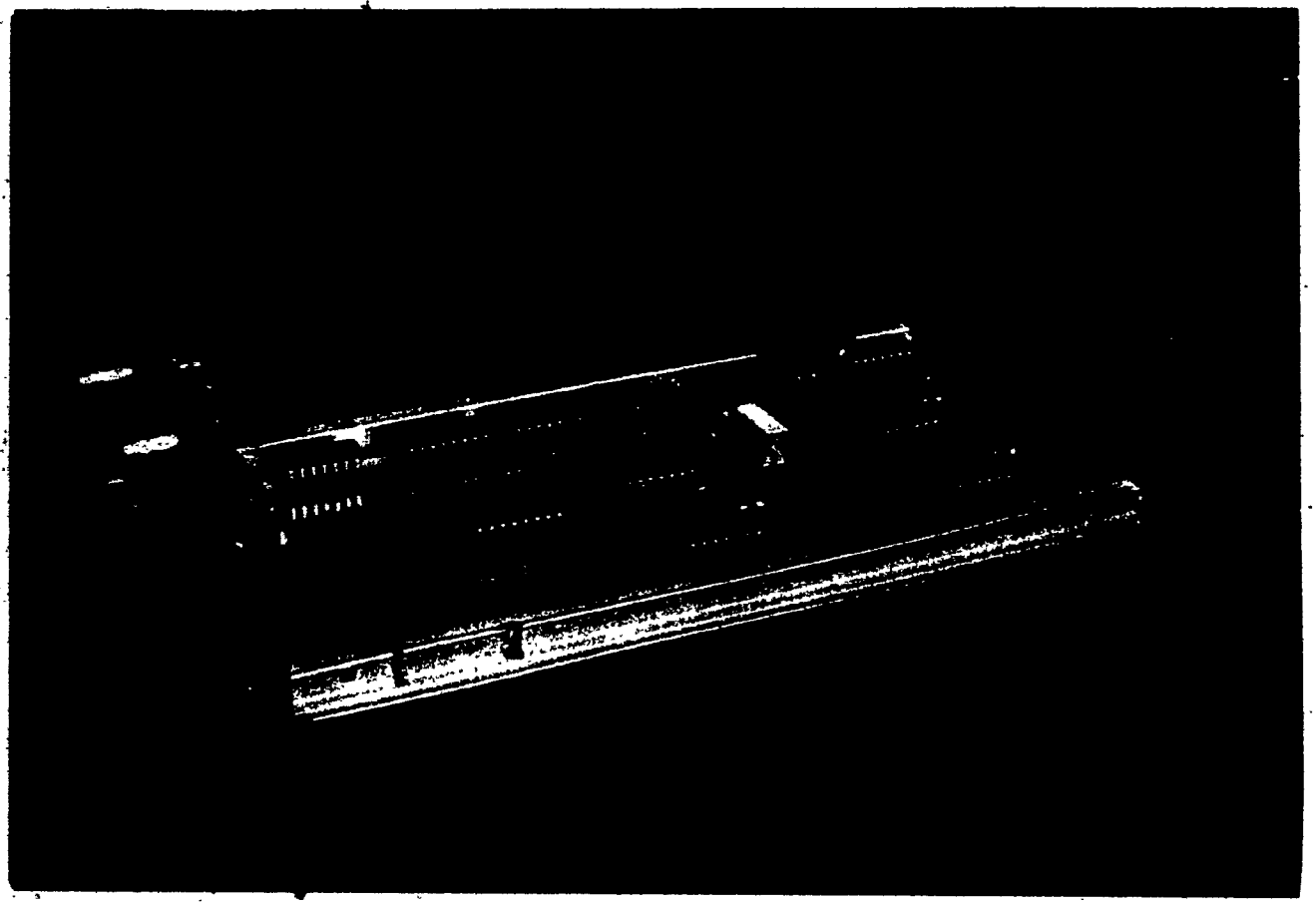

FIG. 5.9 PEM CARD DESIGNED FOR RCA-DAV MODEM TO DETECT THE PERFORMANCE OF THE DATA TRANSMISSION PART

5.7 Measurement Techniques and Test Results

This section describes the different set-ups and techniques utilized in measuring the PEM performances. These measurement results are given.

Fig. 5.10 shows the test bench equipped for medium frequency digital communications performance evaluations.

Excluding the burst measurements, implementation methods applicable to burst type receivers are those used for QPSK Time Division Multiple Access Satellite Systems and Voice Activated Single Channel per Carrier Satellite Systems, the following tests were selected in order to evaluate the character of various types of PEM in different environments:

(i) 2-PEZ measurements by using conventional laboratory equipment, i.e.

(a) P(e) of conventional regenerator versus Eb/No in a Gaussian noise environment.

(b) P(p) versus Eb/No measurement for $\Delta = .5$ and $\Delta = .7$ and their comparison with theoretical predictions.

(c) P(p) versus Eb/No measurement for $\Delta = .5$ and $\Delta = .7$ in the presence of non-Gaussian noise for S/Non-GN 20 dB.

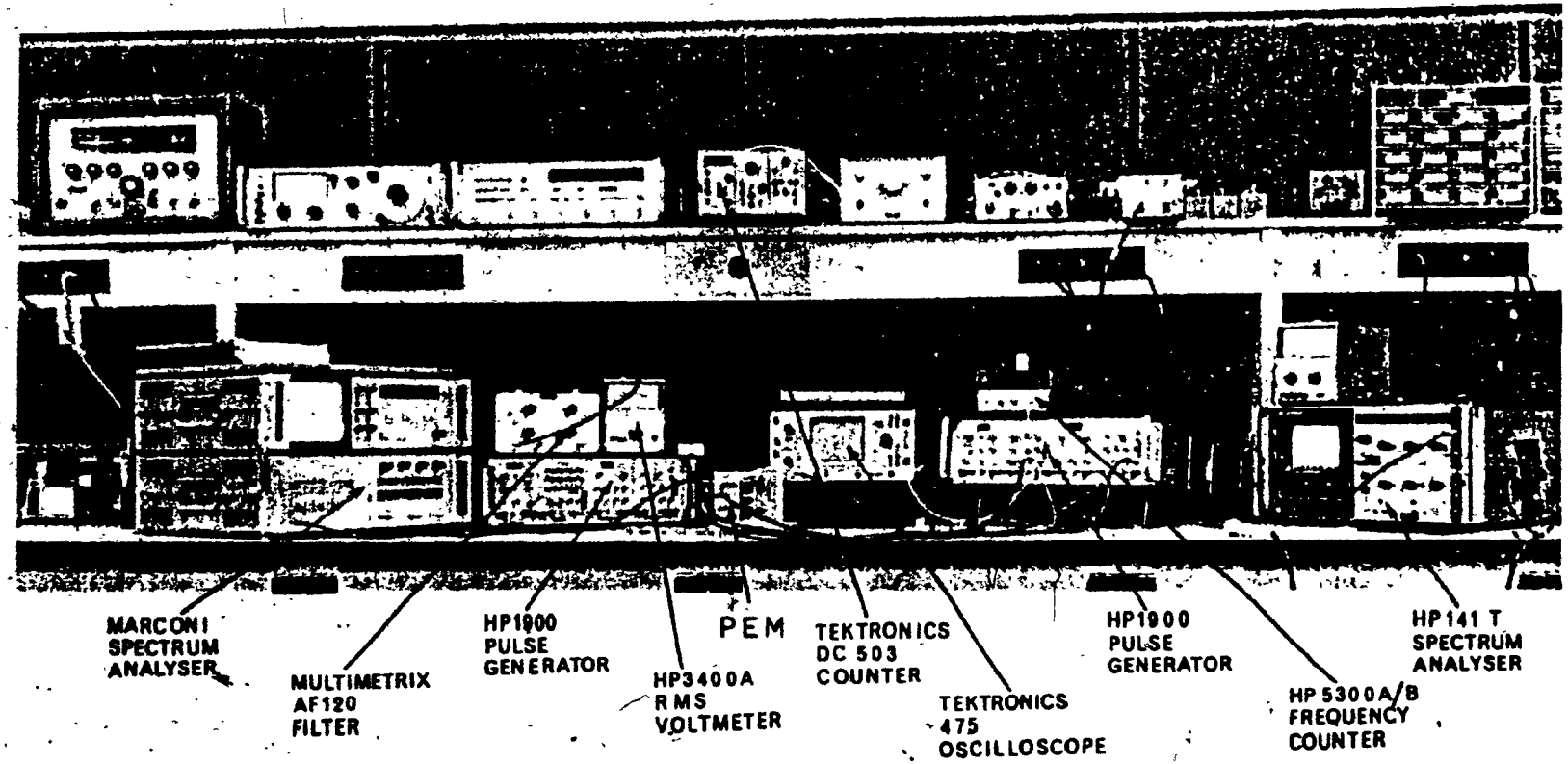

FIG. 5.10 PSEUDOERROR MONITOR TEST SET-UP

(ii) 2-PEZ measurements by implementing the technique on RCA DAV modem, that is:

(a) P(p) versus C/N in Gaussian noise environment for $\Delta = .5$

(b) P(p) versus C/GN in the presence of a 20 dB Carrier to non-Gaussian noise.

(c) P(p) versus C/GN in the presence of a 20 dB Carrier to single frequency tone near the carrier frequency.

(iii) Implementing the PEM Sampling offset technique on RCA DAV modem in Gaussian noise environment with and without 20 dB single tone interference near the modem carrier frequency.

(iv) Measurement of the pseudo-error rate of RCA DAV modem in Gaussian noise environment, implementing the ISI technique.

(v) Measurement of the MPEZ technique utilizing conventional laboratory equipment.

The burst performance of PEM could not be evaluated for the following reasons:

(a) The test equipment available was not suitable to evaluate the burst operation.

(b) This measurement was evaluated in RCA Limited for implementation on the DAV/DAVID Hybrid Transmission system.

The block diagram of the test set-up utilized in evaluating parameters (i) to (v) is shown in Figs. 5.11 and 5.12.

All tests were performed by feeding the PEM with the longest pseudo random binary sequence (220-1) available at the output of the HP 1930A. The data was of NRZ format.

The probability of pseudo-error of the different type of pseudo-error monitored in the presence of various types of interference (Gaussian, non-Gaussian and single frequency tone interference) was evaluated and shown in Fig. 5.13 to Fig. 5.15.

The probability of pseudo-error of 2-PEZ was evaluated using conventional measuring techniques and the block diagram of the test set-up is shown in Figs. 5.11 and 5.12. An amplifier having 20 dB of gain was inserted in the noise path in order to provide adequate noise power in noise bandwidth of less than 100KHz. This filter indirectly limits the amplitude of the noise peaks preventing the amplifier from going into saturation, and deforming the Gaussian probability density function. A 50 to 75 ohms adaptor matches the

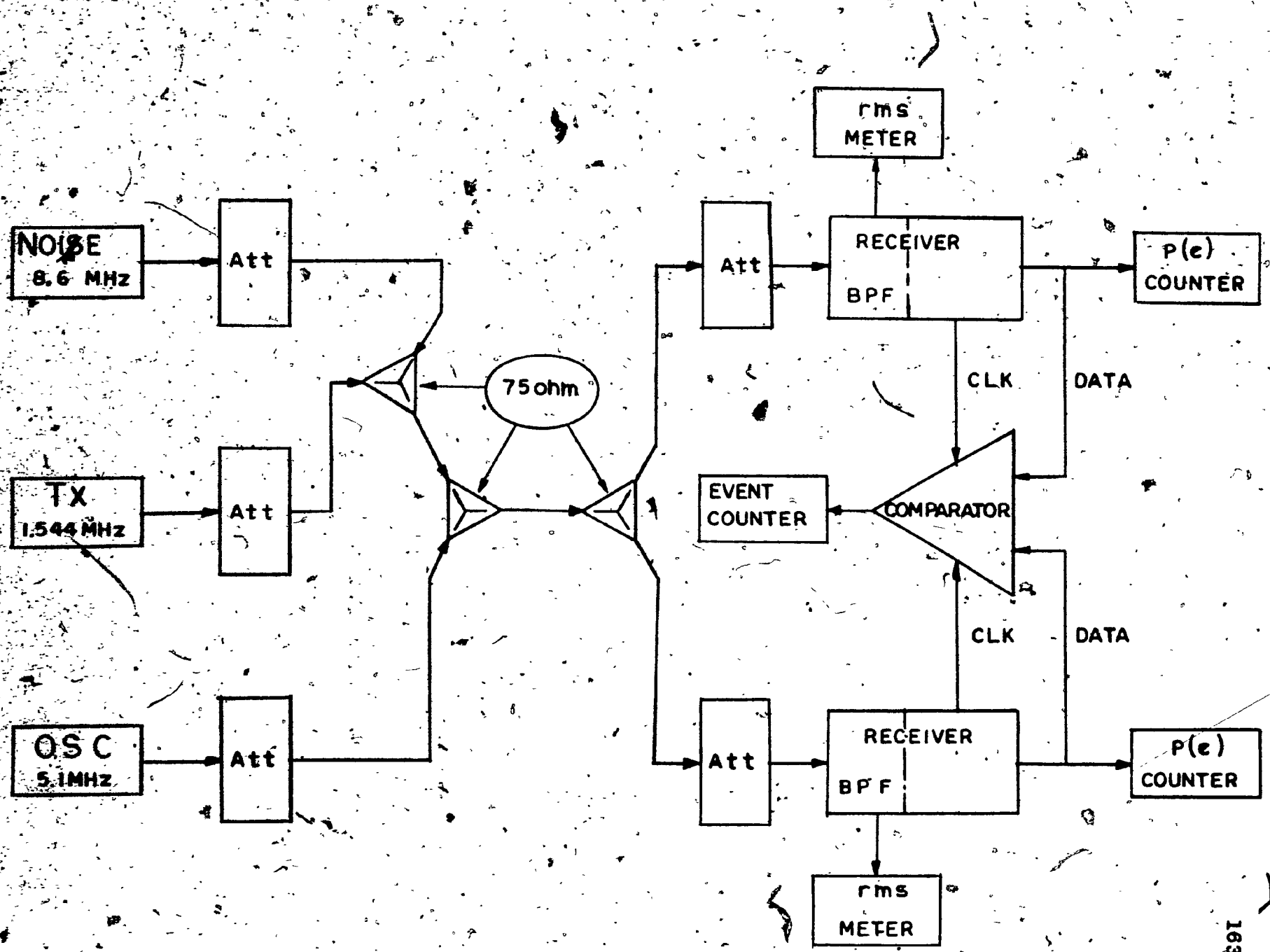

FIG. 5.11 2-PEZ EXPERIMENTAL TEST SET-UP

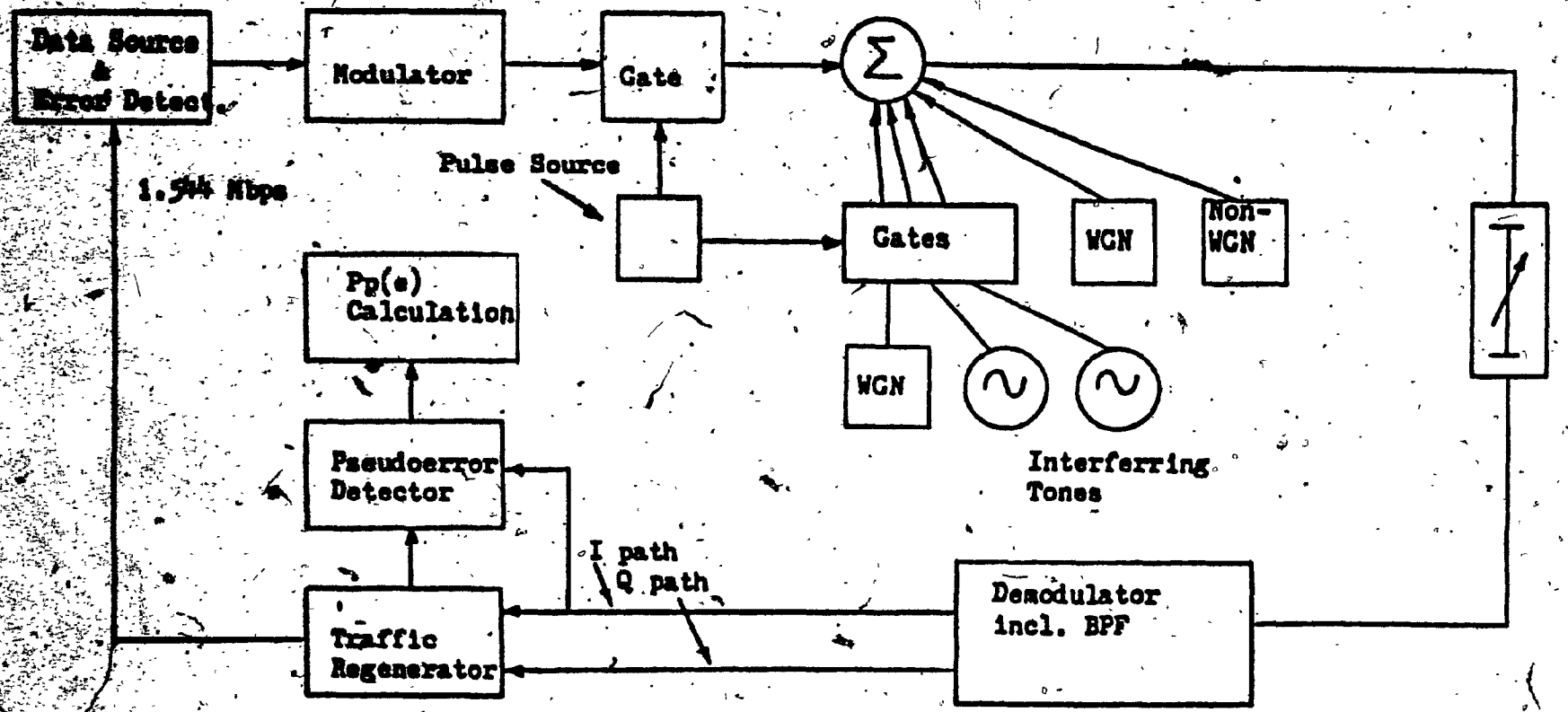

FIG. 5.12 PEM EXPERIMENTAL TEST SET-UP

amplifier output impedance with the variable attenuator. A non-Gaussian noise source was created by passing low-pass band limited Gaussian noise through a nonlinear device (in this case an amplifier was selected operating at its saturation point due to noise power). A linear adder (resistive type T network) combined the Gaussian source output with the non-Gaussian noise source. A second linear adder combined the transmitter output with the noise sources. This is equivalent to an infinite bandwidth noisy channel. An RC low-pass filter LPF-1 preceded the data regenerator limiting the noise and the signal bandwidths in order to approximate an almost optimum receiver. The rest of the set-up is conventional.

To obtain the best P(p) and P(e) performances the regenerator and 2 PEZ has to sample the received signal at its maximum eye opening. This is achieved by adjusting the clock via the variable delay generator (HP-1909A).

The probability of pseudo-error was evaluated as a function of the measured signal to noise ratio, i.e. P(e) = f(S/N), at the regenerator's input. It was then restated in terms of the energy per bit (Eb) over the noise density (No) using the following relation:

$$\frac{Eb}{No} = \frac{S}{N} \cdot \frac{BM}{br} \qquad (5.7.1)$$

where BM is the measured noise bandwidth and br is the bit rate.

If f_c is the RC LPF-1 cut-off frequency, then the equivalent

noise bandwidth, or measured noise bandwidth is:

$$BM = fc \cdot \pi/2 \qquad (5.7.2)$$

Substituting this relation into equation 5.7.1 and expressing Eb/No in dB we obtain:

$$\frac{Eb}{No}_{dB} = 10 \log_{10} \left[\frac{S}{N}\right] + 10 \log_{10} \left[\frac{fc}{br} \cdot \frac{\pi}{2}\right] \qquad (5.7.3)$$

For a bit rate of 1544 kbps a first evaluation of P(p) for $\Delta = 0.5$ was done using the LPF-1 having a measured fc of 1200 KHZ (BM = 1884 KHZ). The results are given in Figs. 5.16 and 5.17. From these graphs we notice that:

(i) The P(p) curve from 2-PEZ, having $\Delta = 0.5$, is approximately 1 dB away from the theoretical prediction. (Chapter 4, equation 4.5.13.)

(ii) The P(p) curve of 2-PEZ having $\Delta = .7$ is approximately .8 dB away from the theoretical prediction (Chapter 4 equation 4.5.13). These divergences are most probably within the measurement accuracy.

A second P(p) measurement was taken introducing both Gaussian and non-Gaussian noise at the same time. The signal to non-Gaussian noise power ratio was 20 dB. In this case, the regenerator P(e) performance was degraded and the 2-PEZ P(p) performance was worse

than the case for Gaussian noise only.

In this case the probability of pseudo-error increased accordingly with the probability of true error rate, i.e. the pseudo-error rate gain factor, the ratio of probability of pseudo-error to probability of true error rate GF = P(p)/P(e), did not vary greatly for bit error rate less than 10^{-6}.

It has to be pointed out that for small values of the 2-PEZ Gain factor (GF) decreases and the reliability of P(p) curve increases. In this case for the same confidence level longer evaluation time is required.

The performance of a MPEZ was evaluated using the same conventional measuring techniques as 2-PEZ. The measurement set-up is similar to that of 2-PEZ. Two additional digital counters were used to count pseudo-error pulses obtained from the remaining pseudo-error zones.

The probability of pseudo-error of the three existing zones were evaluated as a function of the measured signal to noise ratio, i.e. P(p) = f(S/N), at the regenerator's input. It was then restated in terms of Eb/No using equation 5.7.3.

For a bit rate of 1544 Kbps evaluation of P(p), for Δ = .2, Δ = .4 and Δ = .6, was done using the LPF-1 having a measured f_c of 1200 KHZ (BW = 1880 KHZ). The results are given in Fig. 5.18. From this graph we notice that:

(i) The P(P) of each zone is different for a given Eb/No.

(ii) From an evaluation time and confidence level point of view, in a given P(p) range of interest one zone is more reliable than the other.

The test set-up used to evaluate the performance of pseudo-error monitor (PEM) is shown in Fig. 5.12. It depicts a four-phase PSK modulator/demodulator together with instrumentation to introduce various forms of channel impairments and signal interruptions. Note that any combination of noise and single frequency tone can be introduced. The QPSK modem employed for the test operates at 1544 Kbps. The error rate and pseudo-error rate measurements are carried out utilizing one half of the information data from the QPSK demodulator, i.e. the PEM operating bit rate was 772 Kbps. Because of the identical circuits utilizing the QPSK modulator and demodulator path and the scrambled data output from the demodulator outputs with an equal probability of "ones" and "zeros", it is logical to conclude that the P(p) and P(e) obtained from this measurement set-up is half the actual pseudo-error and true error rate of the QPSK modem. The key elements of the test set-up are shown so as to depict with clarity the functions carried out. The regenerator employed in PEM was designed identical to that employed in the modem receiver so that it provided the same traffic data as a reference.

Fig. 5.13 shows the results achieved in tests depicting samples of performance utilizing the methods of sampling offset and the ISI enhancement. These tests show that large gain factors are possible. The gain factor can be varied anywhere from 1 to 5×10^5 in the following ways: by adjustment of the cutoff frequency of the low pass filter (using the ISI method), by adjusting the sampling instant timing and finally, by changing the levels of 2-PEZ. The curves are depicted in terms of four-phase carrier to noise ratios. It should be noted that the gain factor is not the same for all bit error rates, nor is it linear with BER.

Fig. 5.14 shows the performance of the modem and the pseudo-error detector in a situation in which there is additional Gaussian noise as well as a carrier wave tone creating a C/I ratio of 20 dB (Sampling offset, ISI enhancement and 2-PEZ methods of PEM implementation). The traffic data errors and the pseudo errors are both increased by the single frequency tone while the gain factor remains reasonably stable.

By passing low pass band-limited Gaussian noise through a nonlinear device, a non-Gaussian source was created. In order to check that the detector remained stable out of band intermodulation noise was used. This intermodulation noise was similar to a "spiky" noise. It had a greater damaging effect on the P(e) curve than the Gaussian noise had. Both Gaussian and non-Gaussian noise were introduced simultaneously. The carrier to non-Gaussian noise power ratio was 20 dB. There was little change in the gain factor for bit error rates of less than 10^{-5} (see Figs. 5.13, 5.14 and 5.15).

In conclusion one can say that the two most important elements in the performance of a pseudo-error detector are the following:

(1) The ability to achieve a sufficient error gain factor.

(2) The ability to achieve a stable gain factor in a situation in which there are both Gaussian and non-Gaussian perturbations.

The error gain factor has been defined previously as the ratio of P(p) to P(e) at a given bit energy to noise density ratio (Eb/No). If the pseudo-error detector is being used to estimate the BER in a short time span, then high gain factors are usually desirable. It should be noted that the gain factor does not necessarily have to be the same over the range of the BER of interest, but it should be relatively stable.

$R_1 = R_{11}$ - 82Ω

$R_2 = R_{12}$ - 1K

$R_3 = R_{13}$ - 0 to 1K

$R_4 = R_{14}$ - 510Ω

$R_6 = R_{16}$ - 1K

$R_7 = R_{17}$ - 200Ω

$C_1 = C_{11}$ - 0.68μF

$C_2 = C_{12}$ - 0.68μF

$C_4 = C_9$ - 10nF

$C_5 = C_{11}$ - 150μF

$C_3 = C_{12}$ - 10nF

U_1 - LH0033CG - 603

14 - U_2 - MC1035P - 7

14 - U_3 - MC1010P - 7

14 - U_4 - MC1032P - 7

14 - U_5 - MC1010P - 7

14 - U_6 - MC1032P - 7

14 - U_7 - MC1035P - 7

14 - U_8 - MC1030P - 7

TABLE 5.1

PEM COMPONENT DESCRIPTION

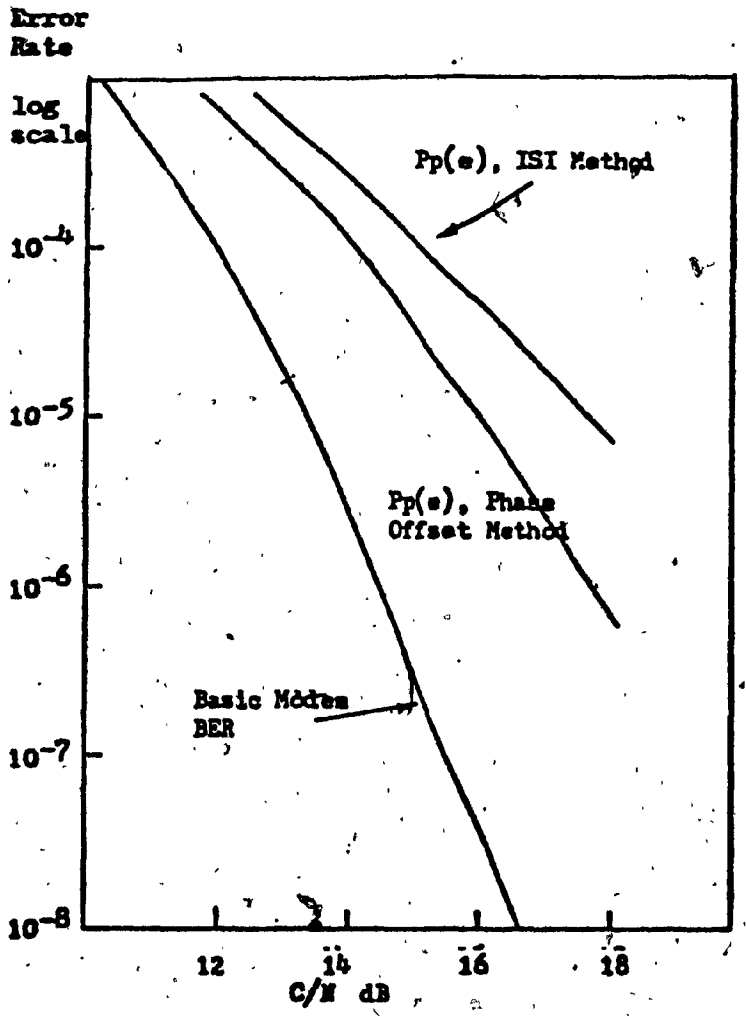

FIG. 5.13 PSEUDOERROR DETECTOR PERFORMANCE IN GAUSSIAN NOISE

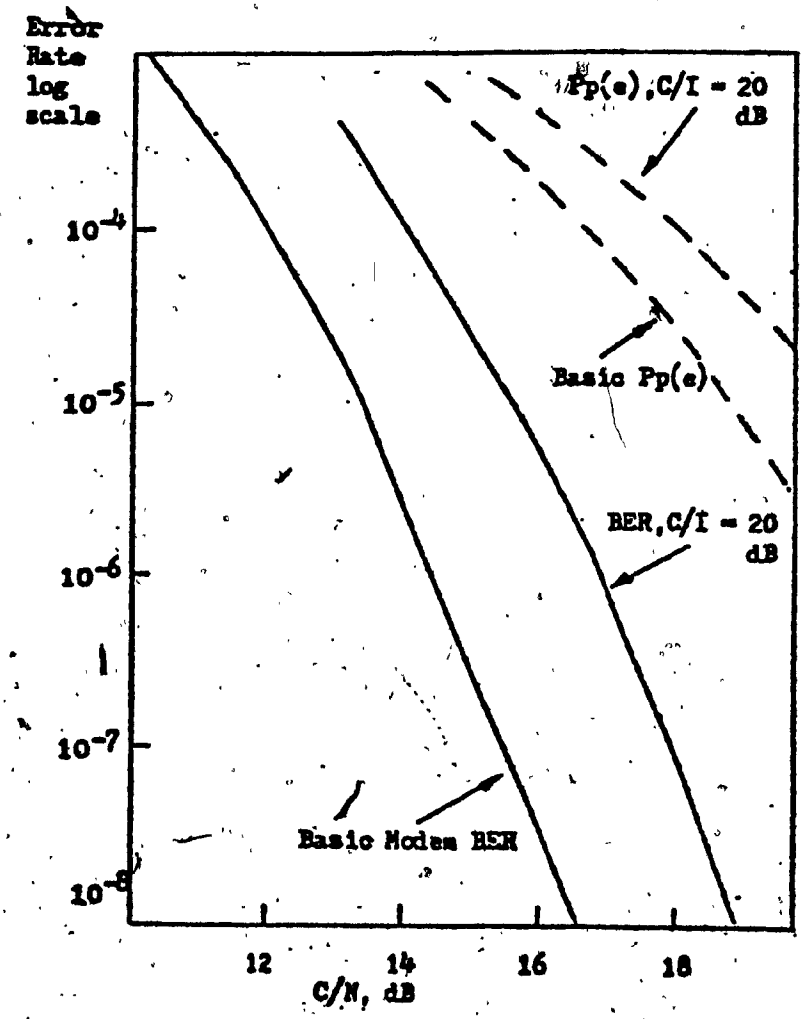

FIG. 5.14 PSEUDOERROR DETECTOR PERFORMANCE IN PRESENCE OF INTERFERRING TONE

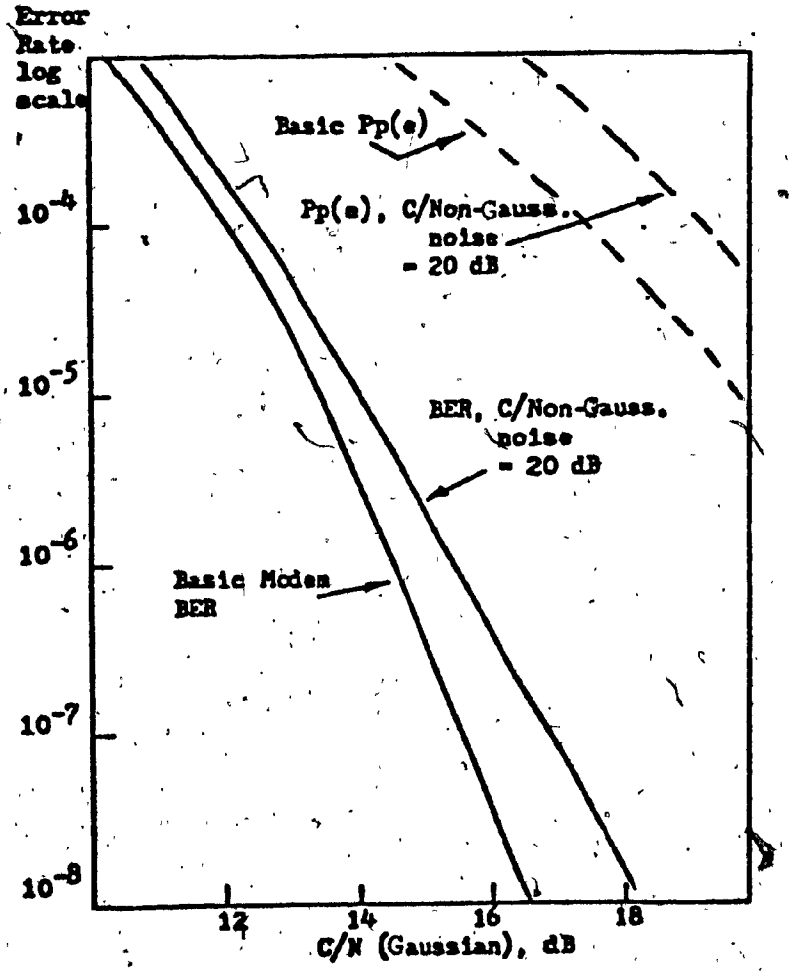

FIG. 5.15 PSEUDOERROR DETECTOR PERFORMANCE IN PRESENCE OF NONGAUSSIAN NOISE

APPENDIX A

Pseudoerror Monitor (PEM) Specifications

1.0 DESCRIPTION

The Pseudoerror Monitor model PEM is an optimum monitoring scheme specially designed for monitoring the BER of digital modems.

It consists of 95 components, analog devices and logic devices.

2.0 INPUT SIGNAL

Pulse Type:	Synchronous NRZ
Bit Rate:	772 kbps
Pulse Amplitude:	100 ± %10 Milli Volts
Impedance:	75 ohms

3.0 INPUT CLOCK

Pulse Amplitude:	1 ± .1 Volts
Pulse width:	100 ± 10 n Sec
Repetition rate:	772 kHz
Impedance:	∞

4.0 OUTPUT SIGNAL

Signal amplitude (75 ohm load): C-MOS or TTL Logic Level to the input of P(p) to P(e) Convertor

5.0 POWER SUPPLY REQUIREMENTS

A: -5.2 ± .1 Volts dC

B: +5 ± .3 Volts dC (For P(p) - P(e) TTL Circuit)

C: +15 ± .3 Volts dC (For P(p) - P(e) C-MOS Circuit)

REFERENCES

1. BENNETT, W.R. & DAVEY, J.R.
   "DATA TRANSMISSION"
   McGraw Hill Book Co., 1965

2. DAVIS, C.G.
   "AN EXPERIMENTAL PULSE CODE MODULATION SYSTEM FOR SHORT-HAUL TRUNKS"
   Bell System Technical Journal, Vol. 41, January 1962

3. LEE, Y.W.
   "STATISTICAL THEORY OF COMMUNICATION"
   John Wiley and Sons, Inc., 1960

4. BENNETT, W.R.
   "ELECTRICAL NOISE"
   McGraw Hill Book Co., Inc., 1960

5. C.C.I.R. (1970-1973) Doc. 9/170E (Japan)
   "20 GHz MULTIPLE HOP DIGITAL RADIO-RELAY EXPERIMENT"

6. MIYAUCHI, K., et al.,
   "A GUIDE MILLIMETER-WAVE TRANSMISSION SYSTEM USING HIGH-SPEED PSK REPEATERS"
   IEEE - GMTT Symposium Digest, P.128, Chicago U.S.A. (1972)

7. GOODING, D.J.
   "PERFORMANCE MONITOR TECHNIQUES FOR DIGITAL RECEIVERS BASED ON EXTRAPOLATION OF ERROR RATE"
   IEEE. Transaction on Communication technology, Vol. Com.16, P-380-387, June 1968

8. LEON, B.J., et al.

"A BIT ERROR RATE MONITOR TECHNIQUES FOR DIGITAL RECEIVERS BASED ON EXTRAPOLATION OF ERROR RATE"

IEEE Transaction on Communication Technology, Vol. Comm-23, No. 5, P. 518-524, May 1975

9. ROSENBAUM, A.S.

"PSK ERROR PERFORMANCE WITH GAUSSIAN NOISE AND INTERFERENCE"

Bell System Tech. J., pp.413-442. Feb. 1969

10. ROSENBAUM, A.S.

"BINARY PSK ERROR PROBABILITIES WITH MULTIPLE CHANNEL INTERFERENCES"

IEEE Trans. Comm. Technol. Vol. Com-18, pp.241-253, June 1970

11. *"NIPPON ELECTRIC COMPANY MICROWAVE PCM SYSTEM"*

Cat.No.317-4-7-E/7004-2000-M; and

"NIPPON ELECTRIC COMPANY TECHNICAL BROCHURE OF MICROWAVE PCM COMMUNICATIONS SYSTEMS"

NEC Ref. No. PCM-70-002

12. WEINSTEIN, S.B.

"ESTIMATION OF SMALL PROBABILITIES LINEARIZATION OF THE TAIL OF A PROBABILITY DISTRIBUTION FUNCTION"

IEEE Trans. Comm. Technol., Vol. Com-19, pp.1149-1155, Dec. 1971

13. LUCKY, SALTZ, WELDON

"PRINCIPLES OF DATA COMMUNICATION"

McGraw Hill, New York, 1968

14. BANDARI, A, FEHER, K

"PSEUDOERROR ON-LINE MONITORING: CONCEPT DESIGN AND EVALUATION"

Canadian Electrical Engineering Journal, Vol.2, No.2, 1977 and Proceedings of the 1976 IEEE Canadian Power and Communication Conference No.1 76-CH-1126, Montreal, Oct.1976